# Multidimensional separation of complex polymers according to microstructure

By

Khumo Gwendoline Maiko

This thesis is presented in fulfilment of the requirements for the degree

**Doctor of philosophy (Polymer Science)**

At the

University of Stellenbosch

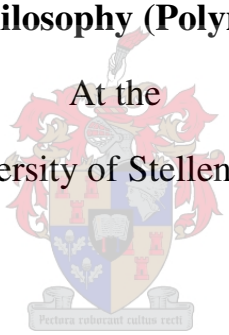


Supervisor: Prof. Harald Pasch

Faculty of Science

Department of Chemistry and Polymer Science

April 2014

## Declaration

I, **Khumo Gwendoline Maiko**, hereby declare that the information contained herein is my own original work and has not previously been submitted in any part at another university for a degree.

Signature : ……

Date : ……..April 2014

# Abstract

Complex polymer systems have multiple distributions with regard to molecular parameters such as molar mass, functionality, chemical composition, molecular architecture and microstructure. These distributions affect the properties of the polymers making it necessary to develop separation methods to be able to correlate structure to property. A single one-dimensional chromatographic method is usually not sufficient to separate these complex polymers with respect to all the distributions. Hence, multidimensional liquid chromatography is necessary for the complete analysis of complex polymers using two or more chromatographic techniques before detection.

In this work, two novel liquid chromatographic methods were developed to separate complex polymers according to microstructure. Comprehensive two-dimensional liquid chromatography (LC x LC) was carried out to observe the correlation between microstructure and molar mass. The separation according to microstructure was coupled to NMR (LC-NMR) to observe, identify and quantify the different microstructural components during chromatographic elution.

The first chromatographic method separated hydrogenated and deuterated polystyrene homopolymers with respect to the isotope effect. For the LC x LC experiments, liquid chromatography at critical conditions (LCCC) was employed as the first dimension separating according to the isotope effect and size exclusion chromatography (SEC) as the second dimension separating according to molar mass. The LC x LC results of the blends showed that there was an improvement in isotopic separation with an increase in molar mass. The LC-NMR coupling using both $^{1}H$ and $^{2}H$ NMR detection allowed for the identification of low molar mass blend components which were not sufficiently separated by liquid chromatography.

The second chromatographic method separated stereoregular poly(methyl methacrylate)s (PMMAs) with respect to tacticity. The LC x LC experiments of stereoregular PMMAs utilised solvent gradient liquid chromatography as the first dimension to separate according to tacticity and size exclusion chromatography (SEC) as the second dimension to separate according to molar mass. The LC x LC results showed a change in the triad composition with

elution of the stereoregular PMMAs with a slight influence of molar mass. The LC-NMR coupling allowed the observation of the triad composition during chromatographic elution.

# Opsomming

Komplekse polimeriese sisteme het meervoudige verspreidings ten opsigte van molekulêre parameters, soos byvoorbeeld, molêre massa, funksionaliteit, chemiese samestelling, molekulêre argitektuur en mikrostruktuur. Hierdie verspreidings beïnvloed die eienskappe van die polimere en dus is dit nodig om skeidingsmetodes te ontwikkel ten einde polimeerstruktuur met polimeereienskappe te kan korreleer. ‘n Enkele een-dimensionele chromatografiese metode is gewoonlik nie voldoende om hierdie komplekse polimere te skei met betrekking tot al die verspreidings nie. Multidimensionele vloeistofchromatografie, met die insluiting van twee of meer chromatografiese tegnieke, is dus nodig om polimere te skei voor waarneming kan plaasvind.

Twee nuwe chromatografiese metodes is ontwikkel om komplekse polimere volgens mikrostruktuur te skei. Twee-dimensionele vloeistofchromatografie (LC x LC) is uitgevoer ten einde die korrelasie tussen mikrostruktuur en molêre massa te ondersoek. Daarna is die skeiding wat op mikrostruktuur gebasseer is, gekoppel aan KMR (LC-KMR) om die verskillende mikrostrukturele komponente gedurende chromatografiese eluering waar te neem, te identifiseer en te kwantifiseer.

Die eerste chromatografiese metode het die gehidrogeneerde en gedeutereerde polistireen geskei met betrekking tot die isotoopeffek. Hier het die LC x LC skeiding bestaan uit vloeistofchromatografie onder kritiese kondisies (LCCC) as die eerste dimensie, wat skeiding bewerkstellig het gebasseer op die isotoopeffek, en grootte-uitsluitingschromatografie (SEC) as die tweede dimensie, wat skeiding bewerkstellig het gebasseer op die molêre massa. Die LC x LC resultate van die vermengings het ‘n verbetering in isotopiese skeiding met ‘n toename in molêre massa getoon. Deur gebruik te maak van die LC-KMR koppeling, waar beide $^{1}H$ en $^{2}H$ KMR waarneming gebruik is, was dit moontlik om die lae-molêre-massa-komponente van vermengings wat nie volledig d.m.v. LC geskei kon word nie, te identifiseer.

Die tweede chromatografiese metode het stereoreëlmatige polimetielmetakrilate (PMMAs) m.b.t. taktisiteit geskei. Die LC x LC skeiding van stereoreëlmatige PMMAs het bestaan uit oplosmiddel -gradiënt-LC as eerste dimensie om volgens taktisiteit te skei, en SEC as tweede dimensie om volgens molêre massa te skei. Die LC x LC resultate het ‘n molêre massa afhanklikheid van stereoreëlmatige PMMAs op taktisiteit getoon. Die LC-KMR koppeling het dit moontlik gemaak om die triade-samestelling gedurende chromatografiese eluering waar te neem.

# Dedication

*This thesis is dedicated to Jayden Bonolo Ndirini.*

# Acknowledgements

Firstly I would like to thank the **Lord Almighty**, for his continued protection and blessings in all aspects of my life especially for all the wonderful gifts I have been blessed with this year.

I would like to extend my deepest gratitude to **Prof. Harald Pasch** for his guidance, support and his unwavering confidence in my abilities.

I would like to thank the National Research foundation, **Prof. H. Pasch** and the University of Stellenbosch for the financial assistance.

I would also like to thank all the staff members at the Department of Chemistry and Polymer science for the assistance whenever I needed it. A special thanks to **Mr Calvin Maart** for his assistance even at unusual times of the morning as well as **Dr G. Harding** for his assistance with my first liquid chromatography experiments.

I would also like to thank the members of the Pasch group past and present: **Nyasha, Helen, Eddson, Monica, Imran, Pritish, Douglas, Trevor, Kerissa, Nadine, Ashwell, Sadiq, Phiri** and **Wisdom**.

I would like to take a moment to remember **Werner van Aswegen.** He was an absolutely wonderful, warm, humble and peace loving soul.

I would like to also thank **Dr W. Hiller** and **Dr M. Hehn** from the Technical University of Dortmund for their assistance and contribution with the liquid chromatography and nuclear magnetic resonance coupling experiments.

To **Peter Kilz**, thank you for the assistance with the PSS software issues.

A heartfelt, thank you to my family and friends for their support, love and inspiration, **Gadifele Maiko**, **Sarah Maiko**, **Thabo Maiko**, **Itshokeng Maiko, Kabelo Maiko, Bonita More, Chandre Willemse, Mpho Phiri, Khotso Mpitso, Lerato Ntlatleng and Yoliswa Jiya**.

Special thanks, to my fiancé **Romeo Ndirini** for being my pillar of strength and support. His advice, suggestions and love has really been of great importance to me. The completion of this thesis would have never been possible without him.

Finally, I would like to thank all the people I may have neglected to mention as everyone's contributions where greatly appreciated.

# Table of contents

# List of figures

# List of tables

# List of abbreviations

| | |
|---|---|
| LC x LC | Comprehensive two-dimensional liquid chromatography |
| ACN | Acetonitrile |
| $^{13}$C-NMR | Carbon-13 nuclear magnetic resonance |
| CCD | Chemical composition distribution |
| DCM | Dichloromethane |
| d-PS | Deuterated polystyrene |
| ELSD | Evaporative light scattering detector |
| FID | Free induction decay |
| FT | Fourier transform |
| FTD | Functionality type distribution |
| h-PS | hydrogenated polystyrene |
| $^{1}$H-NMR | Proton nuclear magnetic resonance |
| $^{2}$H-NMR | Deuterium nuclear magnetic resonance |
| HMBC | Heteronuclear multiple bond correlation |
| HSQC | Heteronuclear single quantum coherence |
| HPLC | High performance liquid chromatography |
| IC | Interaction chromatography |
| *it*-PMMA | isotactic poly(methyl methacrylate) |
| LAC | Liquid adsorption chromatography |
| LED | Light emitting diode |
| LCCC | Liquid chromatography at critical conditions |
| LC-NMR | Liquid chromatography coupled to nuclear magnetic resonance |
| MALDI-TOF | Matrix-assisted laser desorption/ionisation – Time-of-flight |

| | |
|---|---|
| MMD | Molar mass distribution |
| NOESY | Nuclear Overhauser effect spectroscopy |
| NP-LC | Normal-phase liquid chromatography |
| NMR | Nuclear magnetic resonance |
| NR | Neutron reflectivity |
| PB | Polybutadiene |
| PDI | Polydispersity index |
| PEMA | Poly (ethyl methacrylate) |
| PGC | Porous graphitic column |
| PI | Polyisoprene |
| PMMA | Poly (methyl methacrylate) |
| ppm | parts per million |
| PS | Polystyrene |
| RF | Radio frequency |
| RP-LC | Reversed-phase liquid chromatography |
| SANS | Small-angle neutron scattering |
| SEC | Size exclusion chromatography |
| SERS | Surface-enhanced Raman scattering |
| SGIC | Solvent gradient interaction chromatography |
| *st*-PMMA | syndiotactic poly(methyl methacrylate) |
| TGIC | Temperature gradient interaction chromatography |
| THF | Tetrahydrofuran |
| TLC | Thin layer chromatography |
| TOCSY | Total correlation spectroscopy |

| | |
|---|---|
| TMS | Tetramethylsilane |

# List of symbols

| | |
|---|---|
| $\Delta G$ | Change in Gibbs free energy |
| $\Delta H$ | Change in enthalpy |
| $\Delta S$ | Change in entropy |
| $\gamma$ | Gyromagnetic ratio |
| $\sigma$ | Shielding constant |
| $\delta$ | Chemical shift |
| $\alpha$ | Pulse angle |
| $B_0$ | Applied magnetic field |
| $B_{ref}$ | Applied field at reference |
| $B_{sample}$ | Applied field at sample |
| $C_m$ | Concentration of analyte in mobile phase |
| $C_s$ | Concentration of analyte in stationary phase |
| $f$ | Frequency |
| $f_n$ | Number-average functionality |
| $f_w$ | Weight-average functionality |
| h | Planck's constant |
| I | Nuclear spin |
| $k'$ | Retention factor |
| $K_d$ | Distribution coefficient |
| $K_{SEC}$ | Distribution coefficient for size exclusion conditions |
| $K_{LAC}$ | Distribution coefficient at liquid adsorption conditions |
| $M_n$ | Number-average molar mass |

| | |
|---|---|
| $M_w$ | Weight-average molar mass |
| *m* | meso |
| *n* | Peak capacity |
| *N* | Plate number |
| *mm* | meso-meso |
| *mr* | meso-racemic |
| *rr* | racemic-racemic |
| *r* | racemic |
| *R* | Gas constant |
| τ | Residence time |
| *T* | Absolute temperature |
| $T_1$ | Spin-lattice relaxation time |
| $T_{1\ flow}$ | Spin-lattice relaxation time in flow NMR |
| $T_2$ | Spin-spin relaxation time |
| $T_{2\ flow}$ | Spin-spin relaxation time in flow NMR |
| $T_R$ | Retention time |
| $V_R$ | Retention volume |
| μ | Nuclear magnetic moment |
| ν | Resonance frequency |
| $V_0$ | interstitial volume |
| $V_p$ | pore volume |
| $\omega_0$ | Larmor frequency |
| $W_{flow}$ | dwell time in flow NMR |
| $W_{stationary}$ | dwell time in classical NMR |

# List of scientific outputs

## List of publications

1. P. Sinha, G.W. Harding, K. Maiko, W. Hiller, H. Pasch: "Comprehensive two-dimensional liquid chromatography for the separation of protonated and deuterated polystyrene" *J. Chromatogr. A*., **2012**, 1265, 95 – 104.

2. K. Maiko, M. Hehn, W. Hiller, H. Pasch: "Comprehensive two-dimensional liquid chromatography of stereoregular poly (methyl methacrylates) for tacticity and molar mass analysis" *Anal. Chem.*, **2013**, 85, 9793 – 9798.

3. M. Hehn, K. Maiko, W. Hiller, H. Pasch: "Online HPLC-NMR: An efficient method for the analysis of PMMA with respect to tacticity" *Macromolecules*, **2013**, 46, 7678 – 7686.

## Contributions in publications

### Contribution to publication 1

In the first publication I contributed by:

- Employing column temperature experiments to improve the chromatographic separation.
- Establishing new critical conditions and SEC-LAC conditions for the efficient separation of deuterated and hydrogenated polystyrene homopolymer blends by varying column temperature and keeping the solvent composition constant thereby, improving the chromatographic resolution.
- Carrying out the LC x LC experiments using the new chromatographic conditions.
- Data collection and processing of the all results presented in that section.

### Contribution in publication 3

In the third publication I contributed by:

- Implementing and optimising the different chromatographic conditions on the LC-NMR instrument.

- Determining the optimum concentration and injection volumes required to obtain quality NMR spectra without affecting the chromatographic separation.
- Assisting in establishing and improving the different gradient programs used in this publication.

## Oral presentation

1. "Comprehensive two-dimensional liquid chromatography for the separation of protonated and deuterated polystyrene", *12th Annual Unesco/IUPAC conference on macromolecules and materials, 25.03.2013 - 28.03.2013, Stellenbosch, South Africa.*

## Poster presentation

1. "Comprehensive two-dimensional liquid chromatography for the separation of protonated and deuterated polystyrene", *6th International Symposium on the Separation and Characterization of Natural and Synthetic Macromolecules, 06.02.2013-08.02.2013, Dresden, Germany*

# 1. Introduction and aims

## 1.1 Introduction

The high demand of complex polymers with improved properties has led to the development of new synthetic methods. These complex polymers may have various distributions with respect to molar mass, chemical composition, functionality, molecular architecture and microstructure. These distributions affect the properties of the complex systems making it necessary to develop separation methods to be able to correlate structure to property. [1]

High performance liquid chromatography (HPLC) is the technique of choice for separating polymers with respect to their various distributions. There are different HPLC separation modes for polymers, namely size exclusion chromatography (SEC), liquid chromatography at critical conditions (LCCC) and liquid adsorption chromatography (LAC), which will all be described at a later stage.[2]

Since polymers possess more than one distribution, the development of multidimensional techniques is necessary to analyse the multiple distributions with a sole analytical method. To completely analyse a complex polymer a minimum of two characterization methods should be used to obtain two-dimensional information on the molecular distributions.

Deuterated compounds have been assumed to possess similar properties to their hydrogenated analogues. The differences in neutron scattering lengths of deuterium ($^2$H) and hydrogen ($^1$H) have led to their extensive characterization using various neutron scattering and reflective techniques.[3-5] These scattering techniques assume that the thermodynamic parameters of deuterated compounds and their hydrogenated analogues are the same. Previous liquid chromatographic studies have shown that the thermodynamic parameters of hydrogenated and deuterated polymers are quite different.[6, 7] This difference in adsorption behaviour of analytes due to deuteration has coined the term deuterium isotope effect (DIE).[8] This isotope effect (IE) has sparked an interest in developing new chromatographic methods to separate deuterated and hydrogenated polymers.

Poly(methyl methacrylate)s (PMMA)s have various applications as prosthetic and transplant materials due to their biocompatibility to human tissue.[9-11] Various authors have shown that tacticity greatly influences the optical and mechanical properties of PMMA. These properties include thermal degradation,[12] electrical characteristics,[13] and crystalline structure.[14] This discovery incited interest in developing new chromatographic methods to separate PMMAs

according to tacticity. Tacticity refers to the spatial arrangement of substituents along the polymer chain. An extensive literature review revealed that porous graphic stationary phases had never been used to separate polymers according to tacticity at ambient temperature. The numerous advantages that these carbon stationary phases have over silica based stationary phases, especially their sensitivity to closely related compounds without the addition of modifiers, makes them ideal for separating polymers with respect to tacticity.

## 1.2 Aims

1.2.1. The first aim was to develop HPLC methods which would allow for the separation of deuterated and hydrogenated polystyrene homopolymers according to the isotope effect without the influence of molar mass.

The steps taken to achieve this aim included:

i. Developing HPLC methods using liquid chromatography at critical conditions (LCCC) for both deuterated and hydrogenated polystyrene homopolymers.
ii. Separating blends of these homopolymers at each critical condition.
iii. Carrying out comprehensive two-dimensional liquid chromatography (LC x LC) by employing LCCC as the first dimension separating according to the isotope effect and size exclusion chromatography (SEC) as the second dimension separating according to molar mass.
iv. Carrying out on-flow liquid chromatography coupled to nuclear magnetic resonance spectroscopy (LC-NMR) at each critical condition using proton and deuterium NMR detection.

1.2.2. The second aim was to develop a chromatographic method to analyse stereoregular poly(methyl methacrylate)s with respect to tacticity on a porous graphitic column (PGC) at ambient temperature.

The steps taken to achieve this aim included:

i. Developing an HPLC method to separate stereoregular poly (methyl methacrylate) homopolymers according to tacticity on the Hypercarb column at ambient temperature.
ii. Carrying out LC x LC coupling experiments with a HPLC method separating according to tacticity in the first dimension and SEC separating according to molar mass in the second dimension.
iii. Carrying out on-flow LC-NMR coupling with proton detection to observe the tacticity distribution during elution.

# 2. Theoretical and historical background

## 2.1 Theory

### 2.1.1 Polymer distributions

The synthetic method used to prepare a polymer determines its distributed properties. Different molecules in the same polymer will have varying values of that property. The different distributed properties include molar mass, chemical composition, functionality, molecular architecture and microstructure. The broadness of the distribution of the distributed property determines if the polymer will be homogenous or heterogeneous with respect to that property. Monodisperse polymers are homogenous in all distributed properties; polydisperse polymers are heterogeneous in a single distributed property while complex polymers are heterogeneous in more than one distributed property.[2]

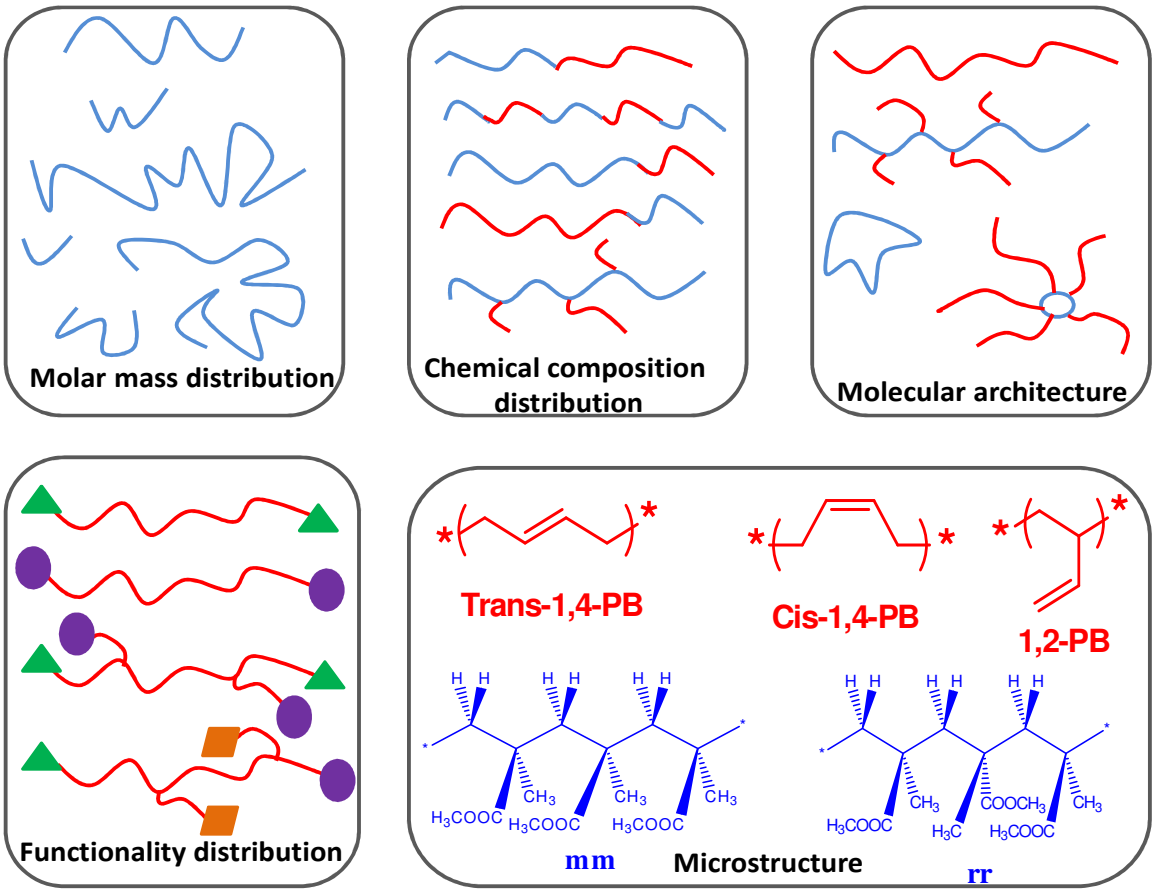


Figure 1: Various polymer heterogeneities of complex polymers.

The most common distribution used to characterise synthetic polymers is the molar mass distribution (MMD). Size exclusion chromatography (SEC) is the technique that is commonly used to experimentally determine the molar mass distribution and molar mass averages by using a calibration. These molar mass averages are the number-average molar mass ($M_n$), weight-average molar mass ($M_w$), viscosity-average molar mass ($M_v$) and Z-average molar mass ($M_z$).

The molar mass polydispersity (PDI) is a measure of the broadness of the MMD which is given by the ratio of $M_w/M_n$. The number-average molar mass ($M_n$), expresses the amount of species by the number of moles of the species as shown by equation 1.

$$\mathrm{M_n} = \frac{\sum n_i M_i}{\sum n_i} \tag{1}$$

Where, $n_i$ is the number of moles and $M_i$ is the molar mass of an individual macromolecule in the sample.

The weight-average molar mass ($M_w$), expresses the amount of species by the mass of the species as shown by equation 2.

$$\mathrm{M_w} = \frac{\sum w_i M_i}{\sum w_i} \tag{2}$$

Where, $w_i$ is the weight of an individual macromolecule in the sample.

Chemical composition distribution (CCD) refers to heterogeneity with respect to the types of monomers incorporated into the polymer chain. The sequences of the monomers in the polymer chain may vary, producing a sequence distribution. There are different types of sequence distributions i.e. alternating, random, block or graft copolymers as shown in Figure 1.

The functional polydispersity is a measure of the broadness of the functionality type distribution (FTD) given by the ratio of $f_w/f_n$, where, $f_n$, is the number-average functionality and $f_w$, is the weight-average functionality. $f_n$ and $f_w$ are represented by the equations 3 and 4, respectively.

$$\mathrm{f_n} = \frac{\sum n_i f_i}{\sum n_i} \tag{3}$$

$$f_w = \frac{\sum w_i f_i}{\sum w_i} \tag{4}$$

The molecular architecture distribution refers to the topology of chain i.e. linear, branched, hyper-branched, comb, star or dendritic as shown in Figure 1.[2]

Polymers may also be distributed with respect to their microstructure. The microstructure simply refers to the detail of the polymer structure i.e. the geometrical, stereochemical and constitutional isomerism that may be observed for the monomer units of the polymer. Constitutional isomers are compounds with the same molecular formula but different bonding patterns. as in the case of the monomers of polyisoprene (PI) and polybutadiene (PB) leading to the formation of 1,2-; 1,4- and 3,4- chain arrangements as shown in Figure 2 a and b.[15]

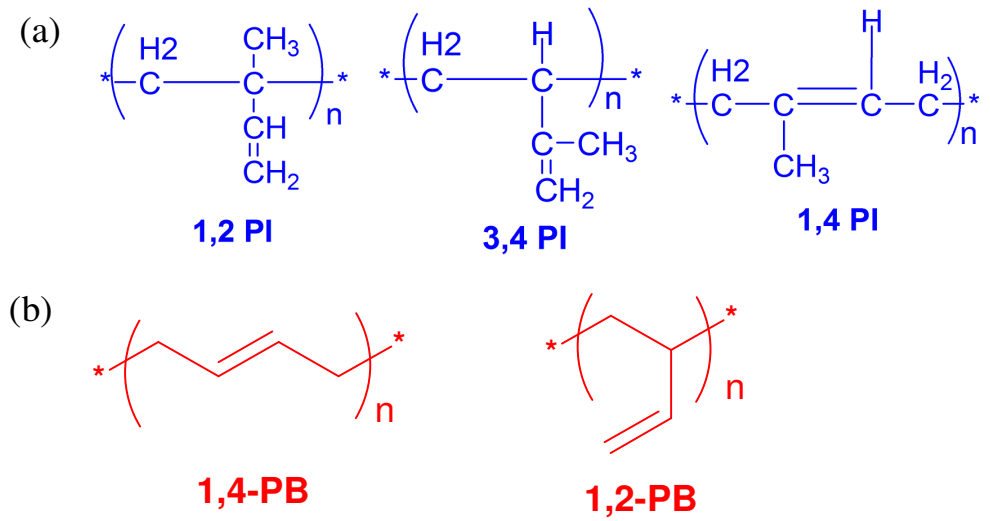


*Figure 2: Constitutional isomerism in vinyl polymers.*

Geometrical isomers are compounds with the same molecular formula but different spatial arrangements of substituents attached on either side of a double bond or ring relative to a reference plane as in the case of monomers of polyisoprenes and polybutadienes as shown in Figure 3 a and b.

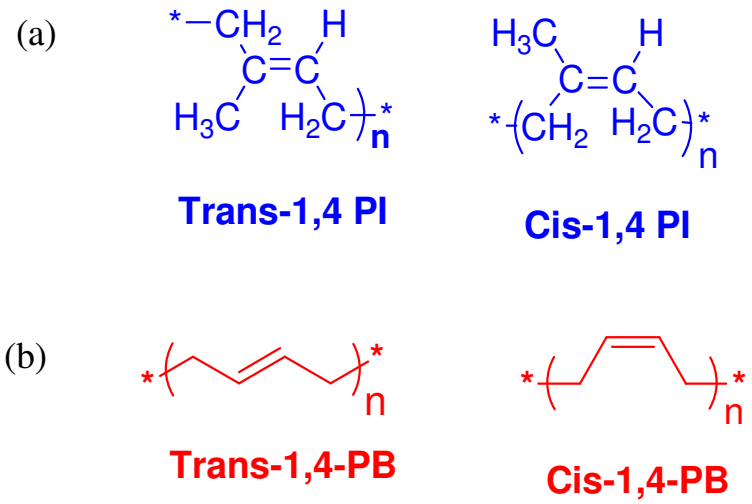


*Figure 3: Geometrical isomerism in vinyl polymers.*

Tacticity refers to the arrangement of the successive configurational repeating units along the main chain of a polymer. There are three tactic arrangements in polymers i.e. isotactic, syndiotactic and heterotactic also referred to as atactic as shown by Figure 4. In an isotactic polymer all the chiral centres have the same configuration (R- or S-) and in a syndiotactic polymer the chiral centres have alternating configurations while, in a heterotactic polymer the chiral centres are randomly arranged.[16]

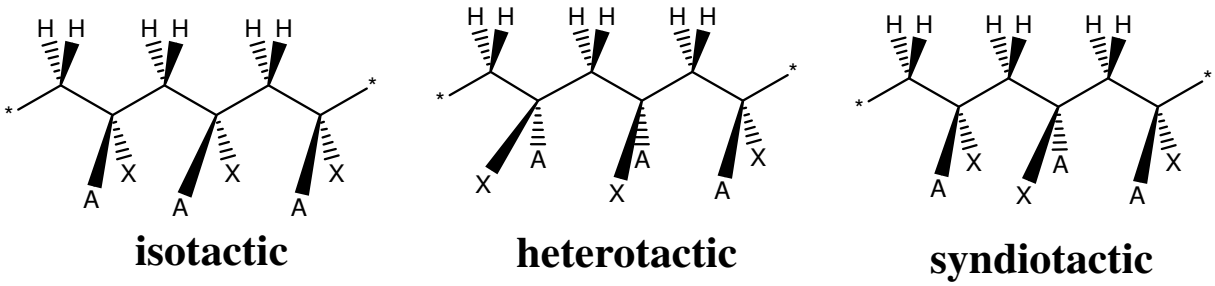


*Figure 4: Tacticity configuration in vinyl polymers.*

### 2.1.2 High performance liquid chromatography of polymers

The chromatographic separation of any analyte refers to the partitioning of that analyte between the mobile and stationary phase. There are four parameters used to describe analyte retention namely retention time ($t_R$), retention volume ($V_R$), retention factor ($k'$) and the distribution coefficient ($K_d$). The distribution coefficient ($K_d$) is a measure of the ratio of the concentration of analyte in the stationary phase ($C_s$) relative to the concentration of analyte in the mobile phase ($C_m$) as shown by equation 5.[2, 17, 18]

$$\mathrm{K_d} = \frac{C_s}{C_m} \tag{5}$$

The change in Gibbs free energy ($\Delta G$) is associated with the analyte partitioning between the mobile and stationary phase as represented by equation 6:

$$\Delta G = \Delta H - T\Delta S \tag{6}$$

Where, $\Delta H$ is the change in entropy of the system attributed to the interactions of the analyte with the pores of the stationary phase, $\Delta S$ is the change in enthalpy of the system attributed to other interactions with the surface of the stationary phase and $T$ is the absolute temperature.

The Gibbs free energy ($\Delta G$) can be related to $K_d$ by equation 7:

$$\Delta G = -RT \ln K_d \tag{7}$$

Where, $R$ is the gas constant.

Combining equations 6 and 7, relates $K_d$ to $\Delta G$ as shown by equation 8:

$$\mathrm{K_d} = \exp\left(\frac{\Delta S}{R} - \frac{\Delta H}{RT}\right) \tag{8}$$

There are three chromatographic separation modes for polymers namely size exclusion chromatography (SEC), liquid chromatography at critical conditions (LCCC) and liquid adsorption chromatography (LAC) as shown by Figure 5.

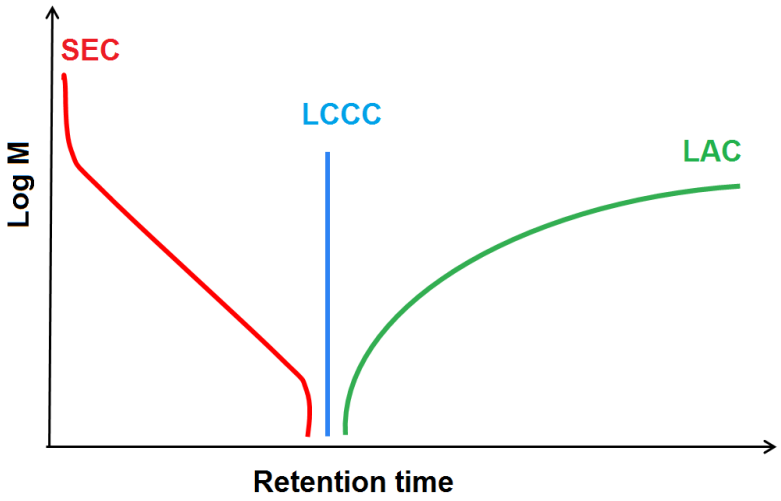


*Figure 5: Plot of the logarithm of molar mass versus retention time showing the three chromatographic modes used for polymers.*[19]

In SEC mode, separation occurs with respect to the hydrodynamic volume of the polymer relative to the pore size of the stationary phase. In ideal SEC, there would be no interaction of the polymer with the stationary phase; hence no enthalpic contribution and the distribution coefficient of ideal SEC ($K_{SEC}$) would be represented by equation 9:

$$K_{SEC} = e^{\frac{\Delta S}{R}} \tag{9}$$

The larger polymer chains are excluded from the pores of the stationary phase ($K_{SEC} = 0$), and are therefore eluted first while the smaller polymer chains can penetrate most of the pore volume are retained longer and eluted last ($K_{SEC} = 1$).

In real SEC, there are enthalpic due to electrostatic interaction of polymer with the pore wall although they are less dominant than the entropic interactions ($T\Delta S > \Delta H$). $K_{SEC}$ can be represented by equation 8. This is the most commonly used separation mode for polymers.

In liquid adsorption mode, separation is determined by the interaction of the polymer with the outer surface of the stationary phase. In ideal LAC, the separation would be directed by the enthalpic interaction with no entropic contribution due to the pore volume not being accessible to the polymer. The distribution coefficient of ideal LAC ($K_{LAC}$) would be represented by equation 10:

$$K_{LAC} = e^{\frac{-\Delta H}{RT}} \tag{10}$$

In real LAC, part of the pore volume can still be accessible to the polymer which means that the equation for $K_{LAC}$ can also be represented by equation 8. This is due to the minor entropic contributions of the polymer to the $K_{LAC}$ together with the dominant enthalpic interactions due to the interaction of the polymer with the surface of the stationary phase ($T\Delta S < \Delta H$).

In liquid chromatography at critical conditions (LCCC), polymers of different molar masses are eluted at the same elution time. This separation mode is sensitive to even the slightest change in eluent composition and temperature. In this separation mode, there is a balance between the enthalpic contributions and entropic contributions ($T\Delta S = \Delta H$) due the pore volume being available to the polymer as well the interaction of the polymer with the stationary phase. The distribution coefficient of critical mode ($K_{LCCC}$) is equal to unity while the Gibbs free energy is equal to zero.[2, 17]

### 2.1.3 Principles of comprehensive two-dimensional liquid chromatography (LC x LC)

Depending on the synthetic method used, polymers can be heterogeneous with respect to multiple distributions i.e. molar mass, functionality and chemical composition. Sometimes a single chromatographic run is not sufficient to have the required peak capacity. Peak capacity is defined as the highest number of resolved peaks that can be separated by a chromatographic method. The peak capacity of a stationary phase is limited by the peak width which depends on the efficiency of the column and the width of the distribution of a particular property. The relationship between peak capacity and column efficiency is described by equation 1: [1, 20, 21]

$$n = 1 + \frac{\sqrt{N}}{4} \times \ln \frac{V_p}{V_0} \tag{11}$$

where, $n$ is peak capacity, $N$ is the plate number, $V_p$ is the pore volume and $V_0$ is the interstitial volume.[1]

To increase peak capacity, a combination of two or more orthogonal separation techniques are used.[22] The total theoretical peak capacity of a LC x LC method is the product of the peak capacities of both dimensions as described by equation 12:[1]

$$n_{LCXLC} = \left(1 + \frac{\sqrt{N_1}}{4} \times \ln \frac{V_{p,1}}{V_{0,1}}\right) \times \left(1 + \frac{\sqrt{N_2}}{4} \times \ln \frac{V_{p,2}}{V_{0,2}}\right) \times \sin\theta \tag{12}$$

Where, $n_{LC\ x\ LC}$ is the peak capacity of a two-dimensional system and $\theta$ is the separation angle between the two dimensions.

A separation angle of 90° is obtained when the two separation methods are completely independent of one another.

The basic LC x LC setup consists of two pump systems, two columns and an electronically controlled transfer valve system equipped with two storage loops and a detector as shown by Figure 6.[20]

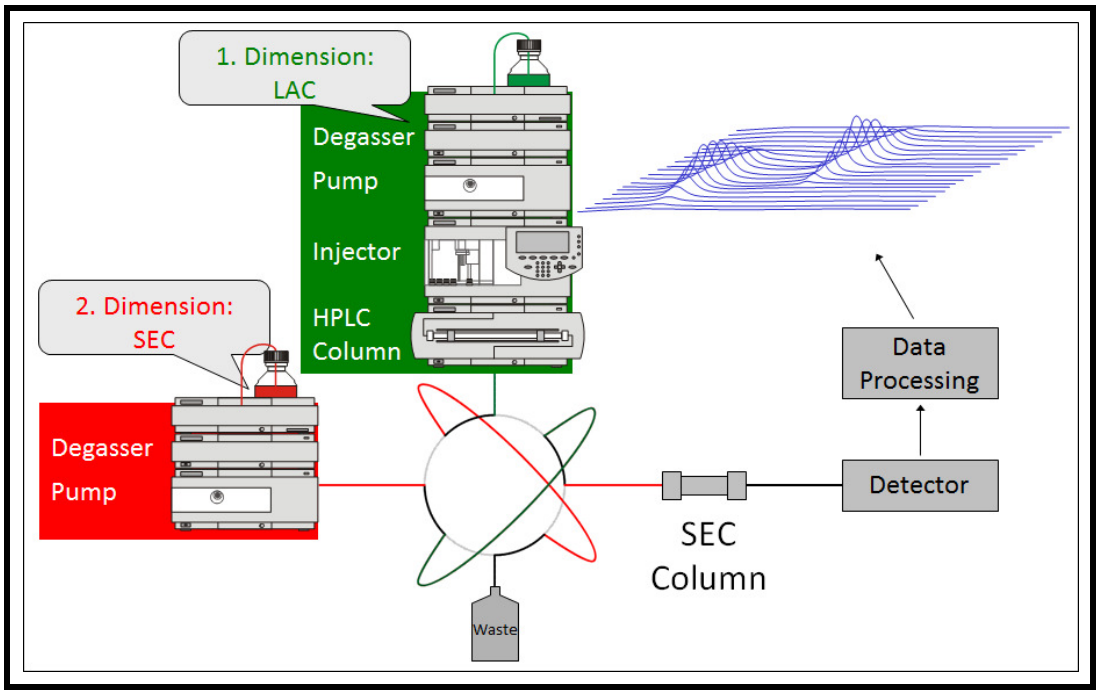


*Figure 6: Basic setup of a LC x LC experiment.* [1]

The first dimension is connected to the second dimension by an electronically controlled transfer valve. This valve transfers fractions from the first dimension into the second dimension. The flow rates of both dimensions are adjusted such that the time it takes to fill one storage loop is equal to the time is takes to analyse the other loop contents in the second dimension. The column type, dimension, particle size, eluent and flow rates in the different dimensions need to be compatible to optimise peak capacity.[23] Having a common solvent in both dimensions reduces breakthrough effects as well as the interferences of the solvent from the first dimension with separation in the second dimension. The advantage of two-dimensional liquid chromatography of polymers is that in a single run you are able to obtain comprehensive information on the different distributions of the polymer. These distributions

can then be correlated to each other to give comprehensive information on the synthetic polymer.[1, 20]

### 2.1.4 Detectors used in liquid chromatography

To obtain more information on the various distributions of the complex polymers numerous detectors are available. Molar mass sensitive detectors i.e. differential viscometer, low-angle laser light scattering (LALLS) and multi-angle light scattering (MALLS) are usually used in conjunction with SEC. In SEC, narrowly dispersed homopolymers are used to construct calibration curves which provide a direct relationship between elution volume and molar mass. Concentration-sensitive detectors i.e. refractive index (RI), ultraviolet (UV) and the evaporating light scattering (ELS) detectors have a response which is dependent on the concentration of the analyte.[1, 2] All these detectors are unable to give information on chemical composition and microstructure.

Selective detectors including mass spectrometry (MS), Fourier transform infrared spectrometry (FTIR) and nuclear magnetic resonance (NMR) are sensitive to molar mass, functionality, chemical composition and microstructure.[1]

In this work the ELS detector was used as a concentration sensitive detector while NMR was used a selective detector to obtain microstructural information.

#### *2.1.4.1 Evaporative light scattering (ELS) detection*

The evaporative light scattering detector (ELSD) is a universal detector, which detects any analyte less volatile than the eluent. The eluent is nebulised by the inlet gas ($N_2$), producing droplets. The droplets enter the evaporating tube where the solvent is removed. The analyte particles are transferred into the detection cell where they are irradiated by a light emitting diode (LED) and photomultiplier positioned at a 120° angle. The intensity of the scattered light is a function of the mass of the particle.[24] The ELSD has been substantially used in the detection of polymers for the past decades.[25]

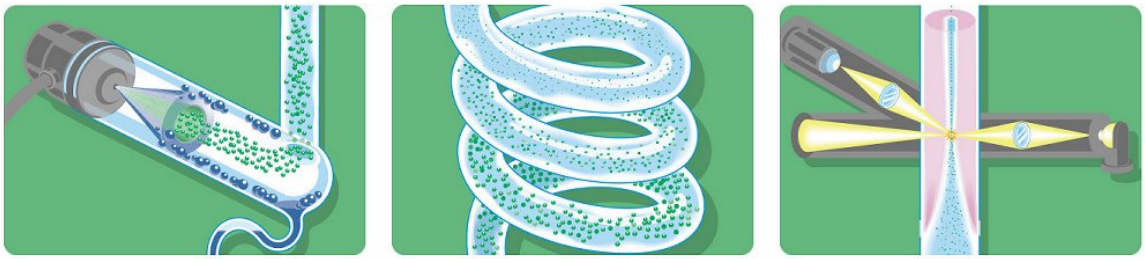

*Figure 7: Three stages of ELS detection, from left to right, nebulisation, evaporation and light scattering detection.*[26]

## 2.1.5 Principles of NMR and LC-NMR hyphenation

### *2.1.5.1 Principles of NMR*

NMR spectrometry is a powerful technique in the detection of polymers due to its ability to observe and quantitatively measure microstructure. For NMR, the most important parameter of the nucleus is the nuclear spin ($I$); this value depends on the mass number and atomic number of the nucleus. Nuclei with a nuclear spin equal to zero have no magnetic moment and cannot be analysed with NMR. The nuclear magnetic moment ($\mu$) of a nucleus is related to the nuclear ($I$) spin by equation 13:

$$\mu = \frac{\gamma I h}{2\pi} \tag{13}$$

Where, $\gamma$ is the gyromagnetic ratio and $h$ is the Planck's constant.

When placed in a magnetic field, $B_0$, the nuclear magnetic field moments orient themselves into specific orientations represented by the magnetic quantum number. The magnetic moment ($\mu$) is aligned parallel or antiparallel to the magnetic field ($B_0$) and the angular magnetic values for the two alignments are -1/2 and +1/2, respectively.[27, 28]

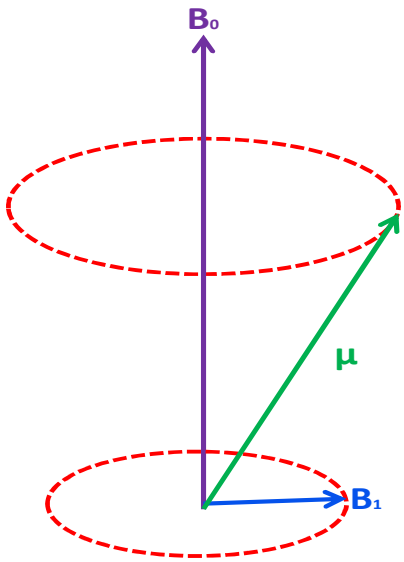


*Figure 8: Nuclear magnetic moment in a magnetic field.*[27]

The energy of the spin states can be related to the magnetic field $B_0$ by equation 14:

$$E = \frac{-\gamma \hbar m B_0}{2\pi} \tag{14}$$

The Larmor frequency ($\omega_0$) of a nucleus is the slow movement of the axis of a charged particle when placed in a magnetic field ($B_0$), around that magnetic field. The Larmor frequency is related to the magnetic field by equation 15:

$$\omega_0 = \gamma B_0 \tag{15}$$

Relaxation processes are transitions during which a nucleus moves from an upper to a lower spin state. The two important relaxation processes that are used to study the molecular motions of a polymer are the spin-lattice and spin-spin relaxation. The spin-lattice relaxation time ($T_1$) is the time it takes for the nuclei to return to thermal equilibrium while spin-spin relaxation time ($T_2$) is the time it takes for the spins of the nuclei to be flipped back into the z plane after being magnetized into the x-y plane.[27, 28]

When a molecule is placed in an external magnetic field ($B_0$) its electrons shield the nuclei from the applied field, causing the nucleus to experience a magnetic field which is less than the originally applied field ($B_0$). The shielding constant ($\sigma$) can be related to the applied magnetic field by equation 16:

$$\nu = \frac{\gamma B_0 (1-\sigma)}{2\pi} \tag{16}$$

This equation shows that the resonance frequency ($\nu$) is proportional to $B_0$.The chemical shift ($\delta$) is then represented by equation 17:

$$\delta = \frac{B_{ref} - B_{sample}}{B_{ref}} \times 10^6 \tag{17}$$

In the above equation, $B_{ref}$, is the magnetic field at reference nuclei and $B_{sample}$ is the magnetic field at the sample nuclei. The unit for $\delta$ is parts per million (ppm). The reference compound for $^1$H NMR spectroscopy experiments is usually tetramethylsilane (TMS).[28]

The type of spectrometer used in this study is a pulse Fourier-transform (FT) spectrometer. In a FT spectrometer, the radiofrequency (RF) radiation is produced by an RF pulse with certain frequency ($f$) called carrier frequency. This pulse is used to excite all the nuclei at the same time which return to thermal equilibrium by releasing energy after the pulse is switched off producing a free induction decay (FID) signal. The FID signal is the oscillating signal decay as a function of time as the phase consistency between the magnetic dipole is lost. The strength of the pulse is described by the pulse angle ($\alpha$) which represented by equation (18):

$$\alpha = \tau \frac{\gamma B_0}{2\pi} \tag{18}$$

Where, $\tau$ is the duration of the pulse and $B_1$ is the amplitude of the RF field. An example of a pulse sequence experiment is shown in Figure 9. The acquisition time is the time needed to obtain the FID. The pulse repetition time is the time between two RF pulses.[27, 28]

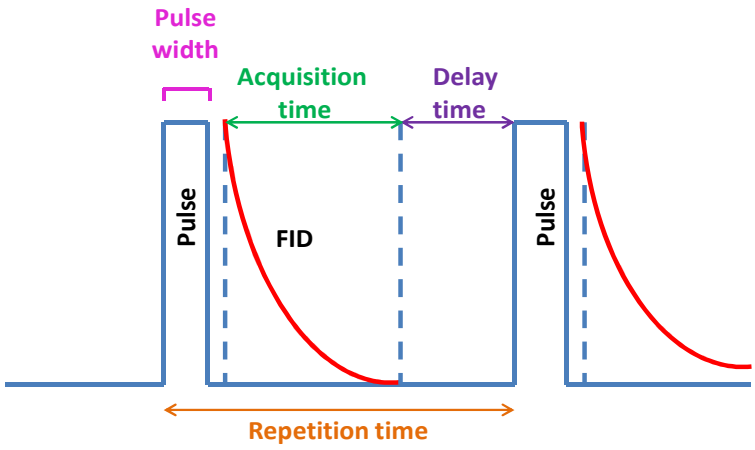


*Figure 9: An example of pulse sequence for an FT NMR experiment.*[27]

The most commonly used nucleus is the $^1$H due to its high abundance and sensitivity, while other observable nuclei include $^{14}$N, $^{19}$F, $^{31}$P, $^{29}$Si and $^2$H. The nuclei of interest for this project

will be the $^{1}H$ and $^{2}H$ nuclei. The $T_1$ relaxation time of the $^{2}H$ nucleus is shorter than that of the $^{1}H$ nucleus.[28]

### *2.1.5.2 LC-NMR hyphenation*

#### *2.1.5.2.1 NMR in a flowing liquid*

In classical NMR the sample remains in the sample tube between the RF detection coils during the whole analysis time. In on-flow LC-NMR the analyte is in motion and the quality of the spectra obtained is determined by the concentration of the sample, flow rate, solvent gradient, magnetic field homogeneity, signal-to-noise ratio and the residence time ($\tau$). The residence time is determined by the volume of the detection cell as well as the chromatographic flow rate.[29, 30] The equation used to calculate the residence time ($\tau$) is shown below:

$$\tau = \frac{detection\,volume}{flow\,rate} \tag{19}$$

In a flowing liquid, the shorter the residence time in the detection coil, the shorter the lifetime of the spin states. The relaxation rates are increased by $1/\tau$ as shown by equation 20:

$$\frac{1}{T_{n\,effective}} = \sum \frac{1}{T_i} + \frac{1}{\tau} \tag{20}$$

Where $T_{n\,effective}$ is the effective relaxation time and $T_i$ is the initial relaxation time.

At a specific detection volume the increase in the flow rate leads to an increase in the signal half-width due to the decrease in $T_2$ relaxation time in on-flow NMR. The following equation shows the effect of detection volume and flow rate represented by dwell time ($\tau$) on the resolution of the continuous flow spectra:

$$w_{flow} = w_{stationary} + \frac{1}{\tau} \tag{21}$$

Where, $W_{flow}$ is the dwell time in on-flow NMR and $W_{stationary}$ is the dwell time in conventional NMR. To obtain maximum sensitivity, theoretically the repetition time should be equal to the dwell time in the flow cell.[29]

*2.1.5.2.2 Conventional NMR versus LC-NMR*

In classical NMR, the analyte is dissolved in a deuterated solvent of choice and placed in a 5 mm cylindrical tube which is placed between the detection coils. The analyte remains in the NMR tube between the detection coils during the entire analysis time. The NMR tube is rotated to remove any magnetic field inhomogeneities.

In LC-NMR, a modified U shaped flow cell with an active detection volume of 60 µL is used. The analyte enters the flow cell through the inlet tubing from the bottom and exits through the outlet tubing to the waste also located at the bottom. The flow cell is not rotated as in classical NMR to eliminate magnetic field inhomogeneities but instead it is inserted into the magnet parallel to the z-direction of the magnetic field to eliminate magnetic field inhomogeneities. The best chromatographic separations are obtained with small flow cells with an active volume of 60 µL or less, although sensitivity of these flow cells may suffer from the limited amount of nuclei present in the detection cell. The larger flow cell volumes produce the best sensitivity but also lead to peak broadening, which sometimes destroys the chromatographic separation. The quality of the LC-NMR spectra depends on the concentration of the sample, the size of the flow cell and the chromatographic flow rate.[29, 30]

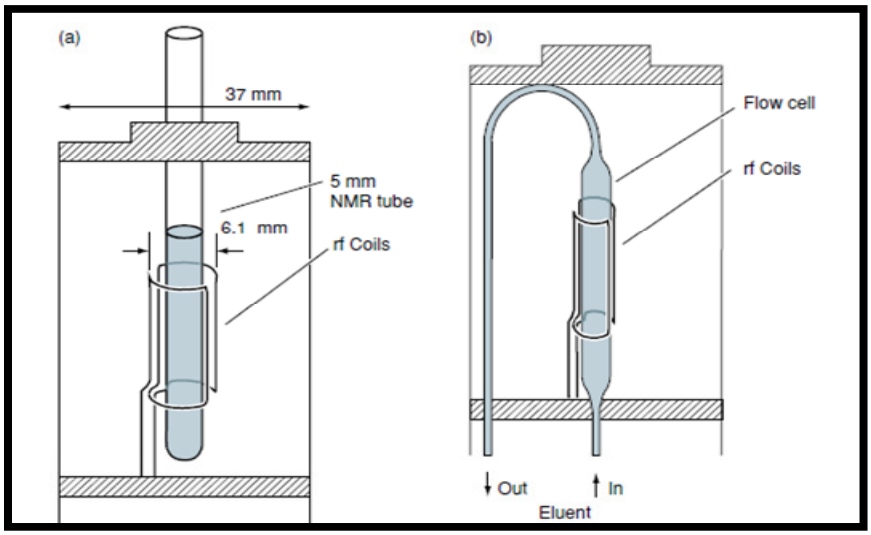


*Figure 10: A conventional 5mm cylindrical NMR tube (a) versus a U shaped LC-NMR flow cell (b).*[29]

*2.1.5.2.3 Solvent suppression*

Solvent suppression is an absolute necessity because the NMR receiver is unable to handle larger solvent signals together with the weaker analyte signals. There are three solvent suppression techniques namely: NOESY pre-saturation, soft pulse multiple irradiation and WET pre-saturation using a z-gradient.

NOESY pre-saturation works on the principle that the nuclei that are unable to relax because ground state and excited state populations are similar do not contribute to the FID after pulse irradiation. Before data acquisition, the pulse irradiates the solvent signals of choice, saturating the solvent signal frequency so that during data acquisition irradiation does not occur. Soft pulse irradiation is also a pre-saturation technique which uses shaped pulses with a broader excitation profile so it is best used with suppression of multiplets.

The WET (Water Suppression Enhanced through $T_1$ effects) sequence uses four solvent selective pulses of different lengths. Each of the four pulses is followed by a dephasing field gradient pulse. The disadvantage of NOESY is that it can only suppress a single signal which would not be effective for solvents with multiple signals as well as for binary solvent systems. Both NOESY and soft pulse multiple irradiation solvent suppression techniques are unable to suppress the $^{13}C$ satellites of the solvent which end up dominating the $^{1}H$ NMR spectra. The WET solvent suppression technique is advantageous because it allows suppression of multiple solvent signals and can be used in conjunction with $^{13}C$ decoupling to remove the $^{13}C$ satellites of the solvent.[29]

For all the LC-NMR experiments in this study WET suppression was employed.

*2.1.5.2.4 LC-NMR modes*

There are three different working modes of LC-NMR namely on-flow, stop-flow and loop storage. The advantages and disadvantages of each of the modes will be discussed below.

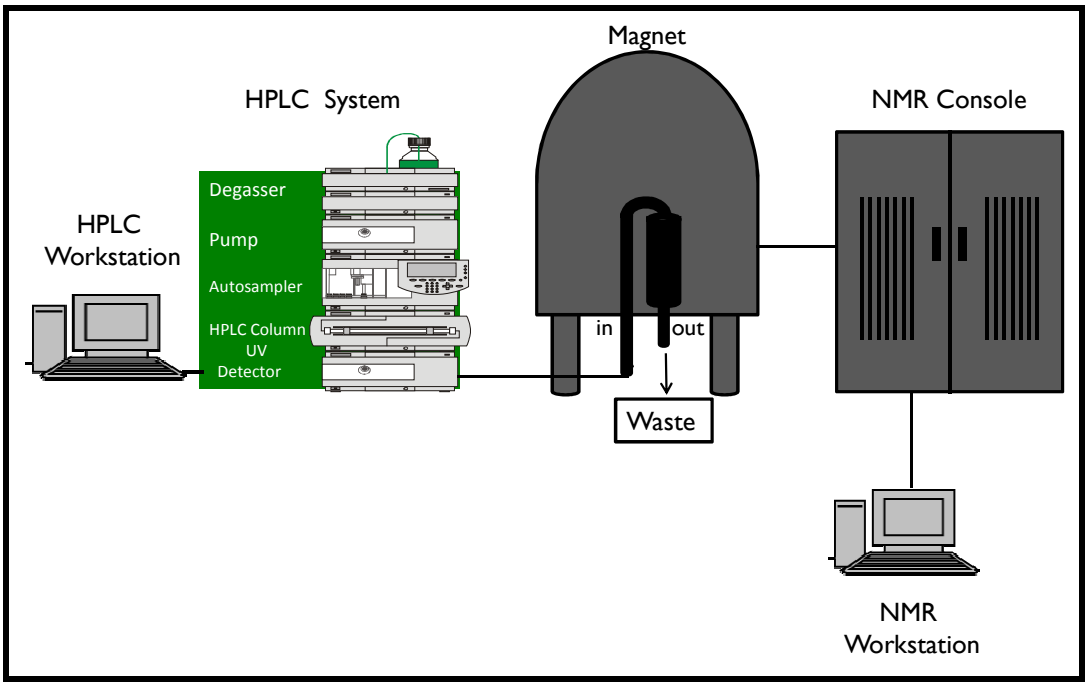


*Figure 11: Basic setup of an on-flow LC-NMR coupling experiment.*

In on-flow LC-NMR, the spectra are obtained continuously while the analyte is eluting out of the chromatographic system without any interruption. The result is a one-dimensional NMR spectrum represented as a two-dimensional matrix covering the whole chromatogram, with one axis showing the retention time scale and the other axis showing the chemical shift scale.

In direct stop flow mode, the spectra are only acquired for a certain part of the chromatogram. The delay time between the LC detector, i.e. UV detector and the NMR spectrometer is calculated. When the peak of interest reaches the NMR spectrometer, the chromatographic separation is stopped. The advantage of this mode is that one may run different types of NMR experiments on selected analytes. The homogeneity of the magnetic field and solvent suppression parameters for each analyte can be adjusted. The disadvantages of this mode are the occurrence of band broadening and diffusion, which will effectively disturb the chromatographic resolution especially for closely eluting analytes.

In loop storage mode, all the components are eluted out of the chromatographic system. The components of interest are transferred in the storage loop. After the chromatographic separation is complete, each of the loop contents are transferred to the NMR spectrometer for analysis. This mode has the advantages of both stop flow and on-flow modes, in that the chromatography is not affected by band broadening and diffusion effects as well as the fact that the homogeneity of the magnetic field and solvent suppression parameters can be adjusted for each stored analyte.[29]

## 2.2 Literature

### 2.2.1 Characterization of polymers according to the isotope effect

Isotopes have the same atomic number but different mass numbers. For example, carbon has two isotopes of which one has an abundance of 98.89% and an atomic mass of 12.000 and the other has an abundance of 1.11% and an atomic mass of 13.003. Oxygen has three isotopes with one having an abundance of 99.76% and an atomic mass of 15.995 and the second having an abundance of 0.04% and an atomic mass of 16.999 while the third has an abundance of 0.20% and an atomic mass of 17.999. Hydrogen has three isotopes, one has an abundance of 98.977% and an atomic mass of 1.007 and the second has an abundance of 0.016% and an atomic mass of 2.014 and the third which has an abundance of 0.20% and an atomic mass of 3.016.

The isotope effects, also known as mass-dependent isotope effects, are the changes in physical and chemical properties of atoms and molecules brought about by isotopic

substitution. These 'mass-dependent isotopic effects' do not include 'magnetic isotope effects' which are brought about by differences in the nuclear spins of isotopes. The isotope effects between hydrogen and deuterium will be the focus of this part of the dissertation.

Deuterium has low systemic toxicity at levels below 20% of body fluid; hence deuterated compounds have been used as stable isotope labels to monitor the metabolism of drugs,[31] and to obtain quantitative data on compounds known to cause rotting of food products.[32] Deuterated compounds are used as tracers to monitor pollutants in water.[33] Deuterated drugs have been used to improve the pharmacokinetic properties of their hydrogenated analogues.[34] Deuterated polystyrenes has been used as scintillators,[35, 36] and as a nuclear fusion targets.[37-40]

Deuterated compounds have been shown to have different molecular volume and polarizability as compared to their hydrogenated analogues. The change in molecular volume is due to the reduced amplitude of C-D bending vibrations, while the polarizability is affected by the increased electron donating abilities of the C-D bond as compared to the C-H bond.[41] The differences in neutron scattering lengths of proton and deuterium have led to extensive characterization of deuterated compounds using small angle neutron scattering (SANS),[42, 43] neuron reflectivity (NR)[44, 45] and surface enhanced Raman scattering (SERS).[46-48] These scattering techniques assume that thermodynamic parameters of deuterated and hydrogenated polymers are similar which, was shown to be incorrect by a few authors who utilised liquid chromatography to prove this point.[6, 7, 49]

For the past two decades, liquid chromatographic separation of small molecules according to the isotope effect has been carried out, proving that thermodynamic parameters are significantly affected by the type of isotope in the molecule.[50-52] Tritium labelled dopamine and dihydroxyphenylacetic acid were separated from their hydrogenated analogues using reversed phase liquid chromatography on a $C_8$ modified silica based stationary phase.[53] Tritium and deuterium isotope effects of isotopologues were extensively investigated on various stationary phases with normal-phase, reverse-phase and chiral liquid chromatography using unlabelled and $^2H$ labelled solvents.[54] Chromatographic separation of racemates according to isotopic chirality has also been reported.[55]

In polymer science, liquid chromatography of polymers according to the isotope effect is relatively new. Tanaka *et al.* carried out one of the first chromatographic separations of polystyrene (PS) with respect to the isotope effect using thin layer liquid chromatography.

They showed that the deuterated PS (d-PS) was more strongly adsorbed on bare silica stationary phase as compared to the hydrogenated PS (h-PS).[49]

Kim *et al.* carried out both normal-phase liquid chromatography (NP-LC) and reverse-phase liquid chromatography (RP-LC) to observe the differences in adsorptive behaviours of d-PS and h-PS. Kim *et al.* utilised NP-LC to show that d-PS was more strongly retained than h-PS. These results were in agreement with those obtained by Tanaka *et al.* using TLC. The inverse was observed with the h-PS more strongly retained than d-PS when RP-LC was utilised.[7, 49] Kayillo *et al.* investigated the thermodynamic differences between d-PS and h-PS using RP-LC; a similar retention mechanism to that observed by Kim *et al.* was also observed. This work showed that there were slight differences between the entropic and enthalpic terms of deuterated and hydrogenated oligomers of similar molar masses, with the h-PS oligomers having higher retention time due to a more negative enthalpic term.[6] Recently, Ahn *et al.*[56] synthesized comb shape polystyrenes with a hydrogenated backbones and deuterated branches; these were then separated using two-dimensional chromatography with normal-phase temperature gradient interaction chromatography (NP-TGIC) separating according to molar mass in the first dimension and RP-LC separating according to the isotope effect in the second dimension.

After an extensive literature review of the separation of polymers with respect to the isotope effect we realised that only two of the HPLC chromatographic modes where used, i.e. SEC and LAC. The use of these chromatographic modes meant that the separation was not only based on the isotope effect but also had a combined molar mass effect The third mode, i.e. LCCC, had never been used for the separation of deuterated and hydrogenated polymers according to the isotope effect.

This brings us to the main aim of this part of the project which is to separate deuterated and hydrogenated polystyrene homopolymer blends according to the isotope effect without the influence of molar mass by using LCCC.

### 2.2.2 Characterization of polymers according to tacticity

Over the past few decades, the separation of small molecules according to different types of isomerism has been conducted. Examples include the separation of constitutional isomers of tetra-, tri-, and di-β-sulphonic phthalocyanine zinc complexes and diaziridines,[57, 58] configurational isomers of cyclic nitrosamines and diesters,[59, 60] and geometric isomers of unsaturated fatty acids and leukotriene antagonist using cyclodextrins,[61, 62] by using various chromatographic techniques.

In polymer science, microstructure is the collective term given to changes in the detail of the polymer structure which includes isomerism. Microstructure is defined as the arrangement of the successive repeating units in the main chain of the polymer. Numerous authors have developed chromatographic methods for the separation of polymers with regard to isomeric structure i.e. polybutadienes,[63] polyacetylenes,[64] and polyisoprenes.[65, 66]

Tacticity describes the relative stereochemistry of chiral centres in successive repeating units within a polymer. The notation used to describe the stereochemistry of polymer is *m* (meso) and *r* (racemic). By extending this notation triads, tetrads, pentads and so on can also be described i.e. *mm* would represent as purely isotactic triad, while *rr* would represent a purely syndiotactic triad. Similarly, *mmm* would represent a purely isotactic tetrad and *rrr* would represent a purely syndiotactic tetrad.[28] The three possible tactic forms in polymers are isotactic, syndiotactic and atactic as shown by Figure 12. In a isotactic polymer the majority of the chiral centres would have the same configuration, in a syndiotactic polymer the majority of the chiral centres will have an alternating configuration and a heterotactic polymer the chiral centres will have no specific arrangement having both isotactic and syndiotactic sequences.[67]

Numerous chromatographic separations with emphasis on tacticity have been developed for various polymers including polypropylene,[68, 69] polystyrene,[70] and PMMA.[71] The focus of this study will be on the tacticity separation of PMMAs.

As shown by Figure 12 on the next page, a purely isotactic PMMA (*mmm*) homopolymer would have all the ester groups on one side of the chain, while a purely syndiotactic PMMA (*rrr*) homopolymer would have the ester groups alternating on both sides of the chain. A heterotactic PMMA (*mrm*) homopolymer would have no specific arrangement of substituents having both isotactic and syndiotactic sequences.

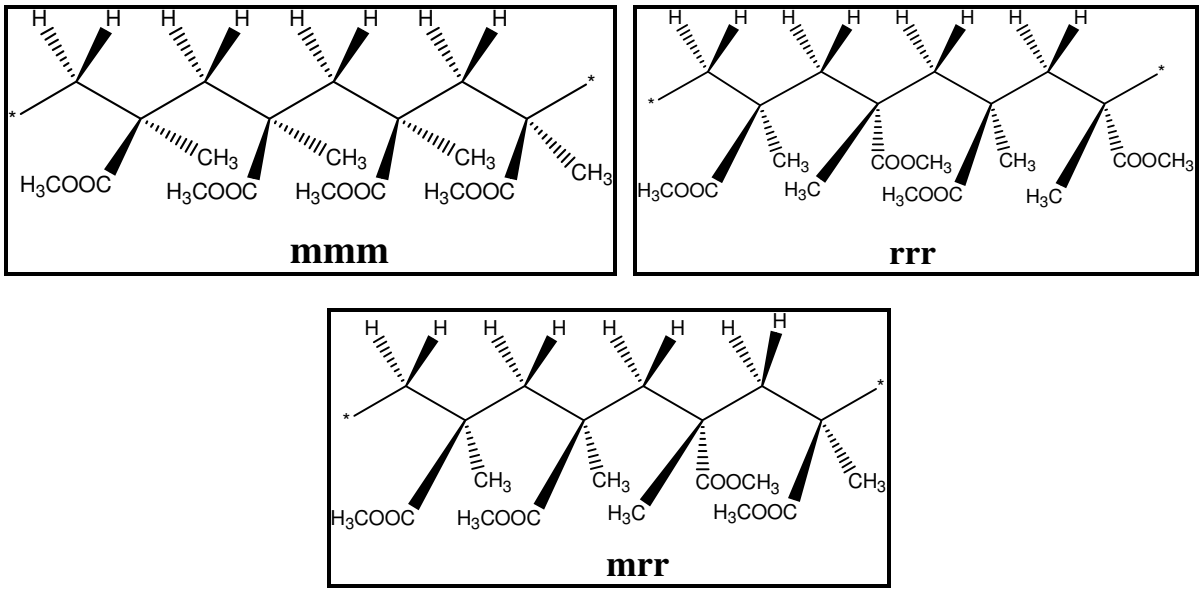


*Figure 12: Structures of an isotactic, syndiotactic and heterotactic poly (methyl methacrylate) homopolymers.*

Solution state NMR spectroscopy is the most frequently used characterization technique for determining polymer microstructure. The $^{1}$H NMR spectra of PMMA shows, that the two methylene protons are non-equivalent and therefore, have different chemical shifts. The α-methyl protons are affected by slight changes in the stereochemical configuration. There are three groups of α-methyl signals observed that are assigned to the *rr*, *mr* and *mm* triad sequences at 0.8, 1.0 and 1.2 ppm, respectively.[28, 72, 73] The tacticity configuration of poly(methacrylate)s has also been investigated using $^{13}$C NMR [74-76] and other two-dimensional NMR experiments i.e. TOCSY, HSQC and HMBC.[77]

The coupling of liquid chromatography with NMR spectroscopy is a powerful technique which allows for the observation of polymer microstructure during chromatographic elution. Hehn *et al.* have used SEC-NMR to characterise PI-b-PMMA copolymers according to microstructure and molar mass.[78] Hatada *et al.* have used SEC coupled to $^{1}$H-NMR to observe the molar mass dependency of PMMA on its tacticity as well as to highlight the advantage of NMR in determining the $M_n$ of polymers whose functionality was known without the need to construct a calibration curve.[79, 80] Although this technique was advantageous for polymers of different molar masses, when polymers of similar molar masses were analysed no further information could be obtained and a chromatographic separation was necessary.

Kitayama *et al.* analysed poly(ethyl methacrylate)s (PEMA) by online LCCC-NMR on a $NH_2$-silica stationary phase using a binary solvent with an elution order of highly isotactic to highly syndiotactic PEMA.[81] Hiller *et al.* have used LCCC-NMR to characterise PI-b-

PMMA copolymers with respect to block length and microstructure. [82, 83] Pasch *et al.* used HPLC-NMR to analyse oligostyrenes with respect to functionality and tacticity. [70]

Other techniques that have been used to characterise PMMAs according to tacticity include FTIR,[84] electron microscopy,[85] light scattering,[86, 87] differential scanning calorimetry (DSC),[88, 89] and X-ray diffraction (XRD).[90, 91] These techniques have shown that changes in the stereochemistry of PMMA affect the crystalline structure and thermal degradation. Other effects include electrical properties,[13] cytotoxicity,[92] and influence on the flexibility of the molecular chain and the free volume morphology.[93]

The majority of studies were on the stereocomplex formation between PMMAs of specific tacticity, especially isotactic PMMA (*it*-PMMA) and syndiotactic PMMA (*st*-PMMA). These articles showed that certain solvents promote the formation of this stereocomplexes, i.e. acetone, toluene, xylene and so on.[85, 94-98] These solvents were split into three groups: the strongly complexing solvents i.e. acetonitrile and acetone, the weakly complexing solvents i.e. toluene and tetrahydrofuran (THF) and the non-complexing solvents i.e. chloroform and dichloromethane.[87, 99, 100] Liquori and colleagues were the first to propose a structure for the stereocomplex. They suggested that in polar solvents the stereo complex has a helical conformation when the ratio of isotactic and syndiotactic PMMAs is 2:1.[97]

The separation of poly (methyl methacrylate)s according to tacticity has been employed for the past four decades. The first liquid chromatographic separation of stereoregular PMMAs was attempted by Inagaki *et al.* using thin layer chromatography. They showed that the separation was influenced by both tacticity and molar mass.[101] Berek *et al.* attempted to separate PMMAs with regard to tacticity using liquid chromatography at limiting conditions on bare silica stationary phases. Although there were slight differences in the curves of different stereoregular PMMAs, the differences were not sufficient for a proper separation.[102] Berek *et al.* used liquid chromatography at critical adsorption point (LC-CAP) on a Nucleosil silica stationary phase using various binary solvents to separate stereoregular PMMAs with respect to tacticity without the influence of molar mass. However, the disadvantage of this method was the total adsorption of high molar mass PMMAs.[103]

Macko *et al.* established the critical conditions of heterotactic PMMA in a single eluent i.e. acetonitrile) and observed that the *st*-PMMA eluted in SEC mode and *it*-PMMA eluted in LAC mode.[104] Janco *et al.* separated PEMAs using online two-dimensional liquid chromatography with SEC as the first dimension separating with regard to molar mass on a

styrene-divinylbenzene (SDVB) stationary phase followed by LC-CAP as the second dimension separating with regard to tacticity on a $NH_2$-silica stationary phase.[105] Cho *et al.* used temperature gradient interaction chromatography (TGIC) coupled with matrix-/ionization time-of-flight mass spectrometry (MALDI-TOF MS) detection for the analysis of stereoregular PEMAs and studied the tacticity effect on the SEC behaviour of stereoregular PEMAs. They showed that TGIC on its own is not sufficient to characterise both tacticity and molar mass.[106, 107]

All the above-mentioned separations used silica based stationary phases. In this study we wanted to use a porous graphitic stationary phase. These carbon-based stationary phase has numerous advantages over silica based stationary phases with the most interesting being its selectivity for closely related small molecules and highly polar analytes i.e. diastereomers, enantiomers.[108-111] They have numerous advantages over silica-based materials in that they are very stable in aggressive solvents, there is no shrinkage or swelling and column bleeding is significantly reduced. They can be utilised over the whole pH range (0-14), at very high temperatures (~200°C) and at high salt concentrations. They can be used with both normal and reversed phase eluents.[109, 112]

This porous graphitic carbon phase (PGC) also known as Hypercarb, was manufactured by impregnating a silica template with phenol-formaldehyde oligomers. The impregnated silica template was heated to 150˚C, producing a phenol-formaldehyde resin, and carbonised by heating to 900˚C under nitrogen to produce a porous carbon. The silica template was not needed anymore and was dissolved with potassium hydroxide. The porous carbon was heated to 2500˚C to graphitize the carbon.[113] The surface of the PGC is crystalline; the particles are spherical and porous. At a molecular level, PGC is made up of intertwined ribbons of carbon. Each ribbon consists of 30 sheets spaced 3.4 Å apart. Each sheet is made up of hexagonally arranged carbon atoms linked by 1.5 order bonds.[112]

In polymer science, the vast majority of separations utilising carbon-based stationary phases are high temperature applications for the analysis of polyolefins. Macko and Pasch have separated polypropylene with respect to tacticity using high-temperature adsorption liquid chromatography.[68, 114] Ginzburg *et al.* carried out high temperature two-dimensional liquid chromatography separating polypropylene with respect to tacticity and molar mass.[115]

There have not been any reports on the chromatographic separation of polymers according to tacticity on carbon adsorbents at ambient temperature. In this study, solvent gradient interaction chromatography (SGIC) was used to separate stereoregular PMMAs with regard to

tacticity on a porous graphitic stationary phase at ambient temperature. This separation was coupled online to SEC for the separation of the PMMA fractions with respect to molar mass to carry out comprehensive two-dimensional liquid chromatography (LC x LC). This SGIC method will also be coupled online to $^{1}$H NMR to observe the triad tacticity distribution during elution.

# 3. Separation of polystyrene with respect to the isotope effect

## 3.1 Introduction

Deuterated compounds although on the expensive side, have found application in pharmacology,[31, 34] and water analysis.[33] Deuterated polymer scintillators,[35, 36] and as nuclear fusion targets.[37-40] Deuteration has been shown to affect the molecular volume and polarizability of the compounds. The differences in neutron scattering lengths of proton and deuterium have led to the characterization of deuterated compounds using various scattering techniques.[42-44, 46-48] The scattering techniques work on the basis that the thermodynamic parameters are not affected by deuteration which, has been proven to be incorrect by various authors using liquid chromatography.[6, 7, 53, 54]

Deuterated and hydrogenated polystyrene blends will be separated according to the isotope effect using LCCC. This chapter will be divided into two major sections, the first section will be on the LC x LC coupling experiments and the second section will be on LC-NMR hyphenation with $^{1}H$ and $^{2}H$ NMR detection of deuterated and hydrogenated polystyrene homopolymer blends.

For the LC x LC experiments, the first dimension separation will be according to the isotope effect using LCCC and the second dimension separation according to molar mass using SEC. For the LCCC-NMR experiments, the isotopic separation will be observed online with $^{1}H$ or $^{2}H$ NMR detection. The LC x LC results present in this section have been published.[116]

Figure 13 shows the different polystyrene sample sets used in this study.

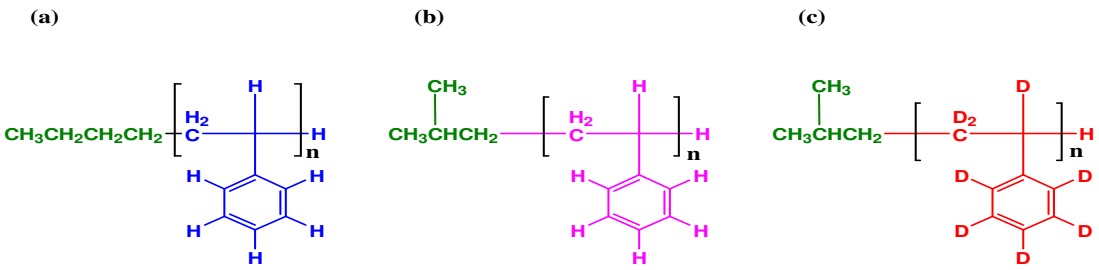


*Figure 13: (a) Hydrogenated PS with n-butyl end group, (b) Hydrogenated PS with a secondary butyl end group and (c) Deuterated PS with secondary butyl end group.*

## 3.2 Experimental section

Three instruments were used for these experiments. The first was an Alliance 2690 HPLC system (Waters Corporation, Milford, USA) used for establishing critical conditions by changing the solvent composition. The second was an Agilent 1200 HPLC system (Agilent technologies, Boeblingen, Germany) used for establishing critical conditions by changing the column temperature. The third was an Agilent 1100/1200 HPLC system (Agilent technologies, Boeblingen, Germany) used for the LC-NMR coupling experiments. All the instruments were equipped with a quaternary pump, auto-sampler, thermostatted column compartment and a UV detector. The first two instruments also had an isocratic pump which was used for the LC x LC coupling experiments and an ELS detector. The processing and recording was carried out with WinGPC software (Polymer Standards Service GmbH, Mainz, Germany) and Origin 7.5. All the NMR spectra were acquired on a Bruker advance DRX 500 Mhz spectrometer (Bruker Biospin GmbH, Rheinstetten, Germany) with a triple resonance flow probe TXi with an active detection volume of 60 µL.

### 3.2.1 Samples

Samples were products of Polymer Laboratories (Church Stretton, England) and Polymer Standards Service GmbH (Mainz, Germany). All samples were synthesised via anionic polymerization using either hydrogenated or deuterated styrene in THF at -78˚C as shown in Figure 14. The initiators used were n-butyl lithium and secondary butyl lithium for the PL and PSS samples, respectively.

Polystyrene homopolymer data as given by each manufacturer is provided in Tables 1 – 3.

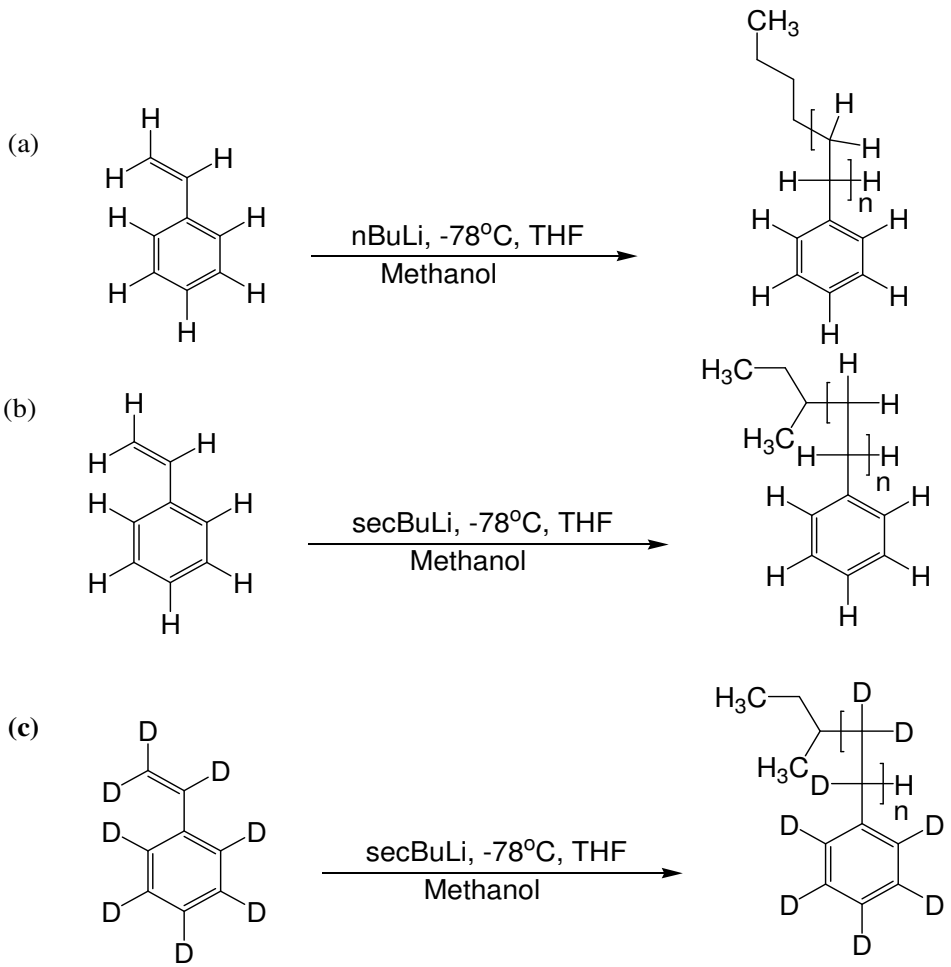


*Figure 14: Synthesis of polystyrene homopolymers (a) PL h-PS, (b) PSS h-PS and (c) PSS d-PS.*

*Table 1: PL hydrogenated polystyrene homopolymer sample overview.*

| Label | $M_p$ (g/mol) | $M_w$ (g/mol) | $M_n$ (g/mol) | PDI |
|---|---|---|---|---|
| **h-PS 2590** | 2590 | 2590 | 2480 | 1.04 |
| **h-PS 5120** | 5120 | 5090 | 4960 | 1.03 |
| **h-PS 10210** | 10210 | 10290 | 10070 | 1.02 |
| **h-PS 19640** | 19640 | 19620 | 19210 | 1.02 |
| **h-PS 38640** | 38640 | 38680 | 37730 | 1.03 |
| **h-PS 72450** | 72450 | 71700 | 70600 | 1.02 |
| **h-PS 132900** | 132900 | 132900 | 131400 | 1.01 |
| **h-PS 275300** | 275300 | 285300 | 273100 | 1.04 |

*Table 2: PSS deuterated polystyrene homopolymer sample overview.*

| Label | $M_p$ (g/mol) | $M_w$ (g/mol) | $M_n$ (g/mol) | PDI |
|---|---|---|---|---|
| **d-PS 2090** | 2090 | 2090 | 1980 | 1.06 |
| **d-PS 5750** | 5750 | 5940 | 5660 | 1.05 |
| **d-PS 15900** | 15900 | 16000 | 15700 | 1.02 |
| **d-PS 28400** | 28400 | 27100 | 25600 | 1.06 |
| **d-PS 49000** | 49000 | 49400 | 48100 | 1.03 |
| **d-PS 112000** | 112000 | 111000 | 109000 | 1.02 |
| **d-PS 211000** | 211000 | 211000 | 208000 | 1.01 |
| **d-PS 658000** | 658000 | 598000 | 540000 | 1.11 |

*Table 3: PSS hydrogenated polystyrene homopolymer sample overview.*

| Label | $M_p$ (g/mol) | $M_w$ (g/mol) | $M_n$ (g/mol) | PDI |
|---|---|---|---|---|
| **h-PS 680** | 680 | 641 | 707 | 1.10 |
| **h-PS 1820** | 1820 | 1770 | 1920 | 1.08 |
| **h-PS 3470** | 3470 | 3260 | 3460 | 1.06 |
| **h-PS 5440** | 5440 | 5270 | 5610 | 1.06 |
| **h-PS 12600** | 12600 | 12000 | 12500 | 1.04 |
| **h-PS 28000** | 28000 | 26600 | 27500 | 1.03 |
| **h-PS 54000** | 54000 | 50000 | 51500 | 1.03 |
| **h-PS 130000** | 130000 | 120000 | 125000 | 1.04 |
| **h-PS 277000** | 277000 | 265000 | 271000 | 1.02 |

### 3.2.2 One-dimensional HPLC experiments

Two types of stationary phases were tested for establishing critical conditions, i.e. Nucleosil silica and Nucleosil $C_{18}$ modified silica. Both stationary phases were from Macherey-Nagel, Düren, Germany. They both had the following dimensions, 5 µm particle size, 300 Å pore size, 250 mm length and 4.6 mm internal diameter. The concentration of the samples was 0.5 mg/mL, with an injection volume of 10 µL. The flow rate used was 0.5 mL/min.

#### *3.2.2.1 Solvent composition experiments*

The solvent varying experiments were carried out on instrument 1 with solvent mixing by pump. The column temperatures were kept constant as follows. The column temperature was set at 31.5˚C for the Nucleosil Silica stationary phase with an eluent composition of THF/cyclohexane which was varied to establish critical conditions for d-PS. The column temperature was set at 30˚C for the Nucleosil $C_{18}$ stationary phase with an eluent composition of THF/ACN which was also varied to establish critical conditions for h-PS.

#### *3.2.2.2 Column temperature experiments*

The column temperature experiments were carried out on instrument 2, on the Nucleosil $C_{18}$ stationary phase. The column temperature was varied while the eluent composition of THF/ACN was kept constant at 47/53 (v/v).

### 3.2.3 Comprehensive two-dimensional liquid chromatography experiments

The concentration of the samples injected in the first dimension was 10 mg/mL, with an injection volume of 50 µL. The first dimension separated according to the isotope effect using either the Nucleosil Silica or Nucleosil $C_{18}$ stationary phase, dimensions specified in the previous section.

#### *3.2.3.1. Solvent composition experiments*

The flow rate used for the first dimension was 0.04 mL/min. An eight port valve system (VICI Valco instruments, Texas, USA) consisting of two 100 µL storage loops was used. The first dimension separated according to the isotope effect details provided in section 3.2.2.1. The second dimension separated according to molar mass using THF as an eluent on a styrene-divinylbenzene (SDVB) stationary phase with the following dimensions, 5 µm particle size, 50 mm length and 20 mm internal diameter. The flow rate used for the second dimension was 4.5 mL/min. The ELSD was used as a second dimension detector, nitrogen was nebulizing gas, the nebulising temperature was 70˚C and the evaporating temperature was 110˚C. These experiments were carried out on instrument 1.

#### *3.2.3.2 Column temperature experiments*

The flow rate used for the first dimension was 0.02 mL/min. The eight port valve system (VICI Valco instruments, Texas, USA) consisting of two 50 µL storage loops was used. The first dimension separated according to the isotope effect details provided in section 3.2.2.2.The second dimension separated according to molar mass using THF as an eluent and a styrene-divinylbenzene (SDVB) stationary phase with the following dimensions, 5 µm particle size, 50 mm length and 20 mm internal diameter. The flow rate used for the second dimension was 4.5 mL/min. The ELSD was used as a second dimension detector, nitrogen was nebulizing gas, with a pressure of 3.0 bars, and the nebulising temperature was 90˚C.These experiments were carried out on instrument 2.

### 3.2.4 On-flow LC-NMR hyphenation experiments

#### *3.2.4.1. SEC-NMR experiments*

Each of the samples in the blends had an average concentration of 2 mg/mL. THF was used as a solvent at a flow rate of 0.2 mL/min with an injection volume of 100 µL for both the $^{1}$H-NMR and $^{2}$H-NMR detection experiments. The SEC experiments were performed on three PSS SDVB 5 µm columns (a guard column, and three columns, $10^{2}$, $10^{3}$ and $10^{5}$ Å with the following dimensions, 300 mm length and 8 mm internal diameter). The on-flow SEC-$^{1}$H NMR experiments were carried out at 8 transients per FID, with an acquisition time of 0.6816 s, a relaxation time of 1 s and a spectral width of 12 ppm. The data were Fourier transformed using 16 Kb data points with an exponential line broadening of 5 Hz. The on-flow SEC-$^{2}$H NMR experiments were carried out at 72 transients per FID, acquisition time of 0.2229 s, a relaxation time of 0.0771 s and a spectral width of 15 ppm. The data were Fourier transformed using 8 Kb data points with an exponential line broadening of 10 Hz.

#### *3.2.4.2 HPLC-NMR experiments*

The h-PS standards had a concentration range of 2.9 – 3.4 mg/mL, while the d-PS standards had a concentration range of 4.8 – 5.8 mg/mL. A solvent composition of THF/ACN 47/53 (v/v) was used at a flow rate of 0.5 mL/min and an injection volume of 50 µL for both proton and deuterium detection experiments. The HPLC experiments were performed on a Nucleosil $C_{18}$ 300 Å Macherey-Nagel (Düren, Germany) with the following dimensions, 250 mm length and 4.6 mm internal and a 5 µm particle size. The on-flow HPLC-$^{1}$H NMR experiments were carried out at 16 transients per FID, an acquisition time of 0.58496 s, a relaxation time of 0.09667 s and a spectral width of 14 ppm. The data were Fourier transformed using 32 Kb data points with an exponential line broadening of 5 Hz. The on-flow HPLC-$^{2}$H NMR experiments were carried out at 64 transients per FID, with an acquisition time of 0.1389 s, a relaxation time of 0.0111 s and a spectral width of 12 ppm. The data were Fourier transformed using 8 Kb data points with an exponential line broadening of 10 Hz.

## 3.3. Results and discussion

The molar masses of the samples ranged from 2000 to 112000 g/mol. The molar masses of the blends used in this section are summarised in Table 4. The blends consisted of equal amounts of each homopolymer present in that blend.

*Table 4: Molar masses of the blends of PL h-PS and PSS d-PS homopolymers for LC x LC experiments.*

| Blend Labels | $M_p$ of d-PS (g/mol) | $M_p$ of h-PS (g/mol) |
|---|---|---|
| B1 | 15900 | 19640 |
| B2 | 15900 | 10210 |
| B3 | 28400 | 38640 |
| B4 | 49000 | 38640 |
| B5 | 49000 | 72450 |
| B6 | 112000 | 72450 |
| QT1 | 49000; 112000 | 38640; 72450 |

B – Binary; QT - Quaternary

### 3.3.1 One dimensional liquid chromatography

The critical conditions for d-PS were established on a silica column while, the critical conditions for h-PS were established on a $C_{18}$ modified silica column, this was due to the fact that d-PS has been shown to be more polar than h-PS, due to the increased electron donating ability of the C-D bond as compared to the C-H bonds.[41]

Figure 15 (a) shows the different separation modes of h-PS in a mixture of THF/ACN on a Nucleosil $C_{18}$ stationary phase at a column temperature of 31.5˚C. The critical conditions for the h-PS homopolymers were established at solvent composition of THF/ACN 49.5/50.5 (v/v). Figure 15 (b) shows that under the critical conditions of h-PS, the d-PS homopolymers eluted in SEC mode.

### *3.3.1.1 LCCC by varying solvent composition*

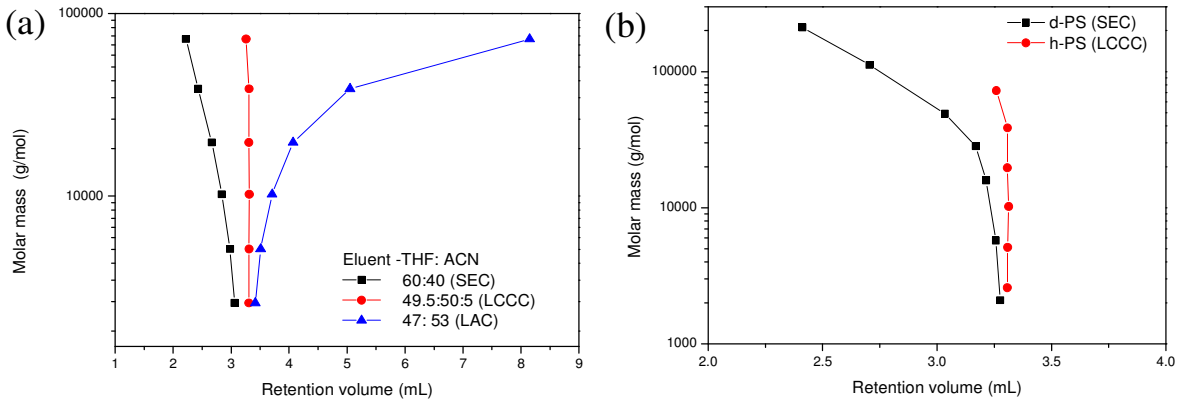


*Figure 15: (a) Plot showing the different separation modes of PL h-PS in various solvent compositions of THF/ACN [■ SEC 60/40; ● LCCC 49.5/50.5; ▲ LAC 47/53 (v/v)] (b) Plot showing PL h-PS in LCCC mode (●) and PSS d-PS in SEC mode (■)in a solvent composition of THF/ACN 49.5/50.5 (v/v) on a Nucleosil $C_{18}$ stationary phase at a flow rate of 0.5 mL/min and column temperature of 30°C using instrument 1.*

The efficiency of the separation was tested with two binary blends. An improvement in separation was observed with an increase in molar mass as shown by Figure 16. This improvement in the separation is due to the elution of the d-PS homopolymers in SEC mode due to the entropic contributions dominating over the enthalpic contributions. This leads to the longer d-PS polymers being excluded from the pores of the stationary phase and eluting earlier than the shorter d-PS polymers thereby, improving separation for higher molar mass blends as shown by Figure 15 (b).

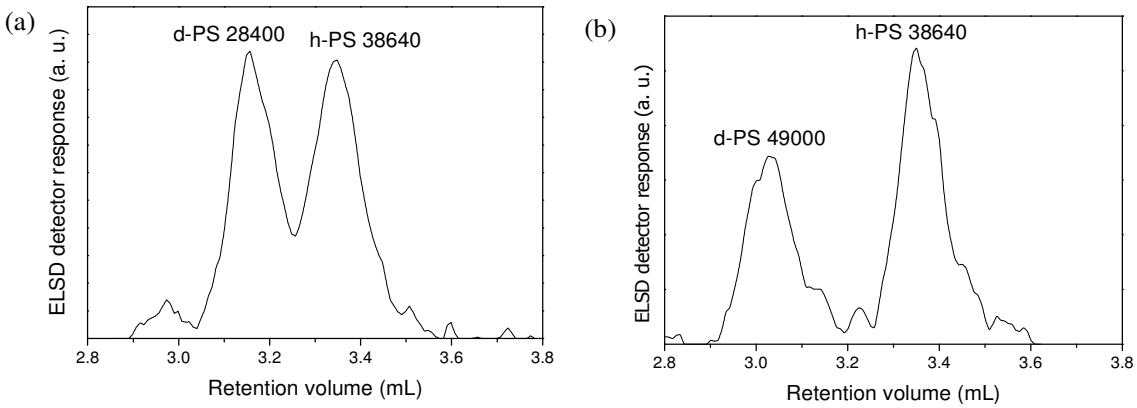


*Figure 16: ELSD chromatograms of two binary blends at the critical conditions of PL h-PS in a solvent composition of THF/ACN 49.5/50.5 (v/v) on a Nucleosil $C_{18}$ stationary phase at a flow rate of 0.5 mL/min and column temperature of 30°C using instrument 1.*

Figure 17 (a) shows the different separation modes of d-PS in a mixture of THF/cyclohexane on a Nucleosil Silica stationary phase at a column temperature of 30˚C. The critical conditions

for the d-PS homopolymers were established at solvent composition of THF/cyclohexane 23/77 (v/v). Figure 17 (b) shows that under the critical conditions of d-PS, the h-PS homopolymers eluted in SEC mode.

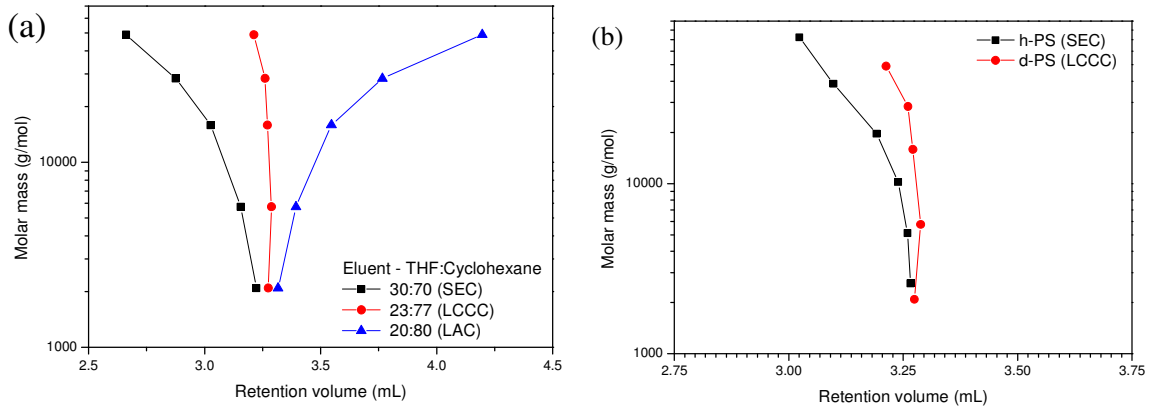


*Figure 17: (a) Plot showing the different separation modes of PSS d-PS in various solvent compositions of THF/Cyclohexane [■ SEC 30/70; ● LCCC 23/77; ▲ LAC 20/80 (v/v)] (b) Plot showing PSS d-PS in LCCC mode (●) and PL h-PS in SEC mode (■) in a solvent composition of THF/Cyclohexane 23/77 (v/v) on a Nucleosil silica stationary phase at a flow rate of 0.5 mL/min and column temperature of 31.5°C using instrument 1.*

The efficiency of the separation was tested using two binary blends. Comparing the separation of the components of blend 3, the separation observed was poorer on the Nucleosil silica stationary phase (Figure 18(a)) than that observed on the Nucleosil $C_{18}$ stationary phase (Figure 16 (a)).

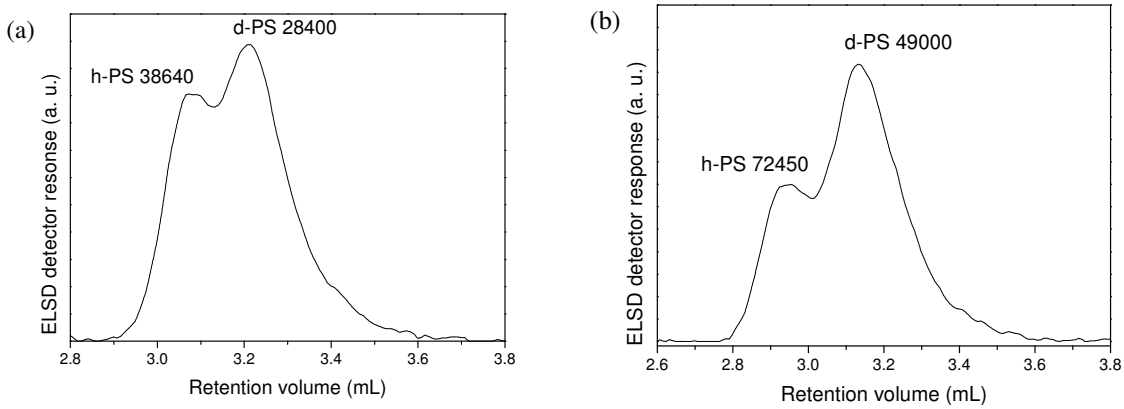


*Figure 18: ELSD chromatograms of two binary blends on at the critical conditions of PSS d-PS at a solvent composition of THF/Cyclohexane 23/77 (v/v) on a Nucleosil silica stationary phase at a flow rate of 0.5 mL/min and column temperature of 31.5°C using instrument 1.*

### *3.3.1.2 LCCC experiments by varying column temperature*

The critical conditions for both the d-PS and h-PS homopolymers were established on the Nucleosil $C_{18}$ stationary phase because of the improved separation that was observed in the previous solvent varying experiments. The solvent composition was kept constant at THF/ACN 47/53 (v/v) and the column temperature was varied to establish the different critical conditions. Figure 19(a) shows the critical conditions of d-PS homopolymers established at a column temperature of 41˚C. As seen previously with the solvent composition experiments, under the critical condition of d-PS homopolymers, the h-PS homopolymers eluted in LAC mode. Figure 19 (c) shows the critical conditions of h-PS homopolymers established at a column temperature of 54˚C. Under these conditions the d-PS homopolymers eluted in SEC mode. During the critical conditions experiments the conditions observed in Figure 19 (b) were established at a column temperature of 45˚C. At these conditions the d-PS homopolymers eluted in SEC mode while the h-PS homopolymers eluted in LAC mode.

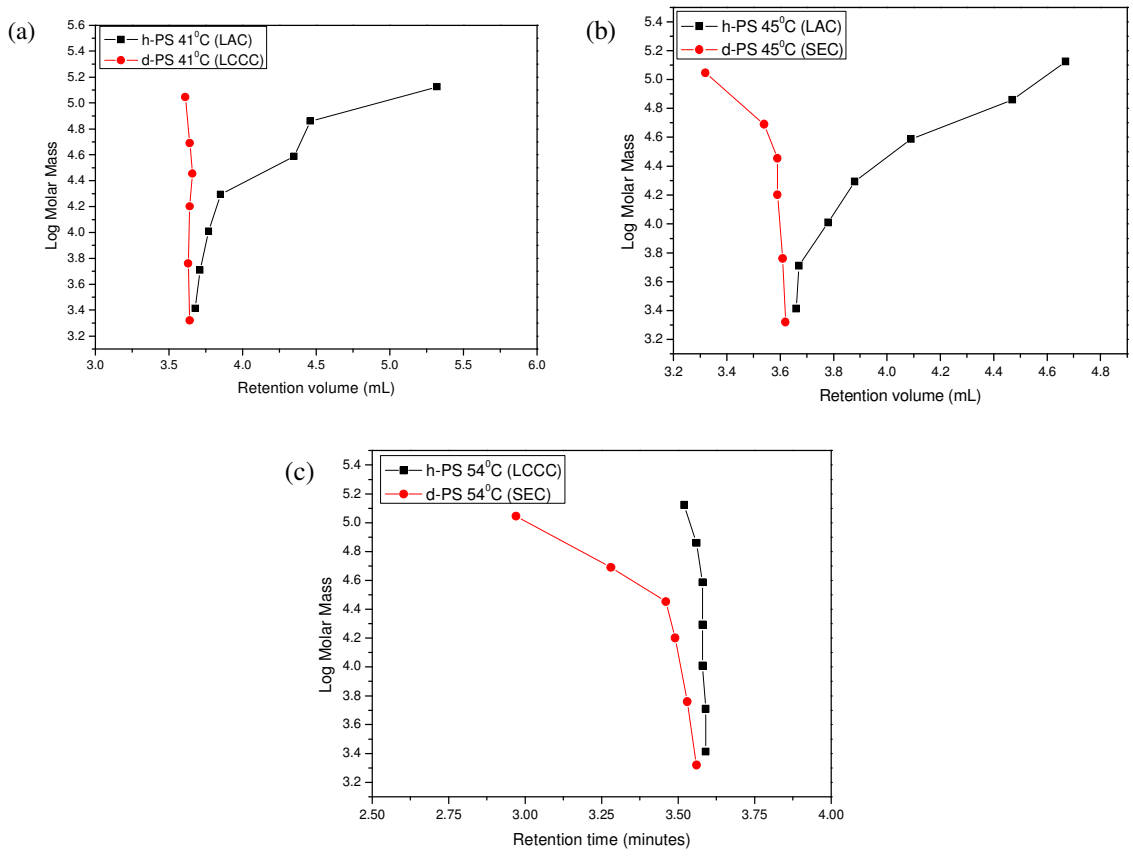


*Figure 19: a) Plot showing PSS d-PS LCCC mode (●) and PL h-PS in LAC mode (■);(b) Plot showing PSS d-PS SEC mode (●) and PL h-PS in LAC mode (■) (c) Plot showing PL h-PS LCCC mode (●) and PSS d-PS in SEC mode (■); the column temperatures of the different conditions were 41°C, 45°C and 54°C, respectively. The eluent was THF/ACN 47/53 (v/v) on a Nucleosil $C_{18}$ stationary phase at a flow rate of 0.5 mL/min using instrument 2.*

Binary blends 4 and 6 were injected to test the efficiency of the separation under the three sets of conditions shown in Figure 19. Figure 20 shows the two binary blends under the critical conditions of d-PS homopolymers; Figure 21 shows the same binary blends at SEC-LAC conditions while Figure 22 shows the same binary blends at the critical conditions of h-PS homopolymers. The separation observed for the critical conditions of d-PS on the Nucleosil $C_{18}$ column (Figure 20) was much better than that observed Nucleosil Silica column (Figure 18). For both binary blends under the three sets of conditions we were able to sufficiently separate and identify each of the binary blend components. An increase in the molar mass of the blend components led to an improvement in the observed separation.

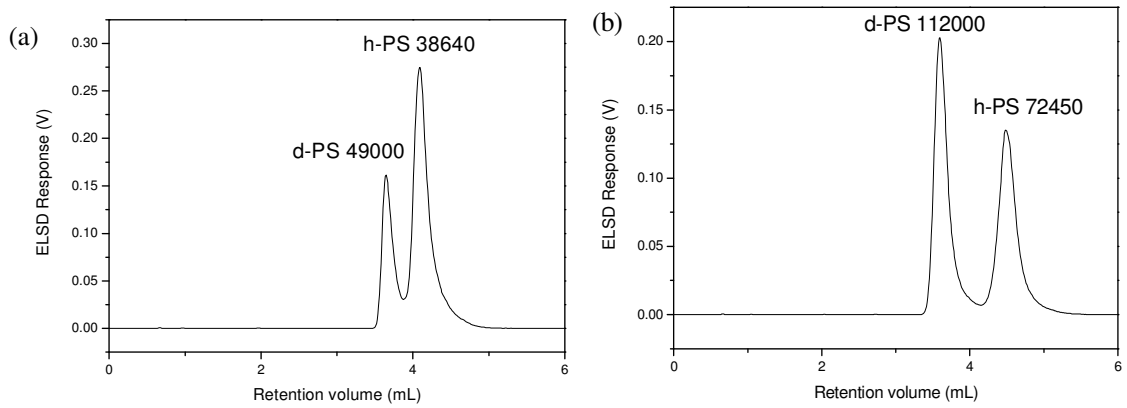


*Figure 20: ELSD chromatograms of binary blends (a) B4 and (b) B6 at LCCC of PSS d-PS at a column temperature of 41°C, eluent composition of THF/ACN 47/53(v/v) and a flow rate of 0.5 mL/min on a Nucleosil $C_{18}$ stationary phase using instrument 2.*

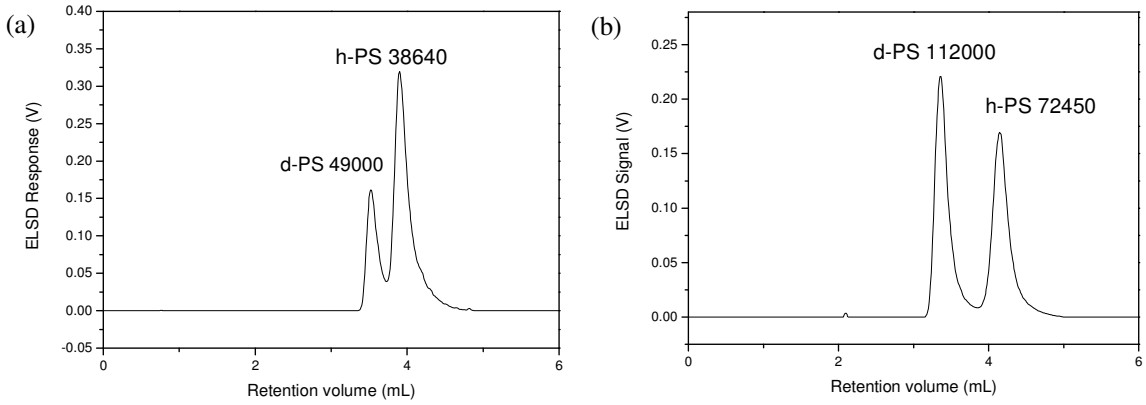


*Figure 21: ELSD chromatograms of binary blends (a) B4 and (b) B6 at SEC-LAC conditions of PSS d-PS and PL h-PS at a column temperature of 45°C, eluent composition of THF/ACN 47/53(v/v) and a flow rate of 0.5 mL/mi on a Nucleosil $C_{18}$ stationary phase using instrument 2.*

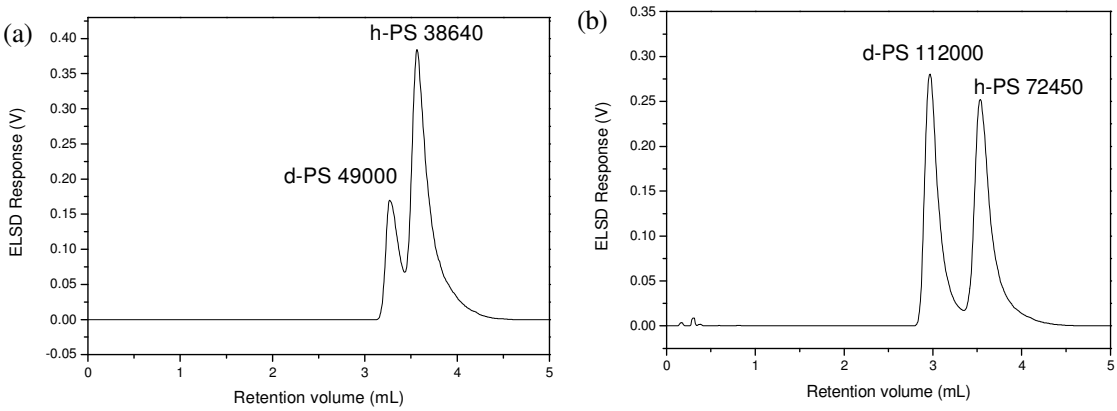


*Figure 22: ELSD chromatograms of binary blends (a) B4 and (b) B6 at LCCC conditions of PL h-PS and at a column temperature of 54°C, eluent composition of THF/ACN 47/53 (v/v) and a flow rate of 0.5 mL/min on a Nucleosil $C_{18}$ stationary phase using instrument 2.*

## 3.3.2. Comprehensive two-dimensional liquid chromatography (LC x LC)

To obtain a comprehensive picture on the isotopic and molar mass separation, two-dimensional experiments were carried out. The first dimension shows the separation with respect to the isotope effect on the y-axis while the second dimension shows separation with respect to the molar mass on the x-axis.

### *3.3.2.1 Solvent composition experiments*

The efficiency of the LC x LC separation for the solvent composition experiments on the Nucleosil $C_{18}$ stationary phase was tested with two binary blends. Figure 23 shows that the separation of the components of blend 3 was not sufficient to identify the blend components as well as to determine their molar mass distributions. The separation of the higher molar mass blend 4 was slightly improved which, allowed for the identification of the blend components and the determination their molar mass distributions.

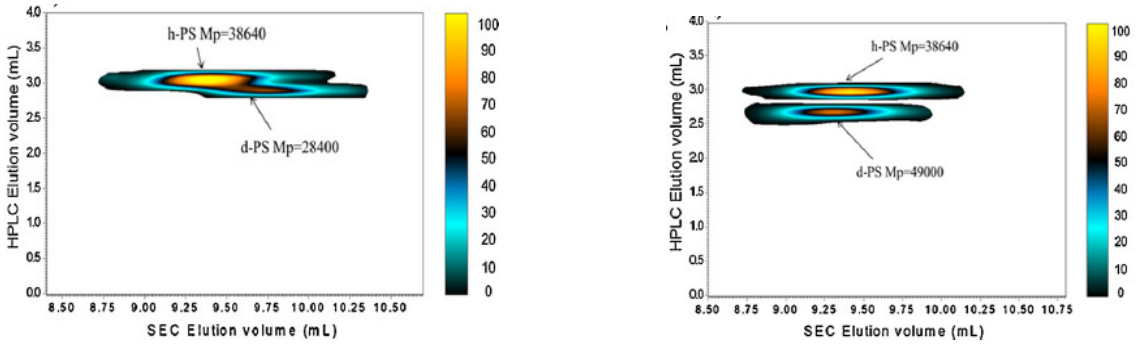


*Figure 23: LC x LC contour plots of two binary blends; B3 and B4 analysed in the first dimension at the critical conditions of PL h-PS in a solvent composition of THF/ACN (49.5/50.5) on a Nucleosil $C_{18}$ stationary phase at a flow rate of 0.04 mL/min and column temperature of 30°C and in the second dimension in THF at room temperature on a SDVB stationary phase at a flow rate of 4.5 mL/min using instrument 1.*

The efficiency of the LC x LC separation for the solvent composition experiments on the Nucleosil silica stationary phase was tested with two binary blends. Figure 24 shows the LC x LC contour plots for blends 3 and 4. The separation of the components of blend 3 and 4 was not sufficient for the identification the blend components as well as for the determination of their molar mass distributions.

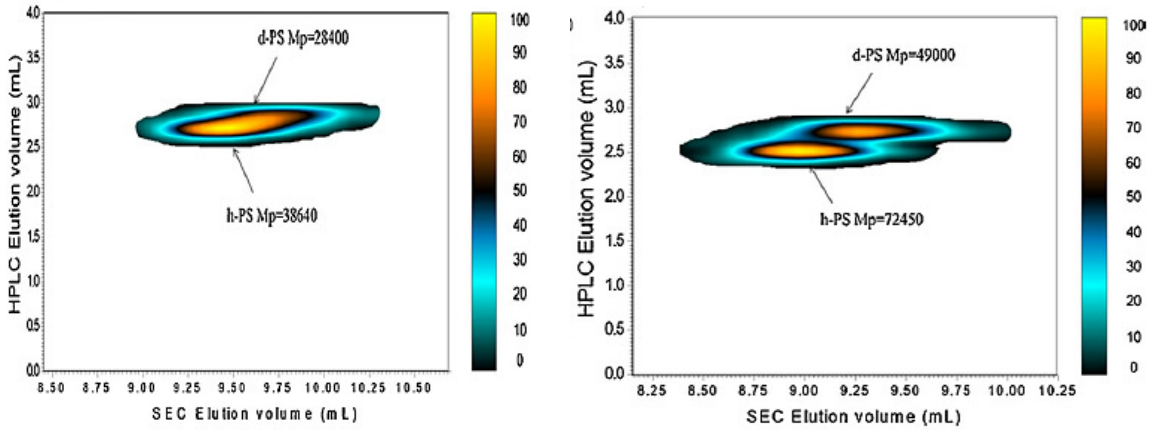


*Figure 24: LC x LC contour plots of two binary blends B3 and B4, respectively, analysed in the first dimension at the critical conditions of PSS d-PS in a solvent composition of THF/Cyclohexane 23/77 (v/v) on a Nucleosil silica stationary phase at a flow rate of 0.04 mL/min and a column temperature of 31.5°C and in the second dimension in THF at room temperature on a SDVB stationary phase at a flow rate of 4.5 mL/min using instrument 1*

### *3.3.2.2 Column temperature experiments*

An improved separation was observed under SEC-LAC conditions at a column temperature of 45˚C for the high molar mass blends. This separation was better due to the fact that the d-PS homopolymers were eluting in SEC mode and the h-PS homopolymers were eluting in LAC mode. The efficiency of the LC x LC experiments was tested with two binary blends and one quaternary blend. Figure 25 (a, b) shows the LC x LC contour plots of the binary blends. For both binary blends we were able to identify the components and determine their molar

distributions. Figure 25 (c) shows the LC x LC contour plot of the quaternary blend; all four blend components could be identified. We could also observe the different modes of separation of the d-PS and h-PS homopolymers.

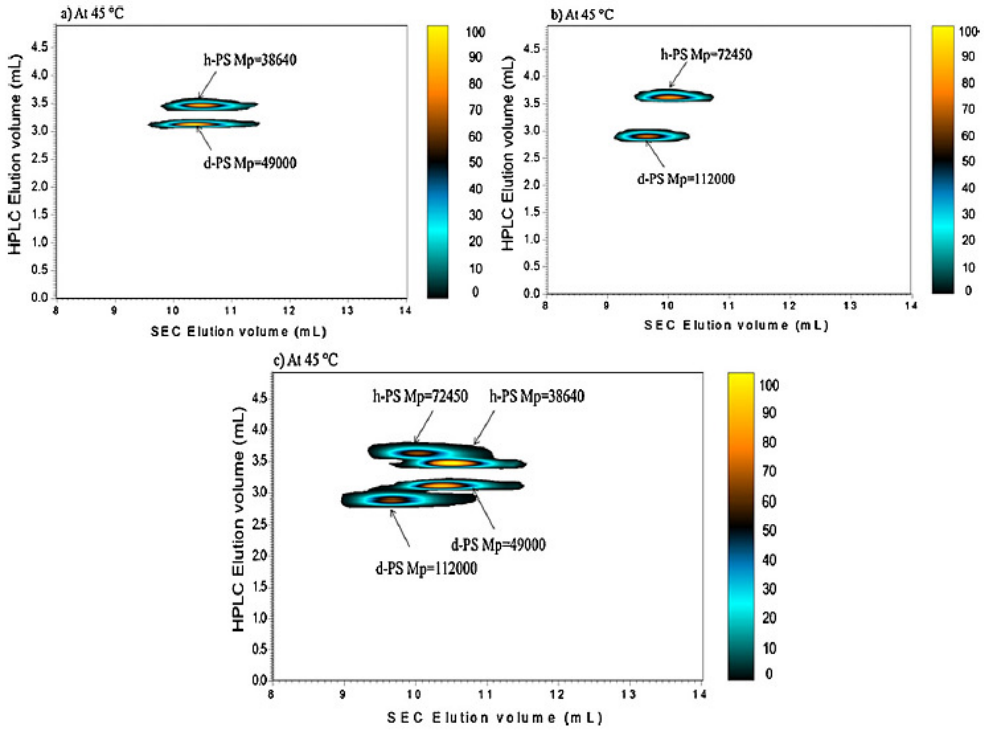


*Figure 25: a) LC x LC contour plot of binary blend B4 (b) LC x LC contour plot of binary blend B6 (c) LC x LC contour plot of quaternary blend QT1; analysed in the first dimension conditions under SEC-LAC conditions of PSS d-PS and PL h-PS in an eluent composition of THF/ACN 47/53 (v/v) on a Nucleosil $C_{18}$ stationary phase at a flow rate of 0.02 mL/min and column temperature of 45°C and in the second dimension in THF at room temperature on a SDVB stationary phase at a flow rate of 4.5 mL/min using instrument 2.*

### 3.3.3 On-flow LC – NMR hyphenation

The developed HPLC methods were coupled online to proton and deuterium NMR for the observation of the isotope distribution with elution. The $^{2}H$ spectrum produced broader signals as compared to the $^{1}H$ spectrum because $^{2}H$ nucleus is a quadrupole nucleus. The longitudinal relaxation times of $^{2}H$ nuclei are shorter than for the $^{1}H$ nuclei, allowing for fast pulse repetitions.[117] The lock coil was used for the $^{2}H$ detection and because this coil was designed to detect large solvent signals and not small analyte signals, the sensitivity of the d-PS homopolymers was quite low. This problem was overcome by increasing the concentration of the d-PS homopolymers as compared to the h-PS homopolymers.

Before LC-NMR hyphenation experiments could be carried out, care should was taken in selecting chromatographic solvents. The signals of these solvents did not overlap with the signals of the analyte. Figure 27 shows the LC-NMR contour plot of PL h-PS 2590 dissolved in THF/ACN at a ratio of 47/53 (v/v) and analysed at the conditions shown on the figure caption. WET solvent suppression was applied to both the signals of THF and ACN. The solvent suppression of ACN was employed at 1.94 ppm while the suppression of THF resonances was employed at 1.72 ppm as well as between the ranges of 3.4 – 3.9 ppm. Signals observed at 2.4 and 5.4 ppm are due to impurities in the solvent since they are constant throughout the chromatogram. The remaining signals are assigned according to Figure 26, the aromatic signals at region of 6.5 – 7.65 ppm are assigned numbers 4-8, the backbone signals at regions 1.4 and 2.4 ppm are assigned numbers 2- 3 and the end group signals at region 0.4 – 1.2 ppm are assigned the number 1. For the sake of clarity, when multiple contour plots are overlaid either the end group region at 0.5 – 1.2 ppm or the aromatic region at 6.5 – 7.5 ppm will be shown.

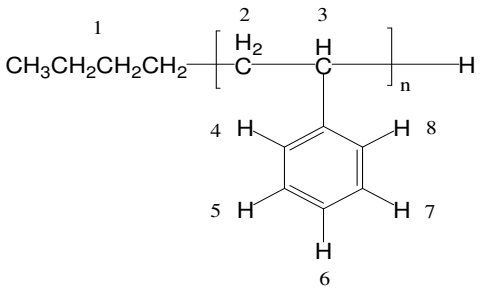


*Figure 26: Structure of PL h-PS 2590 homopolymer.*

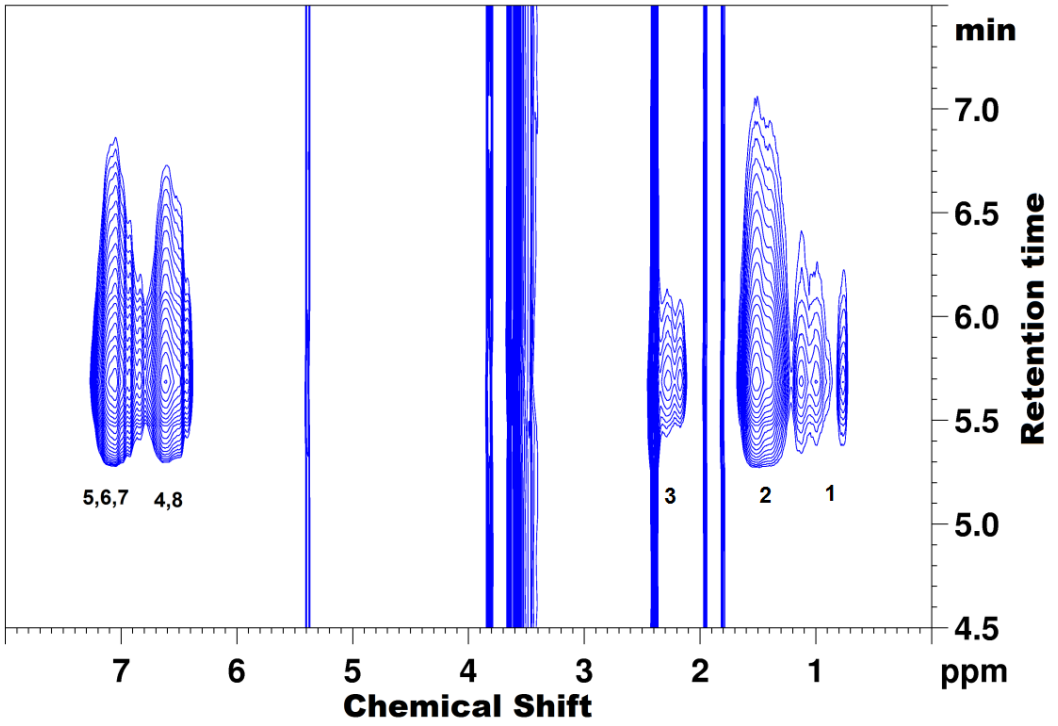


*Figure 27: Full on-flow LC-$^1$H-NMR contour plot of PL h-PS 2590 with a concentration of 3 mg/mL in a solvent composition of THF/ACN 47/53 (v/v) at a flow rate of 0.5 mL/min and a column temperature of 40°C on a Nucleosil $C_{18}$ stationary phase with assignments according to Figure 26.*

Figures 28 (a) and (b) highlight the advantages of LC-NMR hyphenation. Figure 28(a), shows the partial LC-NMR contour plot of two homopolymers, one hydrogenated and the other deuterated with focus on the end group region. These low molar mass homopolymers with comparable molar masses co-elute in the chromatographic dimension at a retention time of 5.7 minutes and have the same end groups as observed in the region 0.5 – 1.2 ppm where there is total overlap of the end group signals. The two homopolymers could be differentiated by making use of $^1$H NMR detection where the hydrogenated homopolymer has a signal at the backbone region between 1.3 – 1.6 ppm while the deuterated homopolymer had no backbone signal at all.

In Figure 28 (b), two homopolymers, both hydrogenated with comparable molar masses differing only in the end group due to the type of initiator used, could be differentiated from each other by using $^1$H NMR detection. Similar to Figure 28 (a), these low molar homopolymers with comparable molar masses also co-elute in the chromatographic dimension at a retention time of 5.7 minutes and because the two homopolymers are both hydrogenated, the use of $^1$H NMR detection allows the observation of the backbone signals for both homopolymers at a region of 1.3 – 1.6 ppm. The two homopolymers could be differentiated at the region of 0.5 – 1.2 ppm where there is a difference in the observed end

group signals showing the differences in the type of end groups present in the two homopolymers.

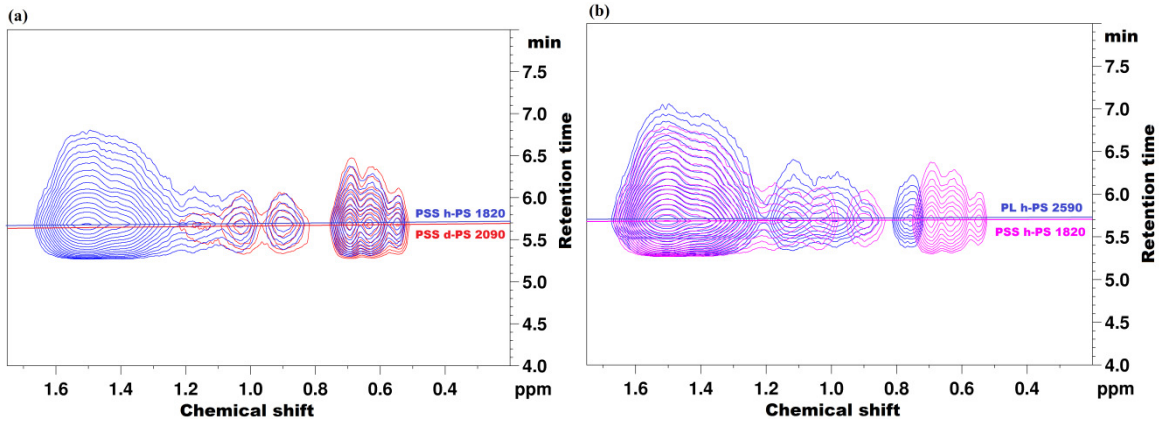


*Figure 28: LC-NMR contour plots with focus on the backbone and end group regions (a) PSS h-PS 1820 and PSS d-PS 2090 (b) PL h-PS 2590 and PSS h-PS 1820 in a solvent composition of THF/ACN 47/53 (v/v) at a flow rate of 0.5 mL/min and a column temperature of 40°C on a Nucleosil $C_{18}$ stationary phase.*

These low molar mass samples could not be differentiated with chromatography alone but they could easily be differentiated with LC-NMR hyphenation.

### *3.3.3.1 SEC-NMR*

SEC-NMR with $^{1}H$ and $^{2}H$ detection was used to observe hydrogenated and deuterated polystyrenes, respectively. SEC-NMR was carried out in hydrogenated THF without lock solvent. In the case of SEC-$^{2}H$-NMR experiments, no solvent suppression was employed due to the low natural abundance of the $^{2}H$ nuclei. The on-flow SEC-NMR contour plots for both the hydrogenated and deuterated polystyrenes show the expected elution order from high to low molar masses with increasing elution time.

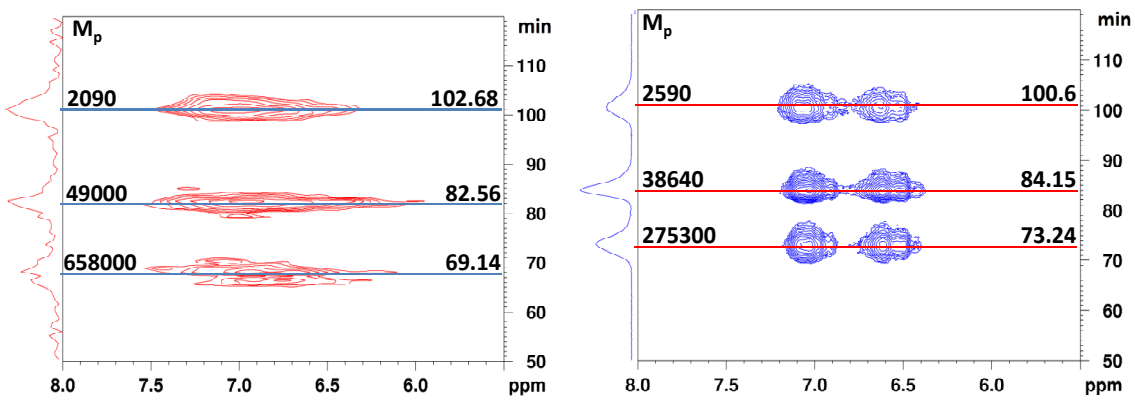

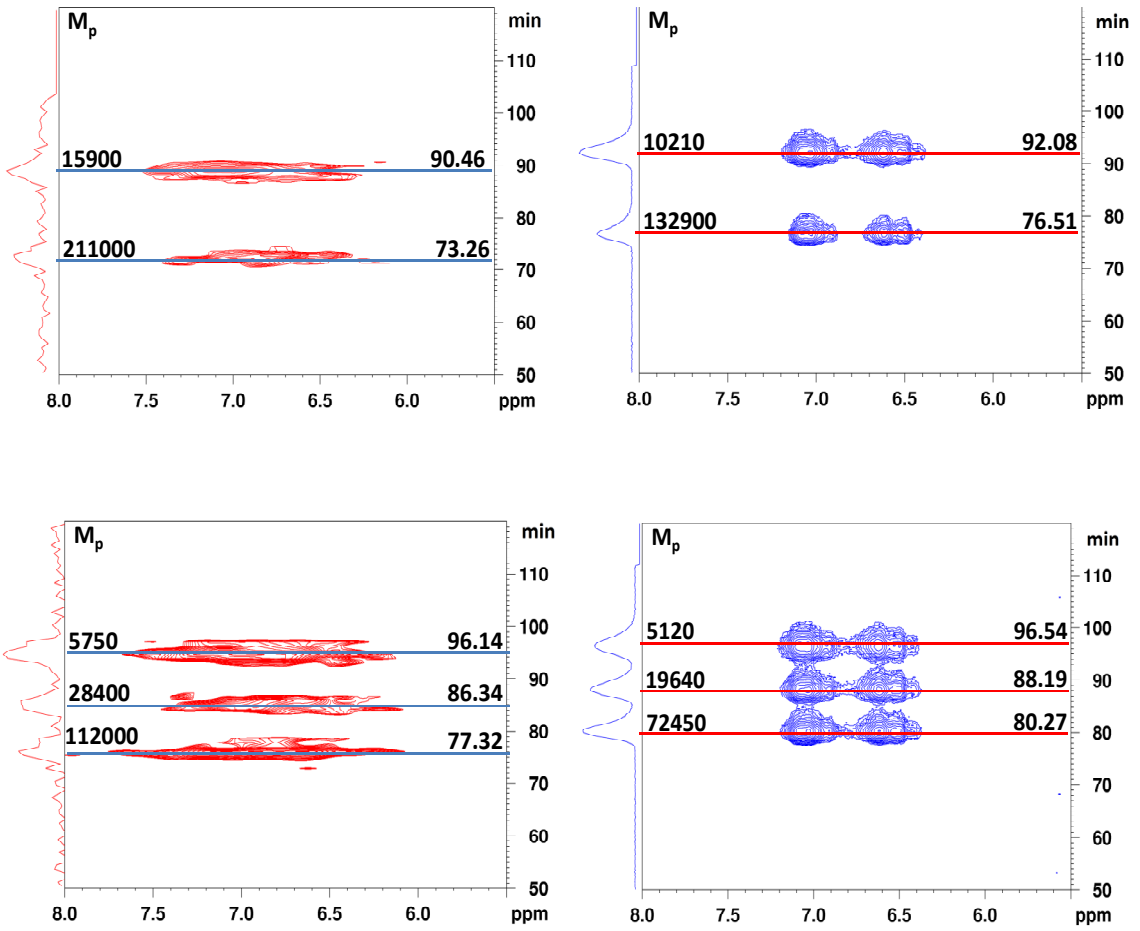


*Figure 29: On-flow SEC-$^{2}$H-NMR contour plots of d-PS (PSS) in red versus SEC-$^{1}$H-NMR contour plots of h-PS (PL) in blue showing the aromatic signals of various molar masses with projections on the y-axis showing the chromatographic elution time. All molar masses are in g/mol. All SEC experiments were carried out on three SDVB columns in 100% THF at room temperature and a flow rate of 0.2 mL/min.*

All the homopolymer standards were measured by SEC-NMR to prepare molar mass calibration curves. The results are shown in Figure 30 with the PSS d-PS calibration curve represented by the red line and the PSS h-PS calibration curve represented by the blue line. The are no significant differences between the two calibration curves that can be observed. Since in SEC, $\Delta S$ contributions are dominant over $\Delta H$ contributions, we can safely assume that the differences between the $\Delta S$ values of deuterated and hydrogenated polystyrenes are not sufficient to show differences in elution volumes.

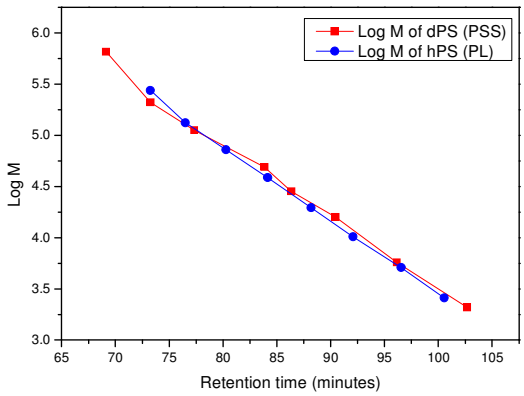


*Figure 30: A comparison of the calibration curves of PSS d-PS (red) and PSS h-PS (blue) as determined by $^{2}H$ and $^{1}H$ NMR detection.*

### *3.3.3.2 LCCC – NMR hyphenation*

Three sets of liquid chromatographic conditions coupled to $^{1}H$ and $^{2}H$ NMR were tested using binary blends of d-PS and h-PS homopolymers. The stationary phase used for all the chromatographic conditions in this section was a Nucleosil $C_{18}$ stationary at a solvent composition of THF/ACN 47/53 (v/v) which was kept constant while varying the column temperature to establish the various conditions. The experiments were carried out on instrument 3. The molar masses of the samples ranged from 1820 to 130000 g/mol. The molar masses of the blends used in this section are summarised in Table 5.

*Table 5: Molar masses of the blend components of PSS h-PS and PSS d-PS blends for LC-NMR experiments.*

| Blend Labels | $M_p$ of d-PS (g/mol) | $M_p$ of h-PS (g/mol) |
|---|---|---|
| B1 | 2090 | 1820 |
| B2 | 28400 | 28000 |
| B3 | 49000 | 54000 |
| B4 | 112000 | 130000 |

B – Binary

*3.3.3.2.1 LCCC of d-PS*

Figure 31 shows the analysis of d-PS homopolymers under critical conditions which were established at a column temperature of 43˚C. As observed previously in the LC x LC experiments, at the critical condition of d-PS homopolymers, the h-PS homopolymers eluted in LAC mode as shown by Figure 32(a, b).

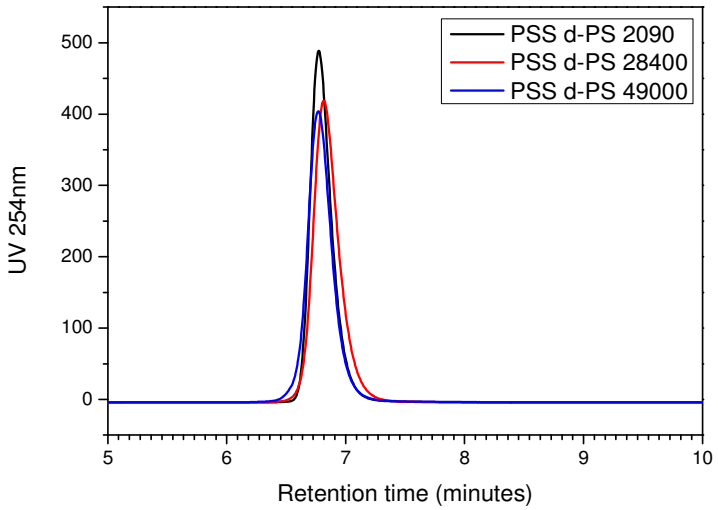


*Figure 31: Overlay of UV chromatograms of individual injections of d-PS homopolymers of various molar masses under the critical conditions of d-PS on a Nucleosil $C_{18}$ stationary phase in a solvent composition of THF/ACN 47/53 (v/v), column temperature of 43˚C and a flow rate of 0.5 mL/min.*

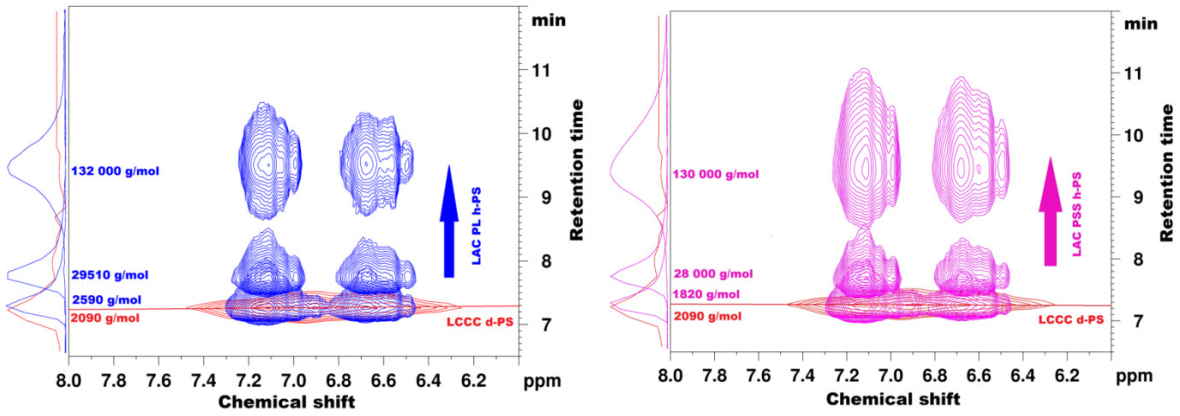


*Figure 32: Overlay of LC-NMR contour plots showing the aromatic region of (a) PL h-PS homopolymers (blue) and (b) PSS h-PS homopolymers (pink) under the critical conditions of PSS d-PS (red) on a Nucleosil $C_{18}$ stationary phase in a solvent composition of THF/ACN 47/53 (v/v) at a flow rate of 0.5 mL/min and a column temperature of 43˚C.*

The efficiency of the LC-NMR hyphenation was tested by injecting binary blends. Figure 33 shows the LC-NMR contour plots of the different blend injections at the critical conditions of PSS d-PS. An improvement in separation was observed with an increase in molar mass of the blend components. Although the chromatographic resolution was low for lower molar mass blends, the different blend components could still be identified by using the aromatic signals of the polystyrene at 6.2 – 7.4 ppm with $^{1}H$ and $^{2}H$ NMR detection.

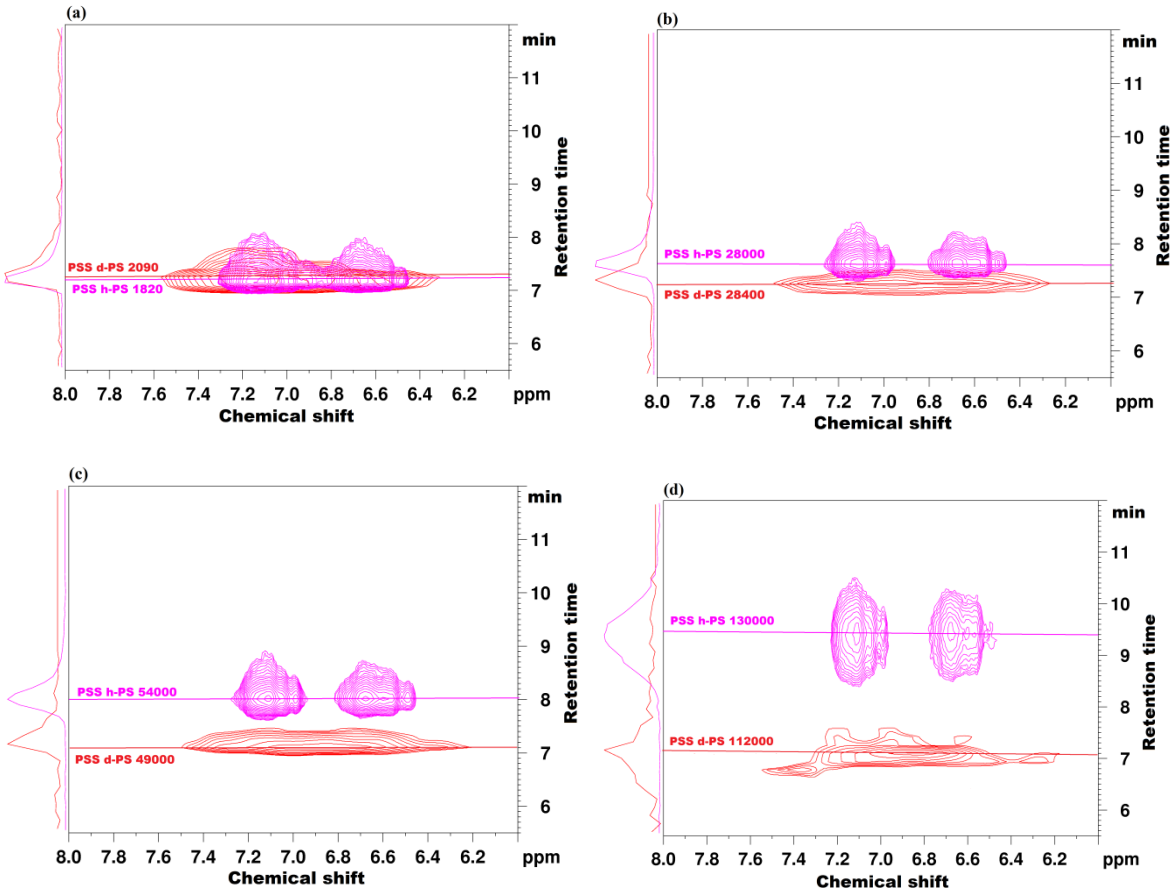


*Figure 33: An overlay of LC-NMR contour plots of four binary blends of PSS d-PS (red) and PSS h-PS (pink) under the critical conditions of d-PS on a Nucleosil $C_{18}$ stationary phase in a solvent composition of THF/ACN 47/53 (v/v) and a flow rate of 0.5 mL/min and a column temperature of 43˚C.*

### *3.3.2.2.2 LCCC of h-PS*

The critical conditions of PSS h-PS homopolymers were established at a column temperature of 53˚C as shown by Figure 34. Similar to the LC x LC experiments, at the critical condition of h-PS homopolymers, the d-PS homopolymers eluted in SEC mode as shown by Figure 35.

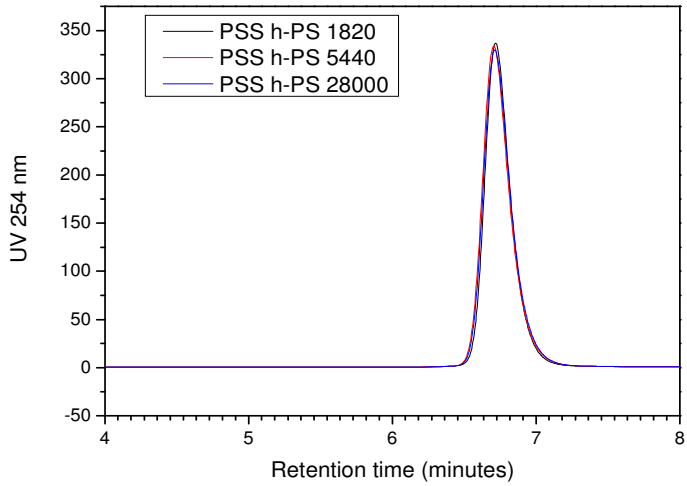


*Figure 34: Overlay of UV chromatograms of individual injections of PSS h-PS homopolymers of various molar masses under the critical conditions of PSS h-PS on a Nucleosil $C_{18}$ stationary phase in a solvent composition of THF/ACN 47/53 (v/v) at a flow rate of 0.5 mL/min and a column temperature of 53˚C.*

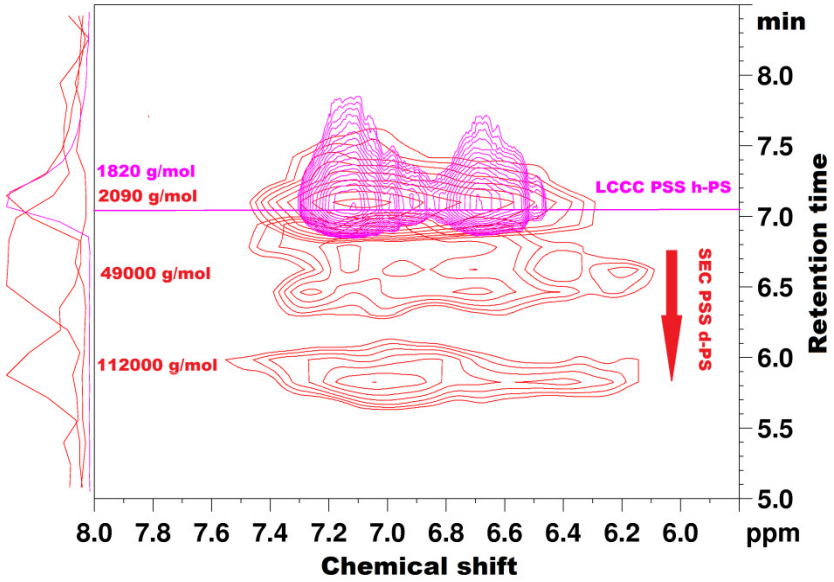


*Figure 35: An overlay of LC-NMR contour plots of PSS d-PS homopolymers (red) at the critical conditions of PSS h-PS (pink) on a Nucleosil $C_{18}$ stationary phase in a solvent composition of THF/ACN 47/53 (v/v) at a flow rate of 0.5 mL/min and a column temperature of 53˚C.*

The efficiency of the LCCC-NMR hyphenation was tested by injecting binary blends. Figure 36 shows the LC-NMR contour plots of the blend injections of varying molar masses at the critical conditions of PSS h-PS. An improvement in separation was observed with an increase in molar mass of the blend components. Lower molar mass components were not sufficiently separated but the high molar mass blend components could be easily distinguished.

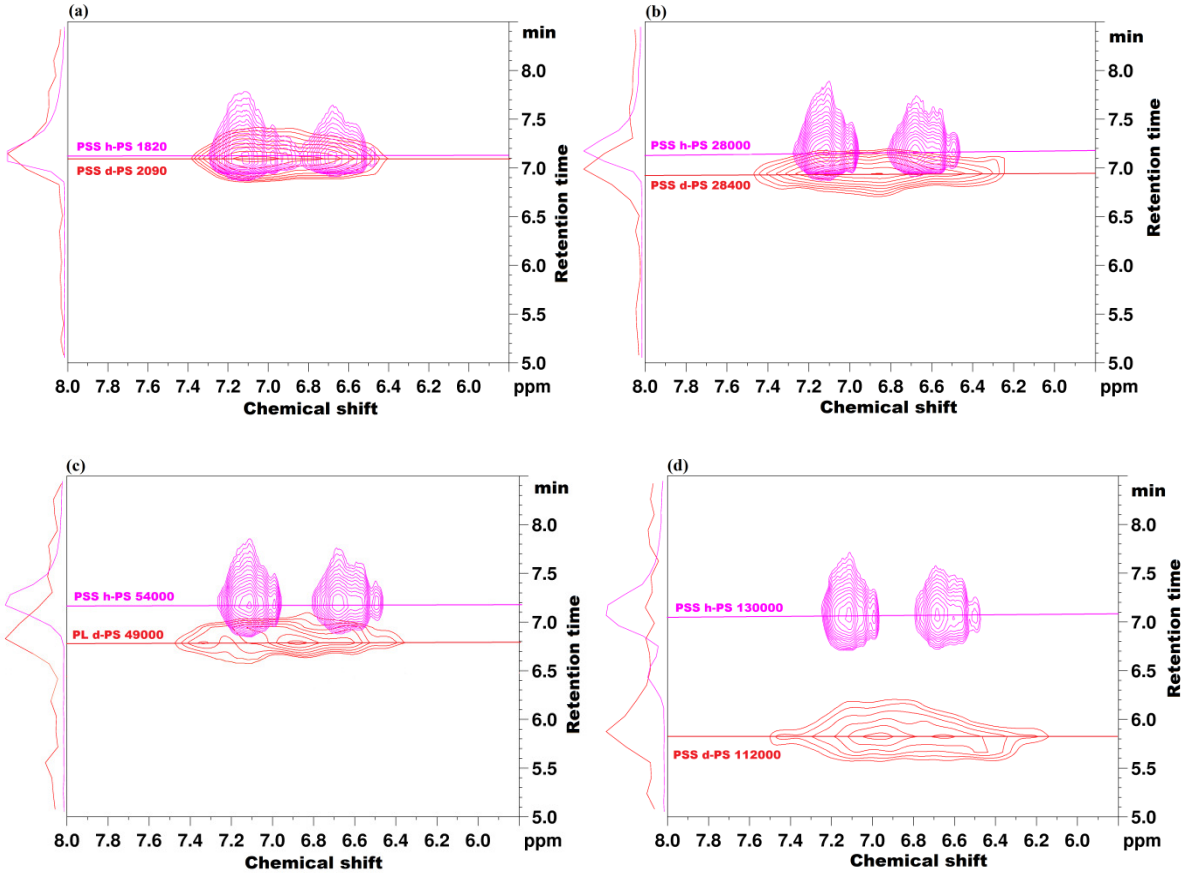


*Figure 36: An overlay of LC-NMR contour plots of four binary blends of PSS d-PS (red) and PSS h-PS (pink) under the critical conditions of h-PS on a Nucleosil $C_{18}$ stationary phase in a solvent composition of THF/ACN 47/53 (v/v) at a flow rate of 0.5 mL/min and a column temperature of 53˚C.*

### *3.3.3.2.3 SEC of d-PS and LAC conditions of h-PS*

SEC-LAC conditions of PSS d-PS and PSS h-PS homopolymers were established at a column temperature of 48.5˚C. The efficiency of these conditions was tested by injecting binary blends. Figure 37 shows the LC-NMR contour plots of the blend injections of varying molar masses at these conditions. An improvement in separation was observed with an increase in molar mass of the blend components, this was due to the high molar mass d-PS homopolymers being excluded from the pores of the stationary phase and eluting earlier than the high molar mass h-PS homopolymers which elute later due to higher retention on the stationary phase. The low molar mass blends had reduced resolution as compared to the higher molar mass blends and could only be distinguished by the use of $^{1}H$ and $^{2}H$ NMR detection.

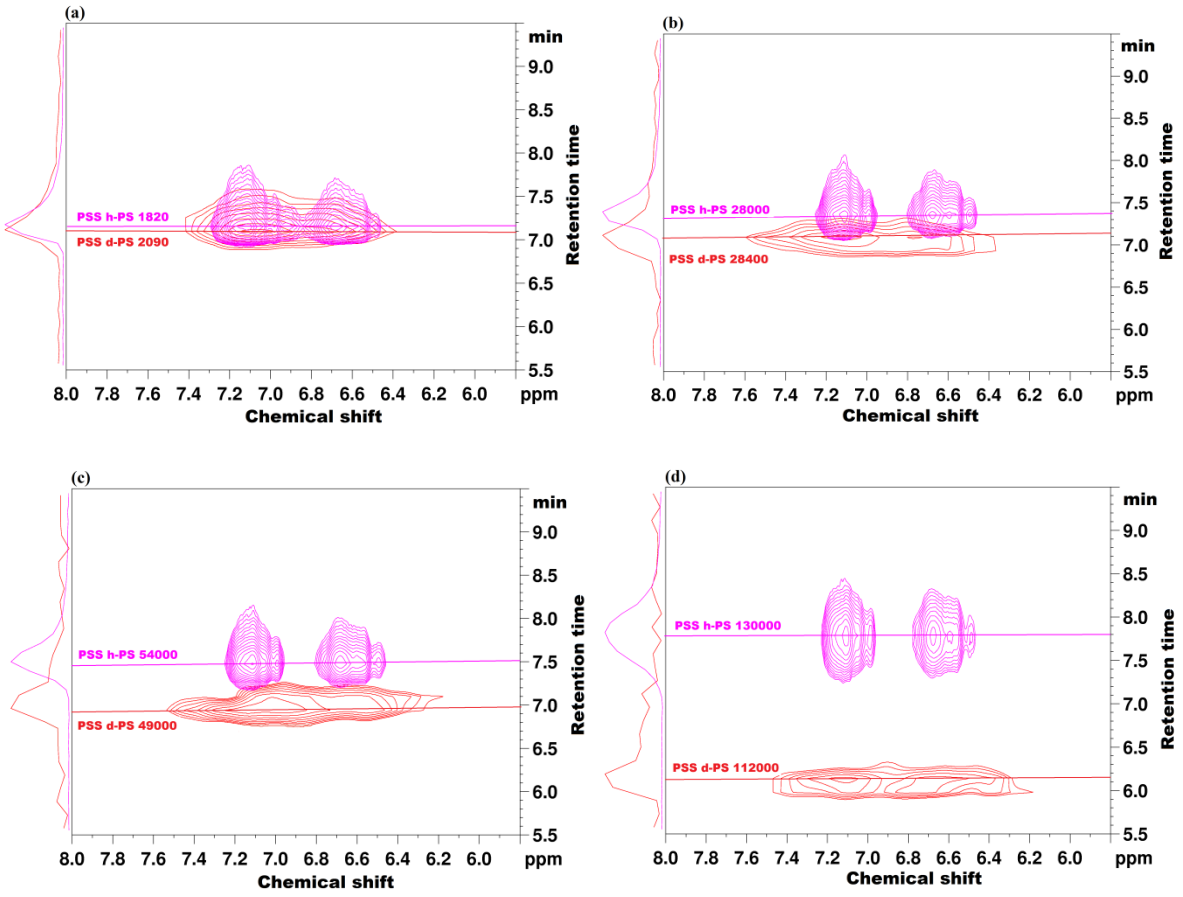


*Figure 37: An overlay of LC-NMR contour plots of four binary blends of PSS d-PS (red) and PSS h-PS (pink) under the SEC of d-PS and LAC of h-PS on a Nucleosil $C_{18}$ stationary phase in a solvent composition of THF/ACN 47/53 (v/v) at a flow rate of 0.5 mL/min and a column temperature of 48.5˚C.*

## 3.4 Conclusions

Deuterated and hydrogenated polystyrenes have been shown to have different adsorptive behaviours using both normal and reversed phase liquid chromatography. This work was aimed at exploring if these differences were sufficient to separate deuterated and hydrogenated polystyrene homopolymers using liquid chromatography at critical conditions. The separation efficiency of the chromatographic methods was tested with binary blends.

Differences in retention behaviours for both the deuterated and hydrogenated polystyrene homopolymers were observed. On a polar stationary phase the d-PS homopolymers adsorbed significantly more than h-PS homopolymers especially at high molar masses. On a non-polar stationary phase, the inverse behaviour is observed.

The critical conditions of deuterated polystyrene homopolymers were established on both bare silica and a $C_{18}$ modified silica columns. At the critical conditions of d-PS on the bare silica stationary phase, the h-PS homopolymers eluted in SEC mode and at the critical conditions of d-PS on a $C_{18}$ modified silica stationary phase, the h-PS homopolymers eluted in LAC mode. The separation on the $C_{18}$ modified silica stationary phase was better as compared to the bare silica stationary phase which is clearly visible on the LC x LC contour plots of both experiments.

The critical conditions for both d-PS and h-PS homopolymers were established on a $C_{18}$ modified stationary phase. At the critical conditions of h-PS, the d-PS homopolymers eluted in SEC mode. A third chromatographic condition was observed, where the d-PS homopolymers eluted in SEC mode while the h-PS homopolymers eluted in LAC mode.

The prepared blends were separated using the established chromatographic conditions. The separation of binary blends with a molar mass higher than 30000 g/mol was shown to be sufficient for the identification of the blend components. While, the separations of low molar masses blend component was not sufficient. This was also observed in the LC x LC contour plots. The LC x LC coupling experiments separated according to the isotope effect in the first dimension and according to molar mass in the second dimension. These LC x LC experiments allowed us to observe the isotopic separation in relation to the molar mass separation. The conditions where the d-PS homopolymers eluted in SEC mode and the h-PS homopolymers eluted in LAC mode showed a much better separation as compared to the critical conditions of both the d-PS and h-PS homopolymers. This showed that molar mass plays a significant

role in the separation with respect to the isotope effect. However, separation was also achieved when the molar mass influence was suppressed at critical conditions.

The coupling of the different chromatographic methods with $^{1}H$ and $^{2}H$ NMR allowed for the identification the blend components of low molar mass blends which were not sufficiently separated with liquid chromatography. This was not possible with one-dimensional liquid chromatography and two-dimensional liquid chromatography. LC-NMR experiments allowed us to be able to distinguish between components with similar chromatographic elution profiles. With LC-NMR coupling experiments, we were able to differentiate two hydrogenated PS homopolymers with similar molar masses and elution times but different end groups. We were also able to differentiate between two PS homopolymers, one deuterated and the other hydrogenated with similar molar masses, elution times and the same end groups. We also used SEC-NMR to show that there are no significant differences between the hydrodynamic volumes of hydrogenated and deuterated polystyrenes.

# 4. Separation of poly (methyl methacrylate)s according to tacticity

## 4.1 Introduction

Polymer tacticity has been shown to influence crystalline structure, thermal degradation, electrical properties, cytotoxicity and flexibility of the polymer chains.[13, 92, 93] The formation of stereocomplexes between *it*-PMMA and *st*-PMMA homopolymers has been shown to be dependent on the temperature, solvent type, weight ratio of the stereoregular PMMAs in the mixture and the amount of time the mixture is allowed to stand.[85, 94-98] These stereocomplexes are believed to have different degrees of crystallinity which will influence the bulk properties of the polymer.[89]

The majority of separations of PMMAs according to tacticity use silica based stationary phases.[101-103, 106] In this study we wanted to use a carbon-based stationary phase because of its numerous advantages over silica based stationary phases, i.e. excellent separation of highly polar analytes, stability at high temperature and salt concentrations as well as its stability in aggressive solvents. The most interesting of these advantages is its selectivity for closely related small compounds without the addition of a modifier. [108-111]

In polymer science, carbon-based stationary phases have been used for high temperature applications for the analysis of polyolefins.[68, 114, 115] There are no reports on the chromatographic separations of polymers on the porous graphitic stationary phases at ambient temperature.

In this study, solvent gradient interaction chromatography (SGIC) was used to separate stereoregular PMMAs with regard to tacticity on a carbon adsorbent at ambient temperature. This separation was coupled online to SEC for the separation of the PMMA fractions with respect to molar mass.

NMR has been shown to be the best characterization technique to observe polymer tacticity.[28, 72, 73] LC-NMR had been shown to be a powerful technique which allows the observation of polymer microstructure during chromatographic elution.[78] In literature, only SEC-NMR has been used to observe molar mass dependency of stereoregular PMMA on tacticity.[79, 80] SEC-NMR is advantageous for analysing polymers of different molar masses, however, when polymers of similar molar masses are analysed co-elution would occur and no further information could be obtained and a chromatographic separation was necessary to observe the different stereoregular polymers.

The developed SGIC method will also be coupled online to $^{1}H$ NMR to observe the tacticity distribution during elution.

Both the LC x LC and LC-NMR results have been published.[118, 119]

## 4.2. Experimental

Two instruments were used for these experiments. The first was an Agilent 1200 HPLC system (Agilent technologies, Boeblingen, Germany) used for the initial one-dimensional and two-dimensional liquid chromatographic experiments (LC x LC). The second was an Agilent 1100/1200 HPLC system (Agilent technologies, Boeblingen, Germany) used for the LC-NMR hyphenation experiments. All the instruments were equipped with a quaternary pump, auto-sampler, thermostatted column compartment and a UV detector. The first instrument was also equipped with an additional isocratic pump and an ELS detector. The processing and recording was carried out with WinGPC software (Polymer Standards Service GmbH, Mainz, Germany). The bulk $^{1}H$ NMR spectra were acquired on a Varian Unity 400 Mhz spectrometer (Agilent, Santa Clara, USA), while the LC-NMR spectra were acquired on a Bruker advance DRX 500Mhz spectrometer (Bruker Biospin GmbH, Rheinstetten, Germany) with a triple resonance flow probe TXi with an active detection volume of 60 µL. All samples were dissolved in $CDCl_3$ for the bulk measurements.

### 4.2.1 Samples

Samples were products of Polymer Laboratories (Church Stretton, England) and Polymer Standards Service GmbH (Mainz, Germany). All samples were synthesised via anionic polymerization using 1,1-diphenyl lithium as an initiator as described by Allen *et al.*[120]

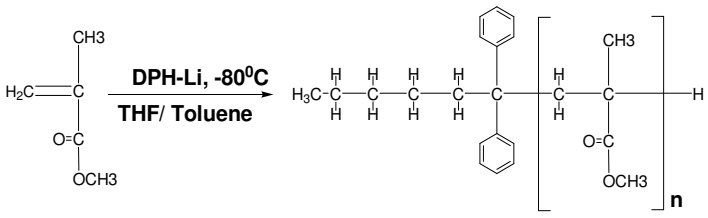


*Figure 38: Synthesis of stereoregular PMMA homopolymers.*

*Table 6: Stereoregular PMMA homopolymer sample overview.*

| Sample Label | $M_p$ (g/mol) | $M_n$ (g/mol) | $M_w$ (g/mol) | Average triad tacticity [a] (%mol) | | |
|---|---|---|---|---|---|---|
| | | | | ***mm*** | ***mr*** | ***rr*** |
| S-2540 | 2540 | 2190 | 2460 | 3.6 | 40.4 | 56.0 |
| S-2810 | 2810 | 2560 | 2770 | 4.0 | 41.6 | 54.4 |
| S-4900 | 4900 | 4530 | 4960 | 3.7 | 39 | 57.2 |
| S-6370 | 6370 | 5880 | 6270 | 3.8 | 38.0 | 58.2 |
| S-8350 | 8350 | 7910 | 8290 | 3.8 | 37.9 | 58.3 |
| S-12600 | 12600 | 12100 | 12600 | 4.0 | 37.1 | 58.9 |
| S-23500 | 23500 | 22500 | 23200 | 4.0 | 35.8 | 60.2 |
| S-392000 | 392000 | 372000 | 380000 | 3.5 | 46.1 | 50.4 |
| HS-7870 | 7870 | 7310 | 7660 | 1.5 | 24.5 | 74 |
| HS-24100 | 24100 | 23200 | 24400 | 1.1 | 21.3 | 77.6 |
| HS-30150 | 30350 | 29580 | 30310 | 1.1 | 20.1 | 78.8 |
| HS-60150 | 60150 | 57450 | 58900 | 1.0 | 19.1 | 79.9 |
| HS-138500 | 138500 | 126200 | 132000 | 1.2 | 19.2 | 79.6 |
| HS-342900 | 342900 | 338100 | 343300 | 0.8 | 17.0 | 82.2 |
| HI-4890 | 4890 | 3750 | 4660 | 86.5 | 3.1 | 9.4 |
| HI-12000 | 12000 | 11500 | 12400 | 92 | 3.0 | 5.0 |

a - Average triad compositions as determined by bulk 1H NMR.

### 4.2.2 One-dimensional HPLC experiments

The solvent gradient method was established on a Hypercarb stationary phase (Thermo Scientific, Dreieich, Germany) with the following dimensions, 5 µm particle size, 250 Å pore size, 150 mm length and 4.6 mm internal diameter. The flow rate used was 0.5 mL/min. The column temperature was kept constant at 30˚C. A solvent gradient program of DCM and acetone was applied as shown in Table 7.

The SEC experiments were carried out on a PL gel Mixed E stationary phase (PL/Varian, Church Stretton, England) with the following dimensions; 3 µm particle size, 300 mm length and 7.5 mm internal diameter. The flow rate used was 1 mL/min. The column was kept at room temperature (~23˚C). All these experiments were carried out on instrument 1. The concentration of the samples was approximately 1 mg/mL and an injection volume of 20 µL

was used. The ELS was used as a detector, nitrogen was the nebulizer gas set at a pressure of 3.0 bars, with an evaporating temperature of 90˚C with a gain of 3.

*Table 7: Solvent gradient used for one-dimensional HPLC experiments.*

| **Time (min)** | **DCM/Acetone (v/v)** |
|---|---|
| 0 | 53.5/46.5 |
| 5 | 53.5/46.5 |
| 10 | 100/0 |
| 12 | 100/0 |
| 14 | 53.5/46.5 |
| 20 | 53.5/46.5 |

### 4.2.3 Comprehensive two-dimensional liquid chromatography

The concentration of the samples was 10 mg/mL, with equal amounts of each component in the blend and an injection volume of 50 µL. The first dimension separated according to the tacticity using the Hypercarb stationary phase at a flow rate of 0.0125 mL/min. The eight port valve system (VICI Valco instruments, Texas, USA) was equipped with two 100 µL storage loops. The second dimension separated according to molar mass using THF as an eluent on a PL gel mixed E stationary phase at a flow rate of 1 mL/min. The ELSD was used as a second dimension detector, nitrogen was nebulizer gas set at a pressure of 3.0 bars, and an evaporating temperature of 90˚C with a gain of 1. These experiments were carried out on instrument 1.

### 4.2.4 On-flow LC – NMR coupling experiments

#### *4.2.4.1. SEC-NMR experiments*

Each of the samples had a concentration of approximately 3 mg/mL. THF was used as a solvent, at a flow rate of 0.8 mL/min. The injection volume was 100 µL. The SEC experiments were performed on three PSS SDV 5 µm columns (a guard column, and three columns) with the following pore sizes; $10^2$, $10^3$ and $10^5$ Å with the following dimensions: column length 300 mm and an internal diameter was 8 mm. The on-flow SEC-$^1$H NMR experiments were carried out at 8 transients per FID, with an acquisition time of 0.82 s, collected data was 8 Kb, with a repetition time of 1s and a spectral width of 10 KHz. The data were Fourier transformed using 64 Kb data points with an exponential line broadening of 5 Hz. The WET suppression technique was used to suppress the THF signals. These experiments were carried out on instrument 2.

#### *4.2.4.2 HPLC-NMR experiments*

For the isocratic runs each of the samples had a concentration of approximately 7 mg/mL. The eluent used had a composition of DCM/Acetone 40/60 (v/v). For the gradient runs each of the samples had an average concentration of approximately 0.5 mg/mL in the blend. Therefore the quaternary blend had a total concentration of 8 mg/mL. The samples were dissolved in the initial conditions of the gradient at a solvent composition of DCM/Acetone 20/80 (v/v). The acetone used in the gradient experiments consisted of a mixture of 75% hydrogenated acetone and 25% deuterated acetone. The gradient program is indicated in Table 8.

The injection volume for all HPLC-NMR experiments was 50 µL and the flow rate was 0.5 mL/min. The HPLC experiments were performed on a Hypercarb stationary phase (Thermo scientific, Dreieich, Germany) with the following dimensions, 5 µm particle size, 250 Å pore size, 150 mm length and 4.6 mm internal diameter. The on-flow HPLC-$^{1}$H NMR experiments were carried out at 16 transients per FID, an acquisition time of 0.82 s, collected data was 16 Kb, with a repetition time of 1s and a spectral width of 5 KHz. The data were Fourier transformed using 32 Kb data points with an exponential line broadening of 5 Hz.

*Table 8: Solvent gradient used for HPLC-NMR coupling experiments.*

| **Time (min)** | **DCM/Acetone Vol%** |
|---|---|
| 0 | 20/80 |
| 1 | 20/80 |
| 17 | 70/30 |
| 22 | 95/5 |
| 30 | 95//5 |
| 33 | 20/80 |

## 4.3. Results and discussion

The molar masses of the samples ranged from 4890 to 138900 g/mol. The molar masses of the blends used in this section are summarised in Table 9. The blends consisted of equal amounts of each homopolymer present in that blend.

*Table 9: Molar masses of PMMA homopolymer blends used for the LC – NMR hyphenation experiments*

| Blend Labels | st-PMMA (g/mol) | Mp of it-PMMA (g/mol) |
|---|---|---|
| B1 | S-4900 | HI-4890 |
| B2 | HS-7870 | HI-4890 |
| B3 | HS-7870 | HI-12000 |
| B4 | HS-60150 | HI-4890 |
| B5 | HS-60150 | HI-12000 |
| B6 | - | HI-4890 + HI-12000 |
| B7 | HS-7870 + HS-24100 | - |
| B8 | S-4900 + HS-138500 | - |
| QT1 | S-4900 + HS-60150 | HI-4890 + HI-12000 |
| QT2 | HS-7870 + HS-24100 | HI-4890 + HI-12000 |

### 4.3.1. One-dimensional liquid chromatography

#### *4.3.1.1. Isocratic HPLC*

Preliminary experiments showed very different adsorptive behaviours for the stereoregular PMMA homopolymers on the porous graphitic stationary phase. Firstly, in 100% DCM both the syndiotactic PMMA (*st*-PMMA) and isotactic PMMA (*it*-PMMA) homopolymers eluted in SEC mode as shown by Figure 39 (a). Secondly, we noted that a decrease in the DCM content in the eluent led to increased adsorption of *it*-PMMA homopolymers as shown by Figure 39 (b). At a solvent composition of DCM/Acetone 40/60 (v/v), there was an increase in retention of *st*-PMMA with an increase in molar mass while *it*-PMMA is almost completely adsorbed onto the stationary phase. At a solvent composition of DCM/Acetone 80/20 (v/v), there was a decrease in retention of *st*-PMMA homopolymers with an increase in molar mass.

The critical conditions of *st*-PMMA were established at solvent composition of DCM/Acetone 53.5/46.5 (v/v), under these conditions all *st*-PMMA elute at the same elution volume irrespective of molar mass. Under the critical conditions of the predominantly *st*-PMMAs, both the predominantly and highly *st*-PMMAs eluted at the same elution volume and could not be differentiated. Under the critical conditions of predominantly *st*-PMMA, *it*-PMMA homopolymers were completely adsorbed onto the stationary phase as shown by

Figure 39 (c). None of the isocratic conditions that we investigated were sufficient for the separation of PMMA homopolymers according to tacticity.

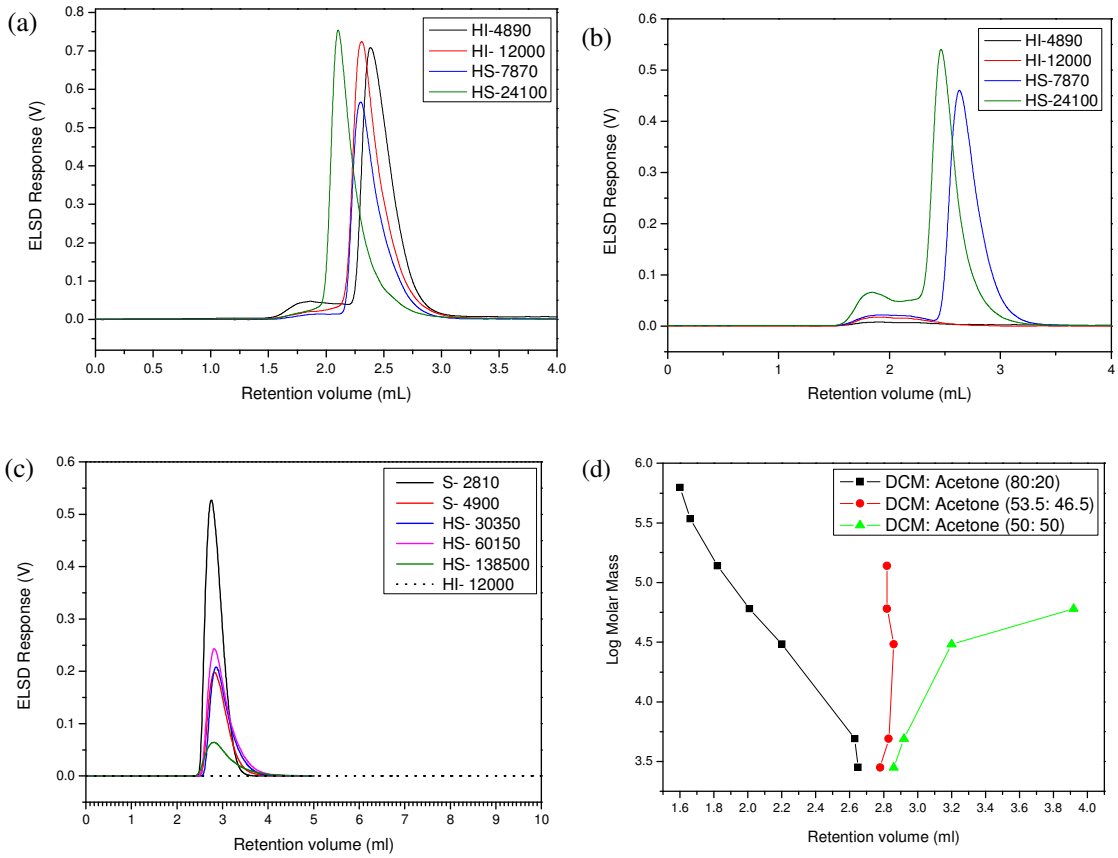


*Figure 39: (a) Highly it- and st-PMMAs in 100% DCM, (b) Highly it- and st-PMMAs in an eluent composition of DCM/Acetone 60/40 (v/v), (c) LCCC conditions of predominantly st-PMMAs in an eluent composition of DCM/Acetone 53.5/46.5 (v/v) and (d) Different modes of elution of st-PMMAs of various molar masses in varying compositions of DCM/Acetone on a hypercarb stationary phase at a flow rate of 0.5 mL/min and a column temperature of 30°C.*

### *4.3.1.2 Solvent gradient HPLC*

The solvent gradient was developed by starting with the critical conditions of predominantly *st*-PMMA followed by an increase in DCM content during elution. The initial solvent composition of DCM/Acetone 53.5/46.5 (v/v) was kept constant for 10 minutes and there after the DCM content was increased linearly from 53.5% to 100% to promote elution of *it*-PMMA. Under these conditions the entire sample was eluted with full recovery.

*4.3.1.2.1 Individual injections*

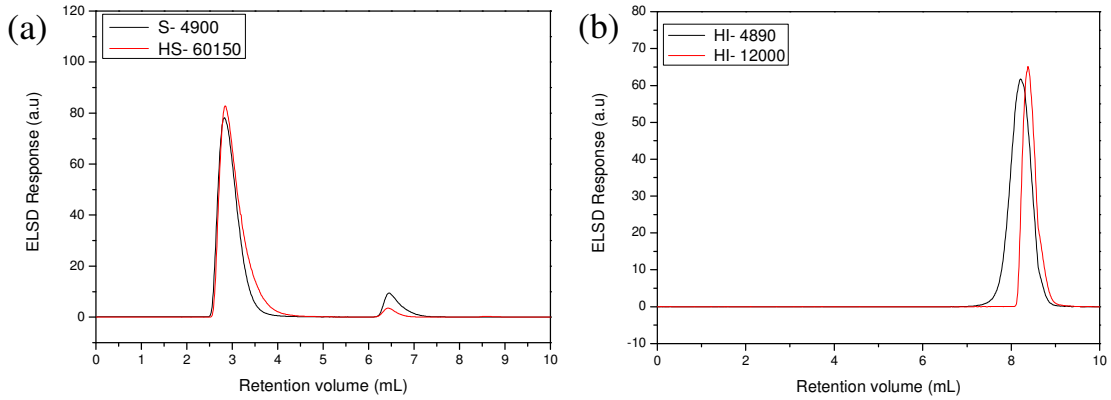


*Figure 40: Individual injections of (a) st-PMMAs and (b) it-PMMAs on a hypercarb stationary phase using the solvent gradient of DCM/acetone shown in Table 8 at a flow rate of 0.5 mL/min and a column temperature of 30˚C.*

The separation efficiency of the solvent gradient was tested with individual injections of stereoregular PMMAs. The *st*-PMMAs eluted in two fractions, the first major fraction which eluted at an elution volume of 2.6 mL, with all molar masses eluting at the same retention volume independent of molar mass and a second minor fraction which eluted slightly later before the elution of *it*-PMMAs. The percentage triad tacticity of syndiotactic sample S-4900 as determined by bulk $^{1}$H NMR was *mm/mr/rr* 4.6/38.2/57.2. The two resulting peaks of this sample were fractionated and analysed with $^{1}$H NMR. The triad tacticity of the first fraction was more or less similar to that determined for the bulk sample *mm/mr/rr* 7.6/35.7/56.7.

The second fraction contained an impurity which overlapped with the *mm* and *rr* triad signals of the PMMA present in this fraction. The high concentration of this impurity could be due to its accumulation during fractionation. We could only accurately determine the average *mr* triad tacticity, which was 45.7 %. This fraction will be labelled as unidentified tacticity PMMA (*ut*-PMMA). Although we are unable to accurately determine the average triad composition of the second fraction, we assumed that this fraction had slightly more *mm* and *mr* triads which led to its increased adsorption was substantiated by the LC-NMR hyphenation experiments. In this gradient the low molar mass *it*-PMMA homopolymer eluted at an earlier retention time as compared to high molar mass *it*-PMMA which eluted at higher retention times as the DCM content increased in the gradient.

*4.3.1.2.2 Blend injections*

The efficiency the solvent gradient was tested with various binary blends of one *st*-PMMA and one *it*-PMMA as shown by Figure 41. All the blends were prepared at 50:50 wt %. For all binary injections two regions of elution were observed. The first belongs to the *st*-PMMA

homopolymers at low retention times and the second belongs to *it*-PMMA homopolymers eluting at higher retention times. Figure 41 (a) shows the superiority of this solvent gradient method in separating two PMMA homopolymers with similar end groups and molar masses only differing in tacticity. The two components of blend 1 are baseline separated with respect to tacticity. The order of elution of the stereoregular PMMAs is in agreement with that observed by Cho *et al.* on a Nucleosil $C_{18}$ stationary phase with the *st*-PMMA eluting earlier than the *it*-PMMA.[106]

An interesting observation was made with *st*-PMMA homopolymers S-4900 and HS-60150. When injected individually these two *st*-PMMA homopolymers eluted in two fractions as shown by Figure 40 (a). In certain binary blends these *st*-PMMAs still eluted in two fractions as shown by Figure 41 (b) and (f), while in other binary blends they eluted in only a single fraction as shown Figure 41 (a), (c), (d) and (e). We tried to correlate this late eluting fraction to an increase in molar mass of the *st*-PMMA but most high molar mass *st*-PMMAs only eluted in a single peak. We also tried to correlate this late eluting *st*-PMMA to an increase in the amount of *mr* triads, as determined from bulk $^1$H NMR. The S-4900 had the following average triad tacticity *mm/mr/rr* 3.8/39/57.2, while the HS-60150 had the following triad tacticity *mm/mr/rr* 1.0/19.1/79.9. Although these two *st*-PMMA homopolymers contained different amounts of the *mr* triad, the second peak for both samples eluted at the same elution volume as shown by Figure 40 (a).

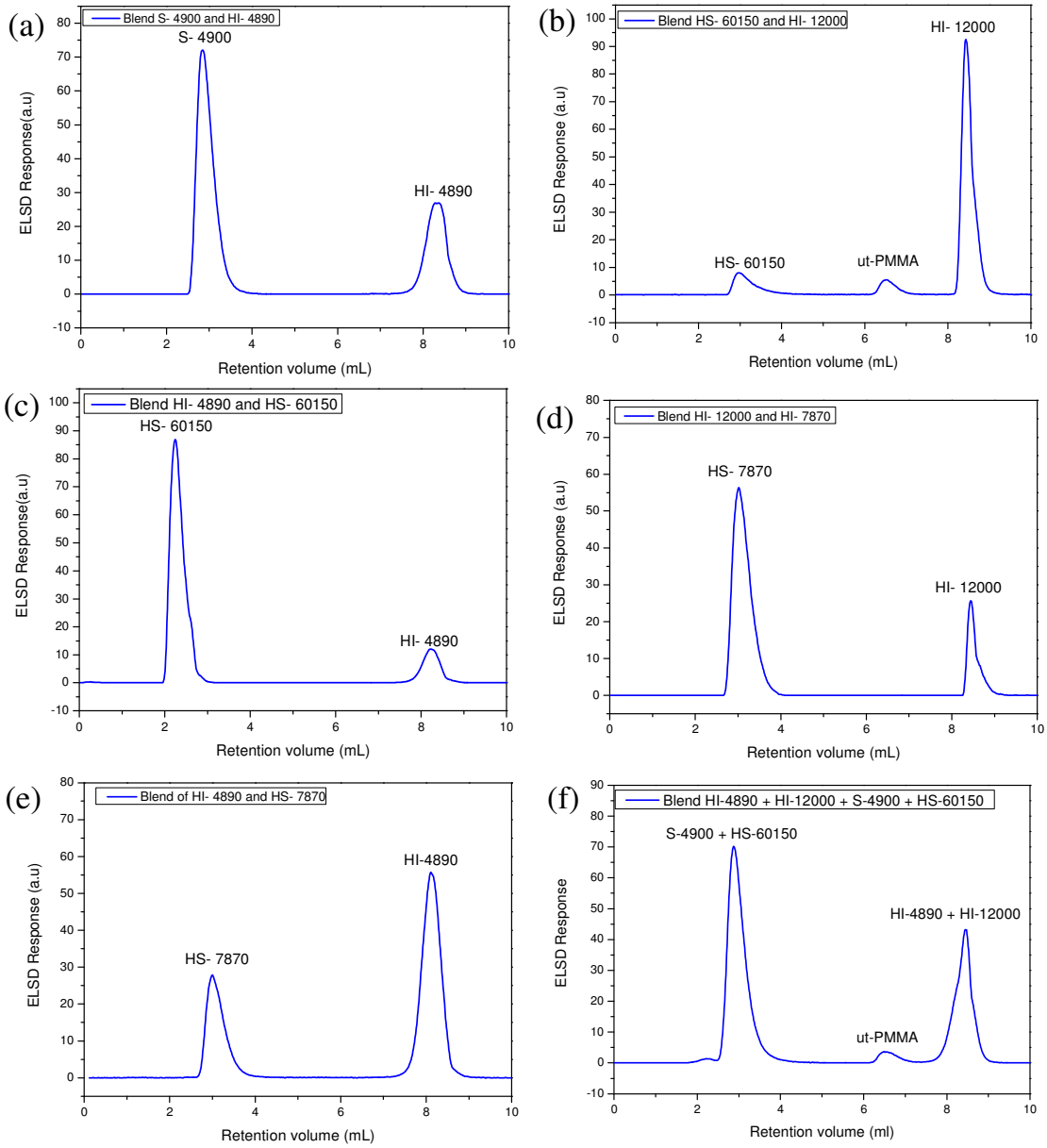


*Figure 41: Chromatograms of binary blends of st-PMMA and it-PMMA on a hypercarb stationary phase using the gradient of DCM/Acetone shown in table 8 at a flow rate of 0.5 mL/min and a column temperature of 30°C*

### *4.3.1.3 SEC*

Figure 42 shows the overlaid SEC chromatograms of certain stereoregular PMMAs. All samples eluted in the expected order from highest to lowest molar mass with increasing retention volume regardless of tacticity. HI-4890 and S-4900 had similar molar mass distributions and end groups with only a difference in tacticity and as expected these two samples had the same elution volume. This shows the inability of SEC to differentiate between samples with the same molar mass and different tacticity distributions.

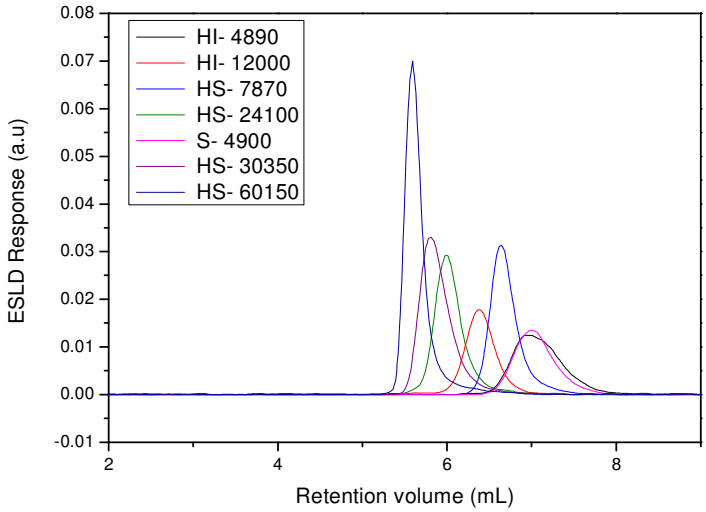


*Figure 42: Overlays of individual chromatograms of PMMAs of various molar masses on a PL gel Mixed E stationary phase in 100% THF at room temperature at a flow rate of 1 mL/min.*

### 4.3.2. Comprehensive two-dimensional liquid chromatography

The developed one-dimensional solvent gradient technique, although successful, does not allow us to observe the true two-dimensional relationship between tacticity and molar mass which would only be possible with comprehensive two-dimensional liquid chromatography (LC x LC). In the LC x LC hyphenation experiments, we separated according to tacticity in the first dimension using the solvent gradient and according to molar mass in the second dimension using SEC. The separation efficiency of the LC x LC method was tested by injecting binary and quaternary blends.

Figure 43 shows the LC x LC contour plot of binary blend 6 made up of two highly *it*-PMMAs which are completely retained on the stationary phase at the start of the gradient. An increase in DCM content promotes elution of the two components with the higher molar mass component eluting at higher retention volume as compared to the low molar mass component. Due to the unavailability of *it*-PMMAs with a molar mass higher than 12000 g/mol, a more detailed study on the resolution could not be conducted.

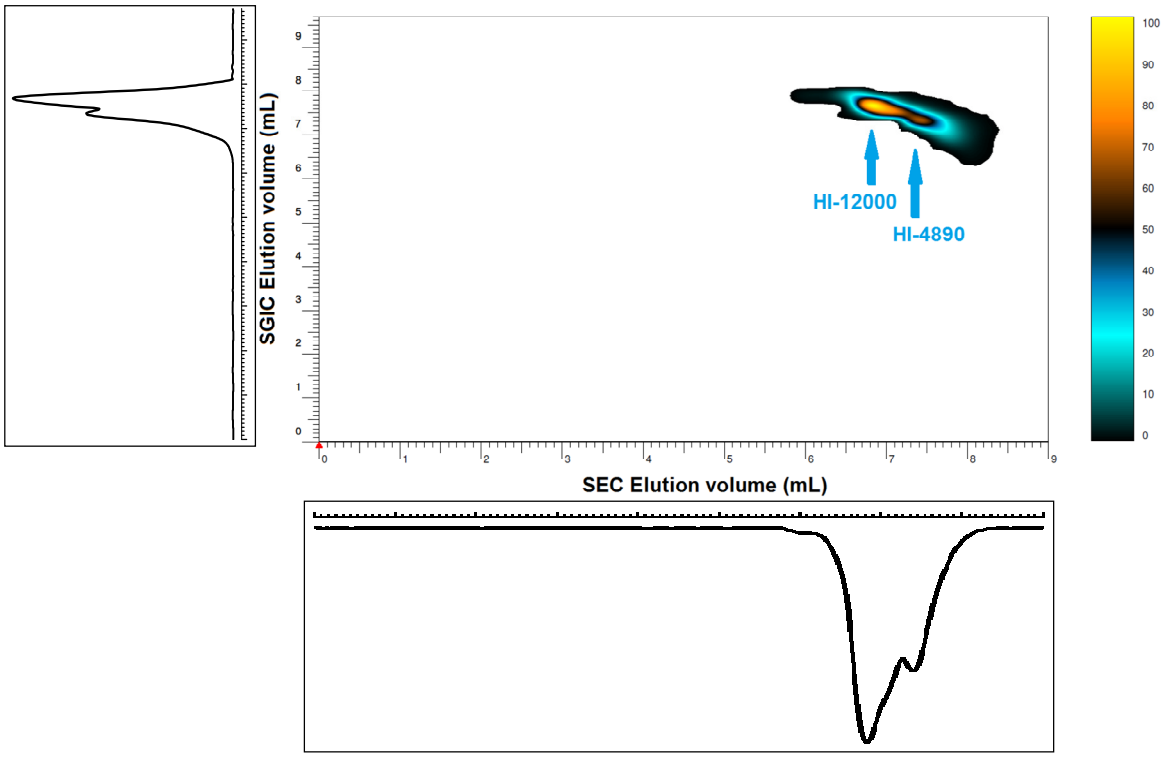


*Figure 43: LC x LC contour plot of binary blend B6 analysed in the first dimension using a solvent gradient of DCM/Acetone on a hypercarb stationary phase at a flow rate of 0.0125 mL/min and a column temperature of 30°C and in the second dimension in THF at room temperature on a PL gel Mixed E stationary phase at a flow rate of 1 mL/min with ELSD detection.*

Figure 44 shows the LC x LC contour plot of two highly *st*-PMMAs eluting early in solvent composition DCM/Acetone 53.5/46.5 (v/v) independent of molar mass. These two contour plots (Figure 43 and 44) show that there are two distinct regions of elution for the *st*-PMMA and *it*-PMMAs. The triad tacticity of the highly *st*-PMMA, HS-24100 as determined by bulk $^{1}$H NMR, was *mm/mr/rr* 1.1/21.3/77.6, while that of HS-7870 was *mm/mr/rr* 1.5/24.5/74.0. The triad compositions of these two samples were comparable hence they eluted at the same region.

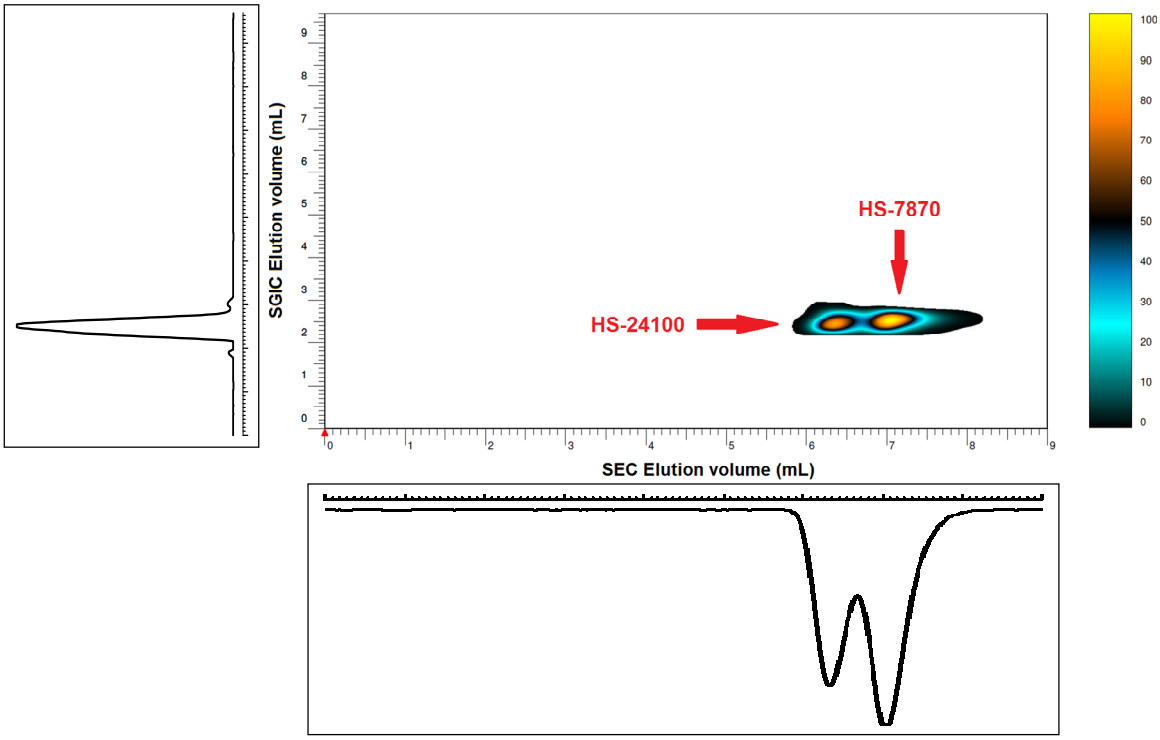


*Figure 44: LC x LC contour plot of binary blend B7 analysed in the first dimension using a solvent gradient of DCM/Acetone on a hypercarb stationary phase at a flow rate of 0.0125 mL/min and a column temperature of 30°C and in the second dimension in THF at room temperature on a PL gel Mixed E stationary phase at a flow rate of 1 mL/min with ELSD detection.*

Figure 45 shows the LC x LC contour plot of two *st*-PMMAs: one highly syndiotactic, HS-138500, with a high molar mass, and the other predominantly syndiotactic, S-4900 with a low molar mass. The triad tacticity of the highly *st*-PMMA; HS-138500 as determined by bulk $^{1}$H NMR was *mm/mr/rr* 1.2/19.2/79.6, while that of the predominantly *st*-PMMA; S-4900 was *mm/mr/rr* 3.7/39.0/57.2. The triad tacticities of these two samples are different but even so they still eluted in the same region as shown by the solvent gradient projection. Both Blend 6 and 7 show unimodal distribution in the tacticity dimension and a bimodal distribution in the molar mass dimension. Blend 8 shows much better separation in the molar mass dimension due to the large molar mass difference between the two *st*-PMMAs in the blend.

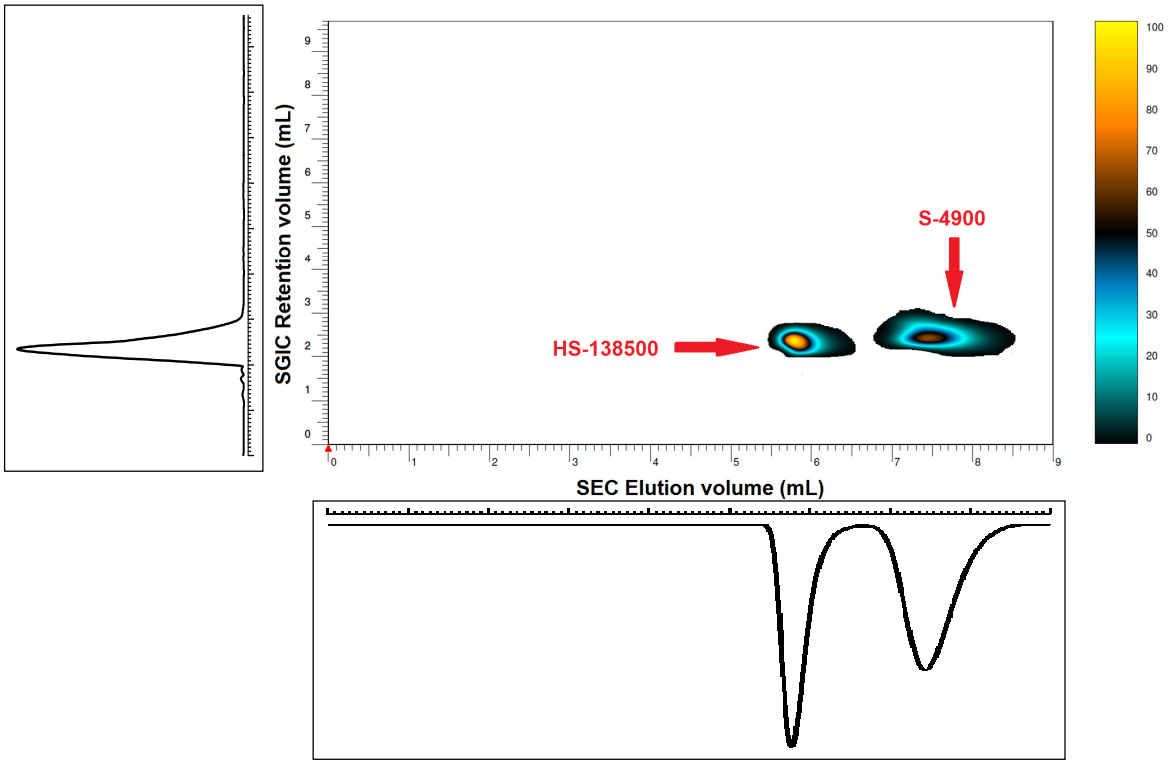


*Figure 45: LC x LC contour plot of binary blend B8 analysed in the first dimension using a solvent gradient of DCM/Acetone on a hypercarb stationary phase at a flow rate of 0.0125 mL/min and a column temperature of 30°C and in the second dimension in THF at room temperature on a PL gel Mixed E stationary phase at a flow rate of 1 mL/min with ELSD detection.*

Figure 46 shows a LC x LC contour plot which highlights the superiority of this gradient method, where binary blend 1 consisting of one highly isotactic and one predominantly *st*-PMMA which are baseline separated in the tacticity dimension. A unimodal distribution is observed in the second dimension due to the two components having similar molar mass distributions.

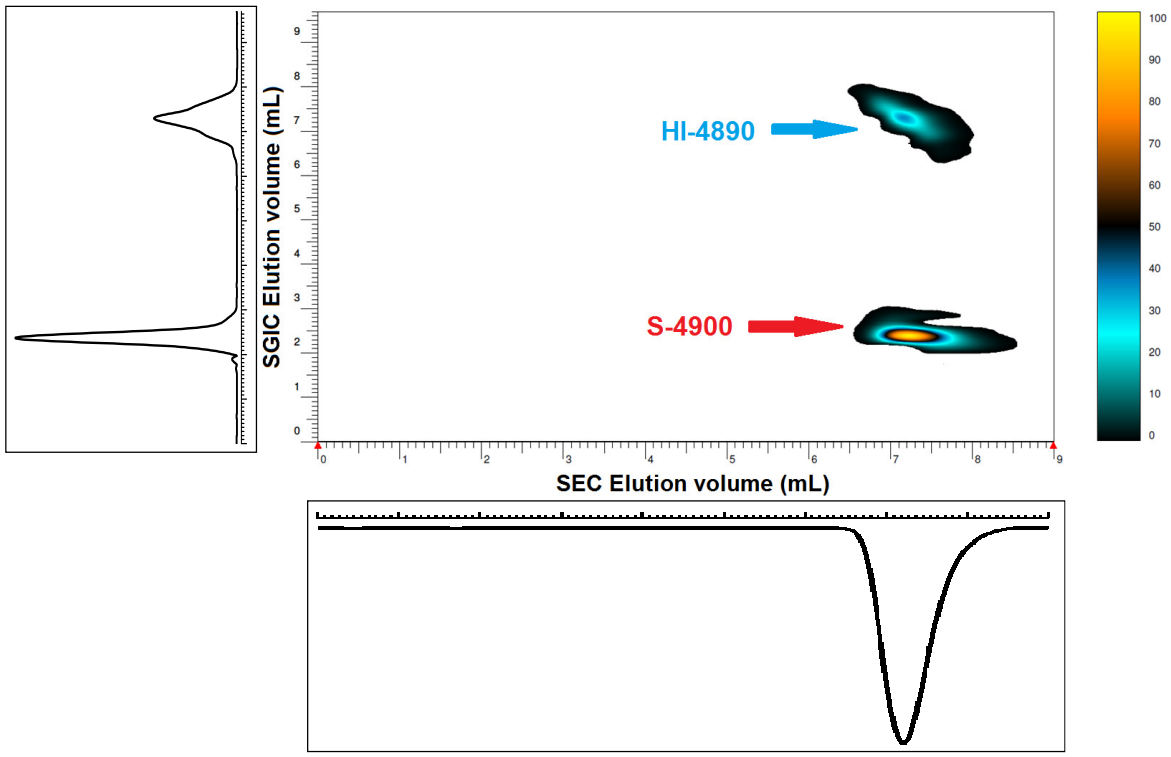


*Figure 46: LC x LC contour plot of binary blend B1 analysed in the first dimension using a solvent gradient of DCM/Acetone on a hypercarb stationary phase at a flow rate of 0.0125 mL/min and a column temperature of 30°C and in the second dimension in THF at room temperature on a PL gel Mixed E stationary phase at a flow rate of 1 mL/min with ELSD detection.*

Figure 47 shows a LC x LC contour plot of binary blend 5 consisting of one highly isotactic and the one highly syndiotactic PMMA, which are sufficiently separated in the tacticity dimension. The *st*-PMMA homopolymer HS-60150 elutes in two peaks, both peaks have similar molar masses as shown by the LC x LC contour plot. As mentioned earlier, the tacticity of the second peak could not be determined due to the presence of an impurity overlapping with the *mm* and *rr* triad signals. Regardless, the highly *it*-PMMA is still baseline separated from the *st*-PMMA components in the blend.

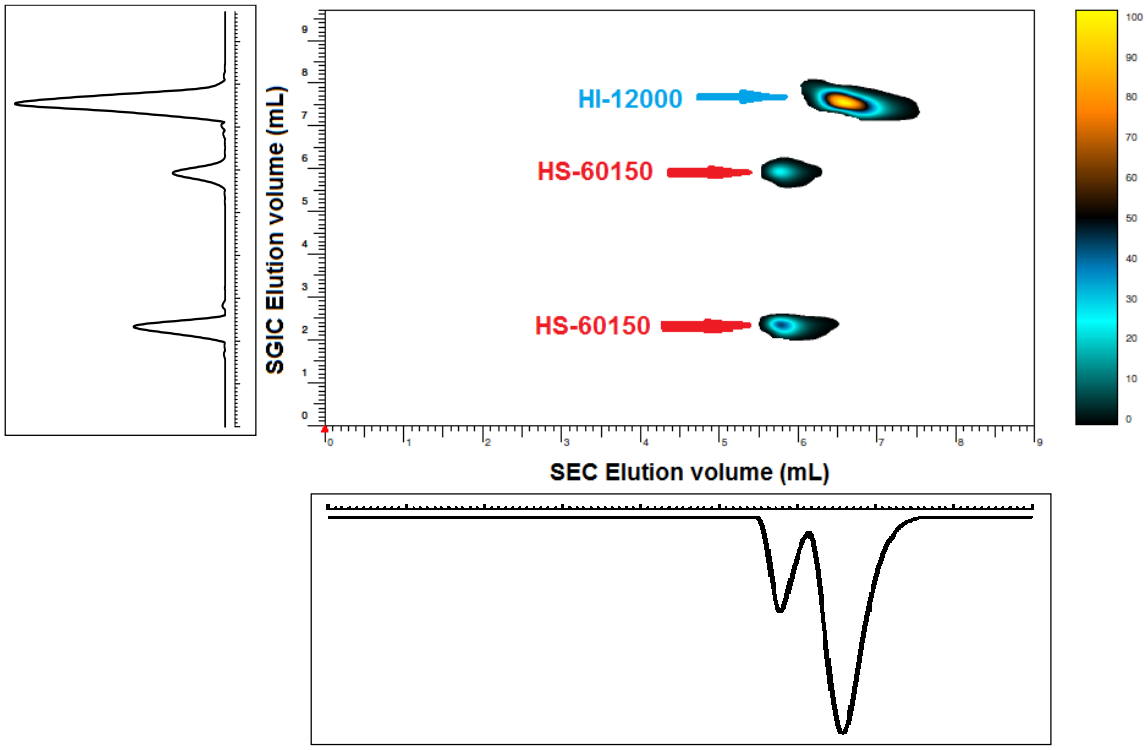


*Figure 47: LC x LC contour plot of binary blend B5 analysed in the first dimension using a solvent gradient of DCM/Acetone on a hypercarb stationary phase at a flow rate of 0.0125 mL/min and a column temperature of 30°C and in the second dimension in THF at room temperature on a PL gel Mixed E stationary phase at a flow rate of 1 mL/min with ELSD detection.*

The LC x LC method was tested by injecting a quaternary blend as shown by Figure 48. The LC x LC contour plot shows two distinct regions of elution in the tacticity dimension. The first region with a unimodal distribution belonged to the *st*-PMMAs eluting independently of their molar masses. The second region with a multimodal distribution belonged to highly *it*-PMMAs, with the higher molar mass homopolymers having a higher retention time than the lower molar mass homopolymers. A multimodal distribution was also observed in the molar mass dimension due to the different molar masses of the blend components.

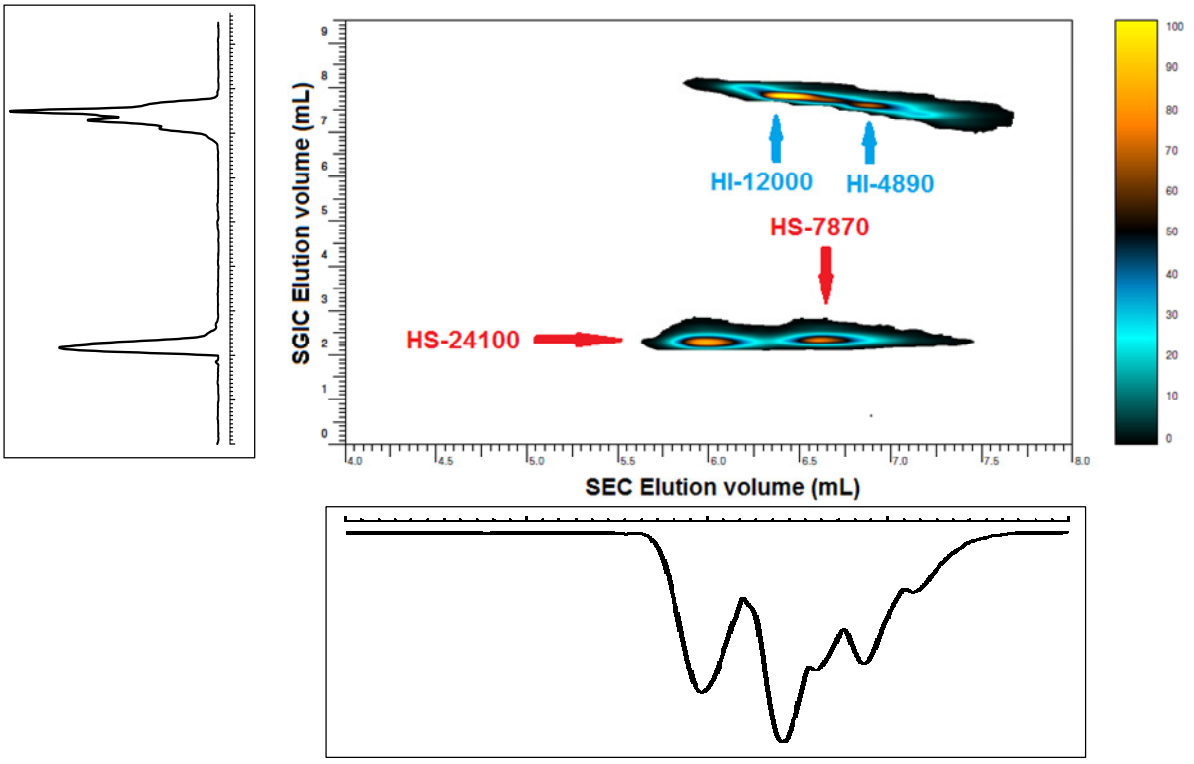


*Figure 48: LC x LC contour plot of quaternary blend QT2 analysed in the first dimension using a solvent gradient of DCM/Acetone on a hypercarb stationary phase at a flow rate of 0.0125 mL/min and a column temperature of 30°C and in the second dimension in THF at room temperature on a PL gel Mixed E stationary phase at a flow rate of 1 mL/min with ELSD detection.*

## 4.3.3. On-flow LC –NMR hyphenation

### *4.3.3.1 SEC-NMR*

In this study, online SEC-NMR was used to study the molecular weight dependence on tacticity. SEC separates polymers with respect to their hydrodynamic volumes. For all the SEC-NMR chromatograms, the green triangles represent the *mm* triad distribution; the red triangles represent the *rr* triad distribution and the blue triangles represent the *mr* triad distribution. All SEC chromatograms showed unimodal distributions.

Figure 49 and 50 show the SEC-NMR chromatograms of the predominantly and highly *st*-PMMAs, respectively. The triad composition of both these sets of samples remains more or less constant during elution.

However, a different observation was made for the SEC-NMR chromatograms of highly it-PMMAs, where a change in both the *mm* and *rr* triad amounts was observed with elution. The *mm* triad amount decreased with elution, while the *rr* triad amount increased with elution.

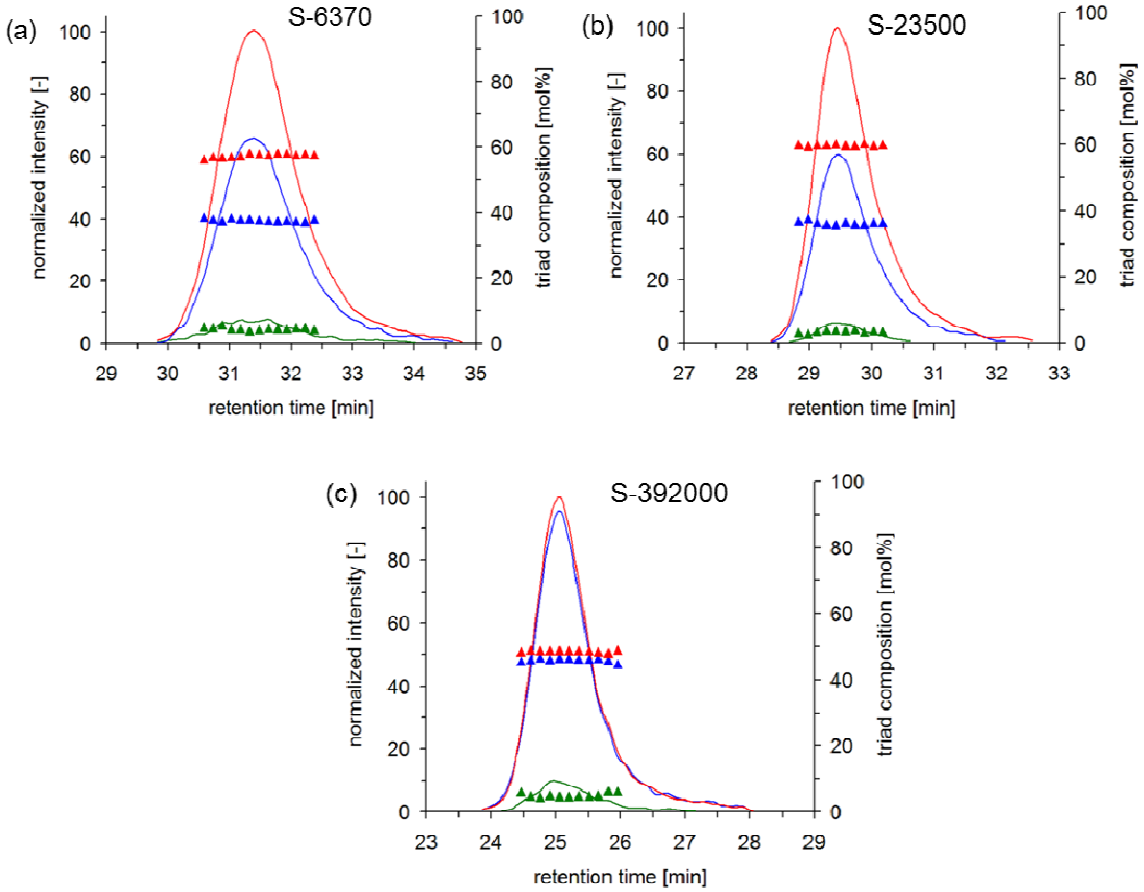


*Figure 49: SEC-NMR chromatograms of predominantly st-PMMAs showing the change in triad composition with elution time on three SDVB stationary phases in 100% THF at room temperature and a flow rate of 0.8 mL/min.*

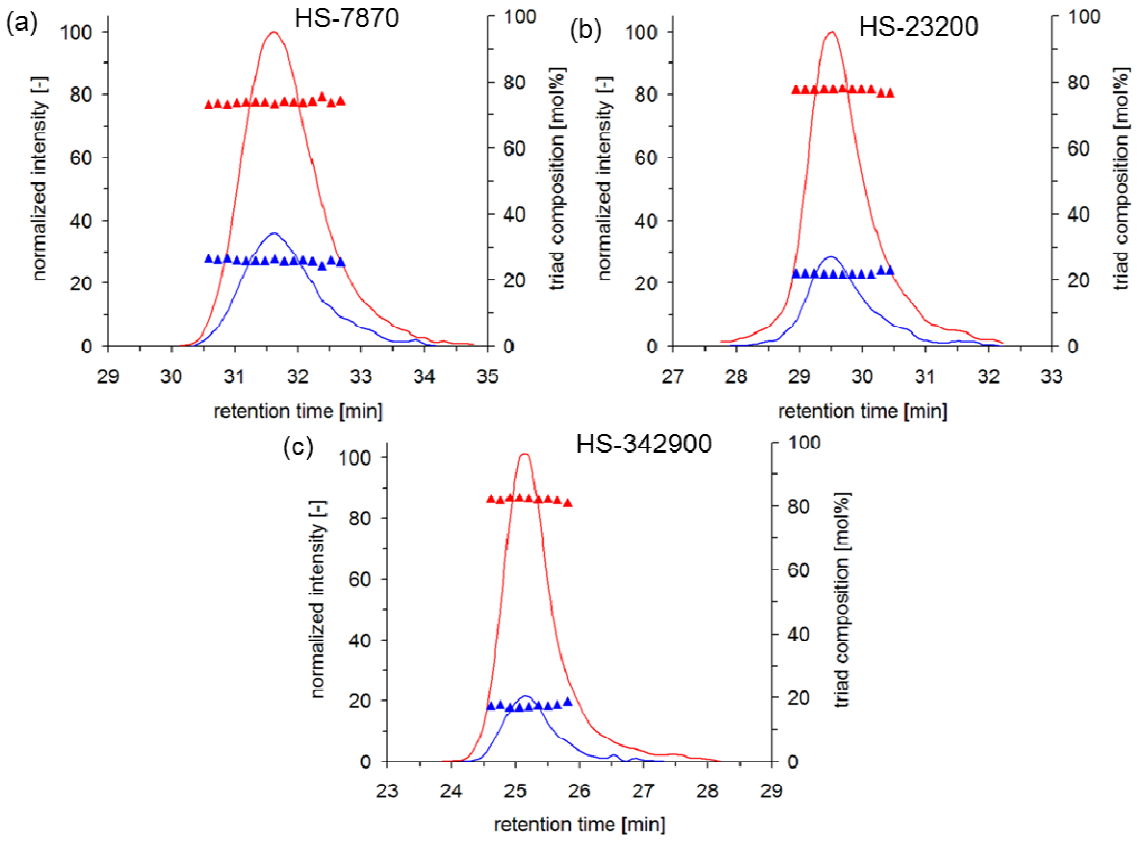


*Figure 50: SEC-NMR chromatograms of highly st-PMMAs showing the change in triad composition with elution time on three SDVB stationary phases in 100% THF at room temperature and a flow rate of 0.8 mL/min.*

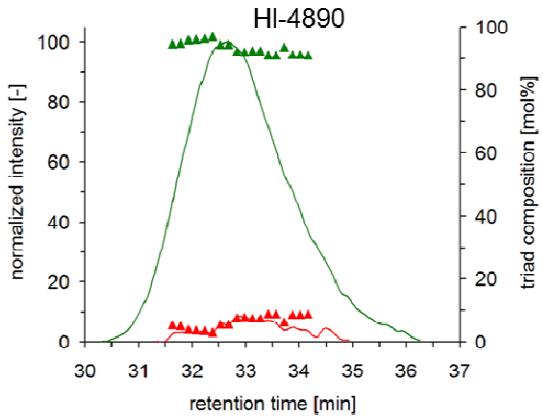


*Figure 51: SEC-NMR chromatograms of highly it-PMMAs showing the change in triad composition with elution time on three SDVB stationary phases in 100% THF at room temperature and a flow rate of 0.8 mL/min.*

All the PMMA homopolymers were measured for the construction of a calibration curve. In Figure 52, the green triangles represent the highly *it*-PMMA homopolymers, the blue triangles represent the predominantly *st*-PMMA homopolymers, while the red triangles represent the highly syndiotactic PMMA homopolymers. Regardless of the tacticity, the $M_p$ values of all the stereoregular PMMA homopolymers could be represented by the same calibration curve as shown by Figure 52. The lack of change in the average triad composition during elution

with SEC-NMR maybe a consequence of band broadening in SEC since the chromatographic system is placed at quite some distance from the flow probe.[121]

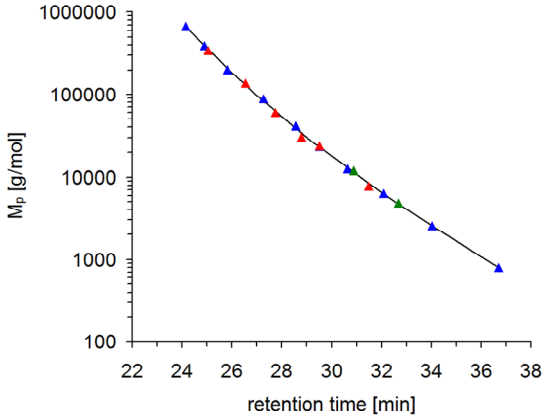


*Figure 52: SEC-NMR calibration constructed using all PMMA homopolymers shown in Table 6.*

The triad compositions of the SEC-NMR spectra over the total elution time where calculated as shown in table 10. These values were in good agreement with the values obtained from the bulk $^{1}$H NMR measurements shown in Table 6.

*Table 10: Average triad composition as measured by SEC-NMR.*

| Sample | Tacticity [mol%] | | |
|---|---|---|---|
| | ***mm*** | ***mr*** | ***rr*** |
| S-8350 | 5.0 | 37.6 | 57.4 |
| S-23500 | 2.8 | 36.6 | 60.6 |
| S392000 | 5.0 | 46.6 | 48.4 |
| HS-7870 | 1.5 | 25.5 | 73.0 |
| HS-24100 | 2.4 | 21.3 | 76.3 |
| HS-342900 | 0.7 | 17.1 | 82.2 |
| HI-4890 | 93.6 | - | 6.4 |
| HI-12000 | 98.3 | - | 1.7 |

### *4.3.3.2 Isocratic LAC-NMR*

Since no change in triad composition was observed with elution of both the predominantly and highly *st*-PMMAs using SEC-NMR, an adsorptive chromatographic technique was utilised to try and observe this change. LAC-NMR was utilised to study the change in triad composition with elution of both *st*-PMMA sample sets. For the LAC-NMR chromatograms,

the green triangles also represent the *mm* triad composition, the red triangles represent the *rr* triad composition and the blue triangles represent the *mr* triad composition. All LAC chromatograms showed a unimodal distribution. At a solvent composition of DCM/Acetone 40/60 (v/v), the *st*-PMMA elutes in LAC mode. With LAC-NMR a significant change in triad composition with elution was observed. Figure 53 shows the isocratic LAC-NMR chromatograms of the predominantly *st*-PMMAs. In these chromatograms, the *mr* and *mm* triad amounts increase with an increase in retention time while, the *rr* triad amount decreases with an increase in retention time.

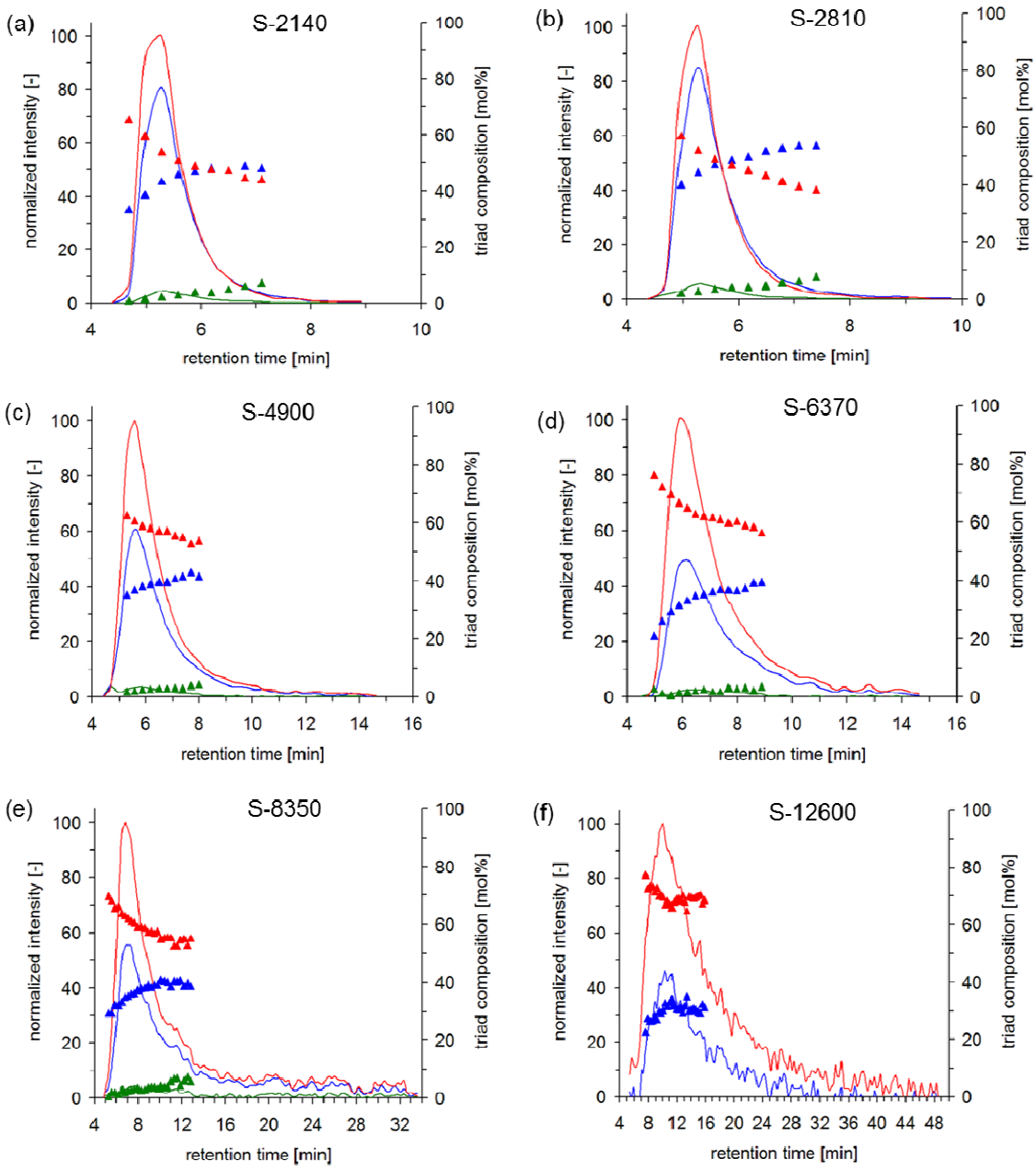


*Figure 53: Isocratic LAC-NMR chromatograms of predominantly st-PMMAs, showing changes in triad compositions with elution time on the hypercarb stationary phase in a solvent composition of DCM/Acetone 40/50 (v/v) at flow rate of 0.5 mL/min and a column temperature of 30°C.*

Figure 54 shows the isocratic LAC-NMR chromatograms of the α-methyl signals of the highly syndiotactic PMMAs. Similar to the predominantly *st*-PMMAs, the *mr* and *mm* triad amounts increase with an increase in retention time, while the *rr* triad amounts decreases with an increase in retention time. The missing *mm* triad data for the higher molar mass *st*-PMMA is due to the high signal-to-noise ratio observed in these experiments due to the increased adsorption.

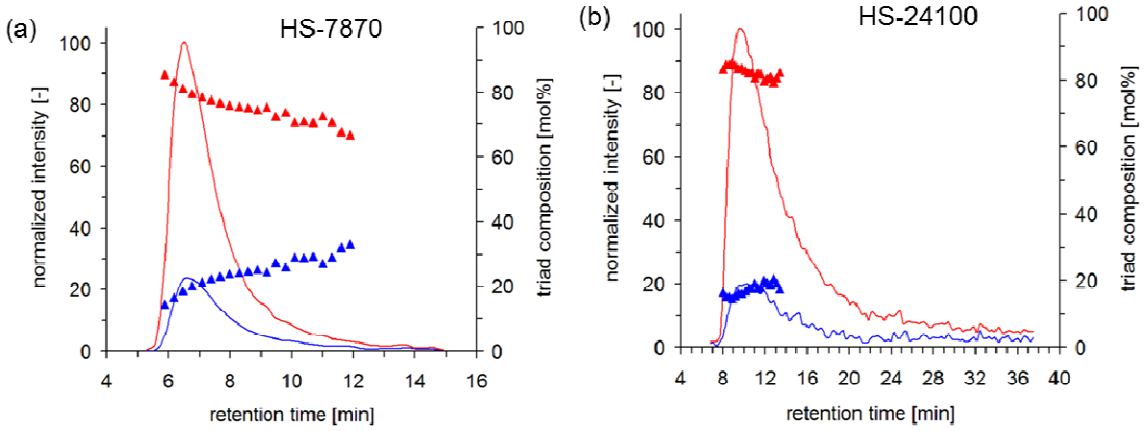


*Figure 54: Isocratic LAC-NMR chromatograms of the α-methyl signals of the highly st-PMMAs, showing changes in triad compositions with elution time on the hypercarb stationary phase in a solvent composition of DCM/Acetone 40/50 (v/v) at flow rate of 0.5 mL/min and a column temperature of 30°C.*

The *st*-PMMAs were analysed for the construction of a LAC calibration curves. In Figure 55, the red triangles represent the predominantly *st*-PMMA homopolymers (S-type samples) while, the blue triangles represent the highly *st*-PMMA homopolymers (HS-type samples). A difference in the calibration curves was observed at high molar masses.

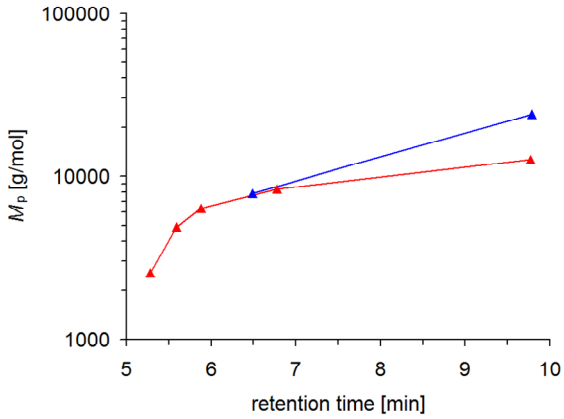


*Figure 55: LAC-NMR calibration curves constructed using the st-PMMA homopolymers.*

Figure 56 (a) and (b) show that an increase in molar mass causes an increase in adsorptive interactions leading to tailing effects. Samples S-8350 and HS-7870 with comparable molar masses, the S-8350 sample with higher *mr* and lower *rr* triad content elutes later than HS-7870 with lower *mr* and higher *rr* triad content. As mentioned previously, an increase in molar mass leads to an increase in adsorption. The slightly higher molar mass of the S-8350 sample also contributes to the increase in adsorptive behaviour. The triad compositions of the LAC-NMR spectra over the total elution time where calculated as shown in Table 11. These values were also in good agreement with the values obtained from the bulk $^{1}$H NMR measurements shown in Table 6.

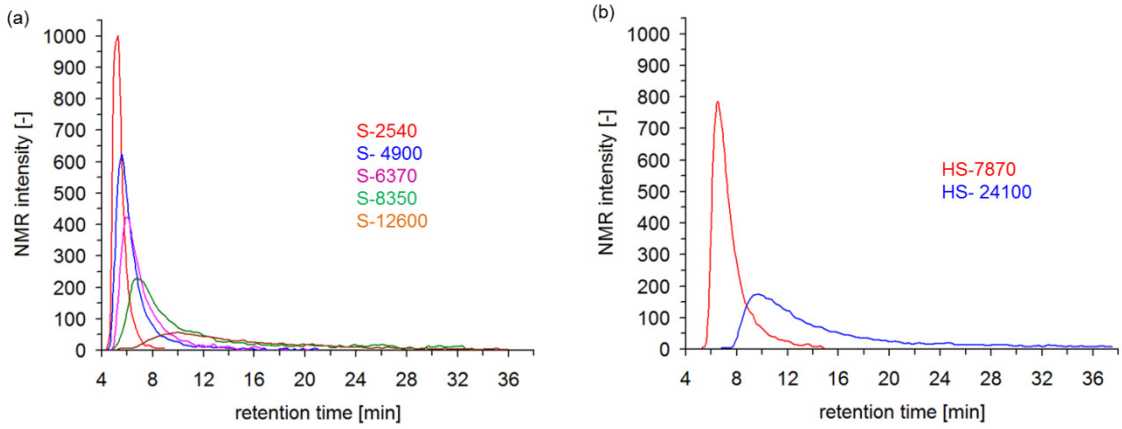


*Figure 56: LAC-NMR chromatograms of st-PMMA homopolymers on a hypercarb stationary phase in a solvent composition of DCM/Acetone 40/60 (v/v) at a flow rate of 0.5 mL/min and a column temperature of 30°C.*

*Table 11: Average triad composition as measured by LAC-NMR.*

| **Sample** | **Tacticity [mol%]** | | |
|---|---|---|---|
| | ***mm*** | ***mr*** | ***rr*** |
| S-25401 | 2.8 | 43.7 | 53.5 |
| S-2810 | 3.8 | 45.8 | 50.4 |
| S-4900 | 3.0 | 38.5 | 58.5 |
| S-6370 | 1.7 | 34.7 | 63.6 |
| S-8350 | 4.5 | 37.6 | 57.9 |
| S-12600 | - | 24.7 | 75.3 |
| HS-7870 | - | 21.8 | 78.2 |
| HS-24100 | - | 20.3 | 79.7 |

#### *4.3.3.3 Gradient HPLC-NMR*

The initial solvent composition of the gradient program was a mixture of DCM/Acetone 20/80 (v/v). The use of a solvent gradient with $^{1}$H NMR leads to a change in chemical shifts during elution. This problem was overcome ensuring the acetone in the reservoir consisted of 25% deuterated acetone with 75% hydrogenated acetone. The deuterated acetone in the eluent allowed for deuterium locking which, allowed for easy homogenization of the magnetic field and frequency tuning producing stable chemical shifts. The presence of deuterated acetone did not alter the chromatography, at DCM/Acetone 20/80 (v/v), the high molar mass *st*-PMMA still eluted at higher retention time as compared to the low molar mass *st*-PMMA which eluted at lower retention times while, *it*-PMMAs were completely adsorbed. An increase in DCM content during elution promoted the elution of *it*-PMMA. The gradient program used is shown in Table 8. The solvent gradient separation efficiency was tested with two sets of quaternary blends shown in Table 12.

Figure 57 shows the LC-NMR contour plots of the two quaternary blends in the above-mentioned gradient. An impurity in the HPLC grade acetone observed at 1.215 ppm, overlapped with the *mm* triad signal. Since the integration of all the α-methyl signals is equivalent to the integration of the methoxy signal, accurate integration of the *mr* and *rr* triad signals will allow for the determination of the *mm* triad amount. The blend compositions were made up in such a way that the S-type *st*-PMMAs in blend 2 had comparable molar masses to the HS-type *st*-PMMAs in blend 1.

Figure 57 shows that for the gradient in Table 8, in both quaternary blends the *st*-PMMA components elute earlier than *it*-PMMAs with, the high molar mass samples eluting at later retention times. In blend 1 samples HS-342900 and HS-24100 are eluting at the same retention time independent of their molar masses at a solvent composition of DCM/Acetone 50/50 (v/v), which is close to the critical conditions that were obtained for *st*-PMMAs on instrument 1. Comparing *st*-PMMA samples of comparable molar masses from the two blends (HS-7870 and S-8290, HS-24100 and S-23500, and HS-342900 and S-392000), the S-type samples with lower amounts of *mm* triads elute earlier than the HS-type samples with a higher amount of *mm* triads.

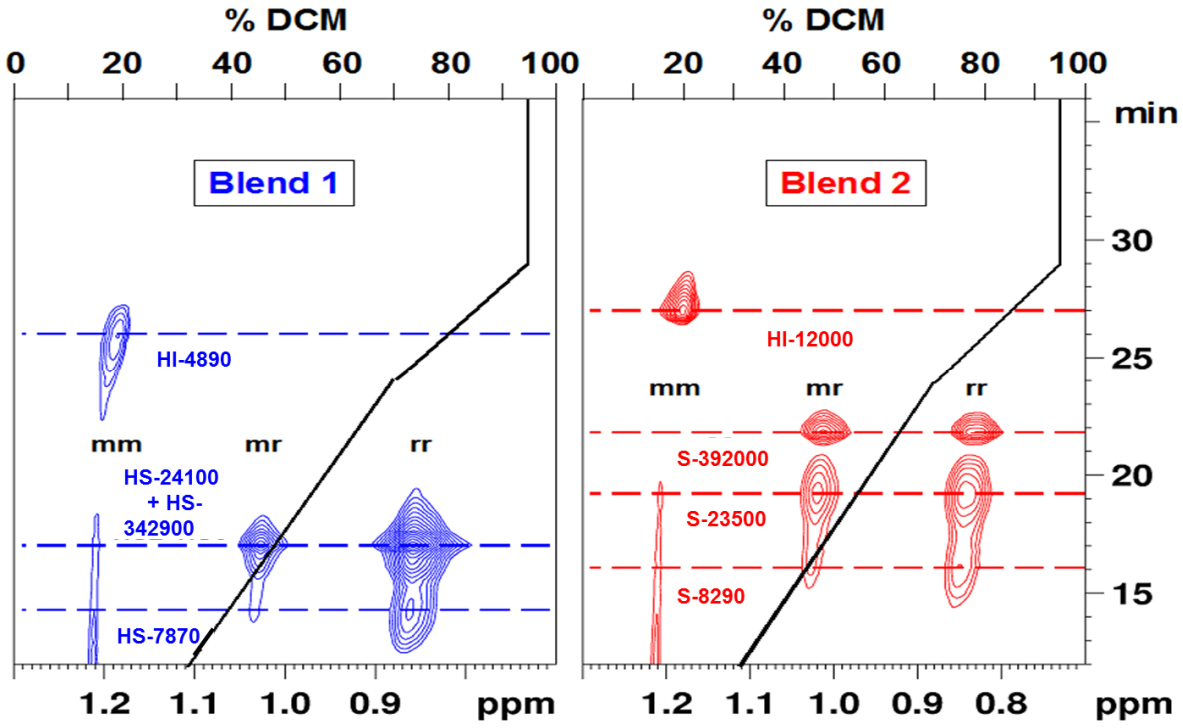


*Figure 57: LC-NMR contour plots of two quaternary blends using the solvent gradient program in Table 8 on a hypercarb stationary phase at a flow rate of 0.5 mL/min and a column temperature of 30°C using instrument 2.*

The integration of the α-methyl signals in the on-flow LC-NMR spectra produced chromatograms of the triad composition of each blend during elution as shown by Figure 58. The triad compositions changed with elution. The amount of *rr* triads decreases with an increase in retention time while the amount of isotactic and heterotactic triads increases with an increase in retention time.

The average triad composition of the blend components in both blends is shown in Table 12. The tacticities of all the *st*-PMMA samples in Table 12 are comparable to the bulk results in Table 6, while the tacticities of the *it*-PMMA samples are different from those obtained by bulk $^{1}$H NMR. The isotactic triad amounts are low while the heterotactic triad amounts are higher.

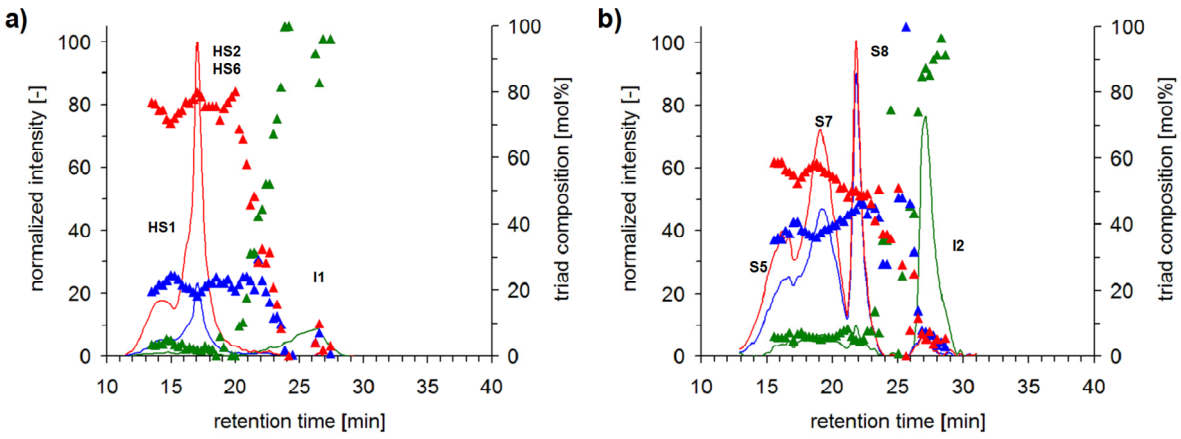


*Figure 58: Gradient HPLC-NMR chromatograms of quaternary blends (a) blend 1 and (b) blend 2, showing the total triad composition.*

*Table 12: Calculated average triad compositions for the different blends using gradient LC-NMR.*

| **Blend** | **Sample** | **Tacticity [mol%]** | | |
|---|---|---|---|---|
| | | ***mm*** | ***mr*** | ***rr*** |
| **1** | HS-7870 | 3.6 | 21.6 | 74.8 |
| | HS-24100 | 1.8 | 18.4 | 79.8 |
| | HS-342900 | 1.8 | 18.4 | 79.8 |
| | HI-4890 | 91.8 | 4.2 | 4.0 |
| **2** | S-8350 | 5.7 | 35.5 | 58.8 |
| | S-23500 | 5.3 | 37.2 | 57.5 |
| | S-392000 | 5.0 | 44.8 | 50.2 |
| | HI-12000 | 87.2 | 7.5 | 5.3 |

## 4.4 Conclusions

Stereoregular PMMAs have been shown to have different adsorptive behaviours on various silica based stationary phases. This work was aimed at using a porous graphitic stationary phase which has numerous advantages over silica-based stationary phases to separate stereoregular PMMAs according to tacticity. Preliminary experiments showed differences in adsorptive behaviours of *st*-PMMA and *it*-PMMA in a solvent composition of DCM/Acetone of various compositions. The critical conditions of predominantly *st*-PMMA were established at a solvent composition of DCM/Acetone 53.5/46.5 (v/v), under these critical conditions, the *it*-PMMA was completely adsorbed while the highly *st*-PMMAs eluted at the same retention volume as the predominantly *st*-PMMAs. Since this method was not efficient in differentiating between st-PMMAs differing in amounts of *rr* and *mr* triads below 20%, this could serve to prove that the amount of *mm* triads in the PMMA drives the separation on this stationary phase. An increase in DCM content was necessary for elution of *it*-PMMAs. Various solvent gradients were developed starting from a low DCM content to a higher DCM content.

The separation efficiencies of the solvent gradients were tested with binary and quaternary blends. Different adsorptive behaviours were observed with *it*-PMMA adsorbed significantly more than *st*-PMMA. For all solvent gradients the *it*-PMMAs were baseline separated from the *st*-PMMAs.

Both LC x LC and LC-NMR results showed two regions of elution belonging to the *st*-PMMAs and *it*-PMMAs. The LC x LC results allowed the observation of tacticity with molar mass separation. The first dimension separated according to tacticity while the second dimension separated according to molar mass. The binary and quaternary blends were baseline separated in the tacticity dimension.

SEC-NMR results of *it*-PMMA showed a decrease in *mm* triad amount with elution and an increase in *rr* triad amount with elution. The same calibration curve could be used to represent all PMMAs regardless of tacticity. Since no change in triad composition was observed with elution using SEC-NMR for the *st*-PMMAs, LAC-NMR was used to observe this change. LAC-NMR showed an increase in both the *mr* and *mm* triad amounts with an increase in retention time, while a decrease in *rr* triad amount was observed with an increase in retention time. Highly *st*-PMMAs and predominantly *st*-PMMAs could not be represented by the same calibration curve at high molar masses.

Gradient HPLC-NMR was used to separate quaternary blends of isotactic and syndiotactic PMMAs. Gradient HPLC-NMR results showed the early elution of the highly *st*-PMMAs (HS-type samples) as compared to predominantly *st*-PMMAs (S-type samples) of comparable molar masses, this might be due to the HS-type PMMAs containing higher *rr* triad amounts as compared to the S-type PMMAs.. Similar to the observations made with SEC-NMR and LAC-NMR, the *mm* triad amount increased with an increase in retention time while the *rr* triad amount decreased with an increase in retention time. The coupling of liquid chromatography with $^{1}$H NMR allowed us to observe the change in triad composition during elution.

# 5. Summary, overall conclusions and recommendations

## 5.1. Summary

### 5.1.1 Separation of polystyrenes according to the isotope effect

Critical conditions of both deuterated and hydrogenated polystyrenes were successfully established. These conditions were used to separate binary and quaternary blends of isotopically different polystyrenes. Two-dimensional liquid chromatography was used to observe the isotopic separation in relation to the molar mass separation. An improvement in separation was observed with an increase in molar mass of the blend components. The low molar mass blends were not successfully separated, making it difficult to distinguish between the different components of the blend.

On-flow LC-NMR with proton and deuterium NMR detection allowed for the observation and differentiation of the components of low molar mass blends although they were not sufficiently separated in the chromatographic dimension.

### 5.1.2 Separation of stereoregular PMMAs according to tacticity

With an eluent composition of DCM/acetone, acetone contents above 50% the allowed for the elution of *st*-PMMA on the porous graphitic stationary phase while *it*-PMMA was completely adsorbed on the column when the acetone content was below 80%. Gradient elution was used for the baseline separation of blends of *it*-PMMA and *st*-PMMA using a solvent composition of DCM/Acetone. Two-dimensional liquid chromatography was used to observe the tacticity separation in relation to the molar mass separation. The first dimension separated with regard to tacticity while the second dimension separated with regard to molar mass. For the LC x LC gradient, *st*-PMMAs eluted regardless of molar mass while *it*-PMMAs elute in adsorption mode with small molar mass PMMAs eluting earlier than large molar mass PMMAs. For the LC-NMR gradient both the *st*-PMMAs and *it*-PMMAs eluted in adsorption mode.

SEC-NMR did not show a change in triad composition with elution for *st*-PMMAs while an increase in syndiotactic triad amount was observed with elution with a decrease in isotactic triad amount with elution for *it*-PMMAs. LAC-NMR showed an increase in both isotactic and heterotactic triads with elution, while a decrease in syndiotactic triad amount was observed with elution.

The gradient HPLC-NMR experiments gave the same results as obtained from both the LAC-NMR experiments, with an increase in heterotactic and isotactic triad amounts with and a decrease in syndiotactic triad amount with elution.

## 5.2. Overall conclusions

### 5.2.1. Separation of polystyrenes with respect to isotope effect

Deuterated compounds have been found to have different properties as compared to their hydrogenated counterparts. The differences between the properties of these compounds have been highlighted by other authors using scattering techniques, which take advantage of the large differences in scattering lengths of deuterium and hydrogen. In literature, liquid chromatography has also been used to prove that the thermodynamic parameters of deuterated and hydrogenated polymers are different.

Numerous authors have made use of both NP- LC and RP-LC to measure the retention differences between deuterated and protonated polymers. Of all the chromatographic methods that have been used to separate isotopically different polymers, liquid chromatography at critical conditions has never been used. None of the chromatographic methods has been coupled online to deuterium and proton NMR for identification of mixtures of these isotopically different polymers.

We decided to evaluate the use of liquid chromatography at critical conditions to separate the isotopically different polymers. The critical conditions of d-PS were established on both bare silica and a $C_{18}$-modified silica stationary phase. The critical conditions for d-PS on a bare silica stationary phase were established at a solvent composition of THF/cyclohexane 23/77 (v/v). Under these conditions the h-PS homopolymers eluted in SEC mode. The critical conditions of d-PS on $C_{18}$-modified silica stationary phase were established at a solvent composition of THF/ACN 47/53 (v/v) at column temperature of 41°C. Under these conditions the h-PS homopolymers eluted in LAC mode. The critical conditions of h-PS on $C_{18}$-modified silica stationary phase were established at a solvent composition of THF/ACN 47/53 (v/v) at a column temperature of 54°C. At these conditions the d-PS homopolymers eluted in SEC mode.

These results were in agreement with those observed by the other authors, with the d-PS homopolymer being more strongly retained on the bare silica stationary phase as compared to the h-PS homopolymer of comparable molar mass. Similarly, the h-PS homopolymer was

more strongly retained on the $C_{18}$-modified silica stationary phase as compared to the d-PS homopolymer of comparable molar mass.

Binary and quaternary blends were analysed using LC x LC and LC-NMR. The LC x LC experiments were conducted with the first dimension separating according to the isotope effect without any molar mass influence and the second dimension separating according to molar mass. An increase in separation was observed with an increase in molar mass of the blend components. With the LC x LC experiments, we were unable to distinguish between the blend components of the low molar mass blends.

Similar to the LC x LC experiments, an increase in separation between the blend components was observed with an increase in molar mass when using on-flow LC-NMR with proton and deuterium detection. Unlike with the LC x LC experiments, the low molar mass blend components could be differentiated using LC-NMR hyphenation even though they chromatographic separation was not sufficient.

We successfully used liquid chromatography at critical conditions to separate deuterated polystyrene from hydrogenated polystyrene at the critical conditions of both polystyrenes. We also successfully coupled the developed chromatographic methods to $^{1}H$ and $^{2}H$ NMR. With the LC-NMR coupling we were able to distinguish between the blend components especially for the lower molar mass blends, which could not be differentiated due to co-elution in the chromatographic dimension.

### 5.2.2. Separation of stereoregular PMMAs with respect to tacticity

Tacticity has been shown to influence various properties of a polymer i.e. crystallinity, cytotoxicity, flexibility of the chain and the electrical properties. The chromatographic separation of PMMA with respect to tacticity has been conducted by various authors on silica based stationary phases. The majority of the studies conducted on stereoregular PMMAs are based on the formation of a stereocomplex between different tacticity PMMAs. The rest of the literature is focused on the separation of PMMAs with regard to tacticity. Some of the developed chromatographic methods had disadvantages which included total adsorption of high molar mass PMMA, insufficient separation and the inability to distinguish the tacticity separation from the molar mass separation, especially with one dimensional liquid chromatography.

The highlight of this study was the use of a porous graphitic stationary phase. This stationary phase has numerous advantages over silica based stationary phase. The most important one for this study is its sensitivity for closely related compounds without the need of adding a modifier.

The preliminary experiments showed differences in the retention behaviours of *st*-PMMA and *it*-PMMA. At a solvent composition of DCM/Acetone 60/40 (v/v) the *it*-PMMA homopolymers were almost completely adsorbed while the *st*-PMMA was eluting in SEC mode. On this stationary phase with a mixture of DCM/Acetone *it*-PMMA was more strongly retained as compared to st-PMMA homopolymer of comparable molar mass.

Binary and quaternary blends were analysed using LC x LC and LC-NMR. The LC x LC experiments were conducted with the first dimension separating according to tacticity and the second dimension separating according to molar mass. The critical conditions of *st*-PMMA were established at a solvent composition of DCM/Acetone 53.5/46.5 (v/v) and incorporated into the LC x LC gradient as the initial conditions. Under these conditions the *st*-PMMA was completely adsorbed and an increase in DCM content was necessary to elute *it*-PMMA. The LC x LC contour plots showed the *st*-PMMAs of different molar masses eluting at the same elution volume of approximately 3 mL while *it*-PMMAs eluted after 6 mL with the low molar masses eluting earlier than the high molar masses.

SEC-NMR results for *it*-PMMA showed a decrease in *mm* triad amount and an increase in *rr* triad amount with elution, while for *st*-PMMA no change in triad composition was observed with elution. LAC-NMR experiments were conducted for the *st*-PMMAs were an increase in isotactic and heterotactic triad amounts with elution was observed, while a decrease in syndiotactic triad amount with elution was observed.

The initial conditions of the LC-NMR gradient were DCM/Acetone 20/80 (v/v). In the LC-NMR gradient both the *st*-PMMAs and *it*-PMMAs eluted in LAC mode with the *st*-PMMAs eluting earlier than *it*-PMMAs. The gradient LC-NMR results showed *st*-PMMAs with higher *rr* triad amounts (>75%) eluting earlier than *st*-PMMAs with lower syndiotactic triad amount (<60%) of comparable molar masses when eluting in adsorptive mode. This is due to the fact that the predominantly syndiotactic PMMAs with *rr* triad amounts < 60% contained higher *mm* ad *mr* triad amounts which have been shown to increase adsorption (Figure 56). LC- $^{1}$H NMR coupling allowed for the observation of triad composition with elution while LC x LC allowed for the observation of tacticity dependence on molar mass.

## 5.3 Recommendations

Suggested future work for the isotopic separation of polystyrenes includes the use of the established two-dimensional liquid chromatography and LC-NMR methods incorporating critical conditions for the separation of copolymers of hydrogenated and deuterated polystyrenes.

Suggested future work for the tacticity separation of poly(methyl methacrylate)s includes investigating the separation efficiency of the current method with a full set of highly and predominantly isotactic, syndiotactic and heterotactic PMMAs of various molar masses. A step gradient would probably be more effective in separating *st*-PMMAs having smaller differences in tacticity. This would allow for the correlation of triad composition with elution volume.

# References


1. Pasch, H. *Polym. Chem.* **2013,** 4, (9), 2628–2650.
2. Pasch, H.; Trathnigg, B., *HPLC of Polymers*. Springer-Verlag Germany, 1999; p 225.
3. Ullmann, R. *Ann. Rev. Mater. Sci.* **1980,** 10, 261– 285.
4. Farrens, D. L.; Holt, R. E.; Rospendowski, B. N.; Song, P. S.; Cotton, T. M. *J. Chromatogr. Sci.* **1989,** 111, (26), 9162-9169.
5. Warner, M.; Higgins, J. S.; Carter, A. J. *Macromolecules* **1983,** 16, (12), 1931–1935.
6. Kayillo, S.; Shalliker, R. A.; Dennis, G. R. *Macromol. Chem. Phys.* **2005,** 206, (20), 2013–2017.
7. Kim, Y.; Ahn, S.; Chang, T. *Anal. Chem.* **2010,** 82, (4), 1509–1514.
8. Iyer, S. S.; Zhang, Z. P.; Kellogg, G. E.; Karnes, H. T. *J. Chromatogr. Sci.* **2004,** 42, (7), 383–387.
9. Kim, S. B.; Kim, Y. J.; Yoon, T. L.; Park, S. A.; Cho, I. H.; Kim, E. J.; Kim, I. A.; Shin, J. W. *Biomaterials* **2004,** 25, (26), 5715–5723.
10. MacTaggart, J. N.; Pipinos, I. I.; Johanning, J. M.; Lynch, T. G. *J. Vasc. Surg.* **2006,** 43, (1), 180–183.
11. Yao, J.; Tao, S. L.; Young, M. J.; Tadokoro, H. *Polym. J.* **2011,** 3, 899–914.
12. Wondraczek, K.; Adams, J.; Fuhrmann, J. *Macromol. Chem. Phys.* **2002,** 203, (18), 2624–2629.
13. Park, J. O.; Hwang, D. K.; Lee, J.; Im, S.; Kim, E. J. *Thin Solid Films* **2007,** 515, (7–8), 4041–4044.
14. Biros, J.; Larina, T.; Trekoval, J.; Pouchly, J. *J. Colloid Polym. Sci.* **1982,** 260, 27–30.
15. Bovey, F. A.; Mirau, P. A., *NMR of polymers*. Academic Press, Inc.: California, USA, 1996; p 118 – 154.
16. Woo, E. M.; Chang, L., Tacticity in Vinyl Polymers. In *Encyclopedia of Polymer Science and Technology*, John Wiley & Sons, Inc.: 2011; pp 1–19.
17. Chang, T. *J. Polym. Lett.* **2005,** 43, (13), 1591–1607.
18. Striegel, A. M.; Yau, W. W.; Kirkland, J. J.; D.D., B., *Modern Size exclusion liquid chromatography*. 2nd ed.; John Wiley and sons Inc: New Jersey, 2009; p 19 –26.
19. Chang, T. *Adv. Polym. Sci.* **2003,** 163, 1–60.
20. Svec, F. *Chem. Educator* **1997,** 2, (6), 1 – 8.
21. Stoll, D. R.; Li, X.; Wang, X.; Carr, P. W.; Porter, S. E. G.; Rutan, S. C. *J. Chromatogr. A* **2007,** 1168, (1–2), 3-43.

22. Cohen, S. A.; Schure, M. R., *Multidimensional liquid chromatography: Theory and applications in industrial chemistry and life sciences*. John Wiley and sons, Inc: New Jersey, 2008.
23. Malerod, H.; Lundanes, E.; Greibrokk, T. *Anal. Methods* **2010,** 2, 110 – 122.
24. Mourey, T. H.; Oppenheimer, L. E. *Anal. Chem.* **1984,** 56, 2427 – 3434.
25. Arndt, J. H.; Macko, T.; Brüll, R. *J. Chromatogr. A* **2013,** 1310, 1–14.
26. http://jsb.klantdemo.nl/?id=260&title=ELSD Principles of ELSD. (17 August 2013),
27. Bovey, A. B.; Mirau, P. A., *NMR of polymers*. Academic Press Inc: California, 1996; p 1 – 24.
28. Hatada, K.; Katayama, T., *NMR Spectroscopy of polymers*. Springer-Verlag: Germany, 2004; p 228.
29. Klaus, A., *Online LC-NMR and related techniques*. John Wiley and sons Ltd: Germany, 2002; p 295.
30. Gonnella, N. C., *LC-NMR expanding the limits of structure elucidation*. Taylor and Francis Group, LCC: Boca Raton, USA, 2013.
31. Pons, G.; Rey, E. *Pediatrics* **1999,** 104, (3), 9.
32. Lin, J.; Welti, D. H.; Vera, F. A.; Fay, L. B.; Blank, I. *J. Agric. Food. Chem.* **1999,** 47, (7), 2813–2821.
33. Thierrin, J.; Davis, G. B.; Barber, C. s. *Ground Water* **1995,** 33, (3), 469–475.
34. Sharma, R.; Strelevitz, T. J.; Gao, H.; Clark, A. J.; Schildknegt, K.; Obach, R. S.; Ripp, S. L.; Spracklin, D. K.; Tremaine, L. M.; Vaz, A. D. N. *Drug Metab. Dispos.* **2012,** 40, (3), 625– 634.
35. Akimov, Y. K., *Instruments and experimental techniques*. Russia, 2000; Vol. 43.
36. Lee, S.; Park, S.; Lee, K.; Cha, H. *Rev. Sci. Instrum.* **2012,** 83, (12), 123504–123505.
37. Bruno, M.; D'Agostino, M.; Lombardi, M. *Lett. Nuovo Cimento* **1978,** 22, (14), 556–558.
38. Gillich, D. J.; Kovanen, A.; Danon, Y. *J. Nucl. Mater.* **2010,** 405, (2), 181–185.
39. Nemoto, K.; Maksimchuk, A.; Banerjee, S.; Flippo, K.; Mourou, G.; Umstadter, D.; Bychenkov, V. Y. *Applied Physics Letters* **2001,** 78, (5), 595–597.
40. Lin, Z.; Yongjian, T.; Chifeng, Z.; Xuan, L.; Houqiong, Z. *Nucl. Instrum. Meth. A* **2002,** 480, (1), 242–245.
41. Bates, F. S.; Wignall, G. D. *Phys. Rev. Lett.* **1986,** 57, (12), 1429–1432.
42. Hammouda, B.; Nakatani, A. I.; Waldow, D. A.; Han, C. C. *Macromolecules* **1992,** 25, (11), 2903–2906.

43. Takeno, H.; Koizumi, S.; Hasegawa, H.; Hashimoto, T. *Macromolecules* **1996,** 29, (7), 2440–2448.
44. Composto, R. J.; Stein, R. S.; Kramer, E. J.; Jones, R. A. L.; Mansour, A.; Karim, A.; Felcher, G. P. *Physica B* **1989,** 156–157, (0), 434–436.
45. Ogawa, H.; Kanaya, T.; Nishida, K.; Matsuba, G.; Majewski, J. P.; Watkins, E. *J. Chem. Phys.* **2009,** 131, (104907), 1–7.
46. Anema, J. R.; Brolo, A. G.; Felten, A.; Bittencourt, C. *J. Raman Spectrosc.* **2010,** 41, (7), 745–751.
47. Hong, P. P.; Boerio, F. J.; Clarson, S. J.; Smith, S. D. *Macromolecules* **1991,** 24, (17), 4770–4776.
48. Hong, P. P.; Boerio, F. J.; Smith, S. D. *Macromolecules* **1993,** 26, (6), 1460–1464.
49. Tanaka, T.; Donkai, N.; Inagaki, H. *Macromolecules* **1980,** 13, (4), 1021–1023.
50. Tanaka, N.; Araki, M. *J. Am. Chem. Soc.* **1985,** 107, (25), 7780–7781.
51. Tanaka, N.; Yamaguchi, A.; Hashizume, K.; Araki, M.; Wada, A.; Kimata, K. *J. High Res. Chromato.* **1986,** 9, (11), 683–687.
52. Sarma, V. V. S. S.; Abe, O.; Saino, T. *Anal. Chem.* **2003,** 75, (18), 4913–4917.
53. van der Krogt, J. A.; van Valkenburg, C. F.; Belfroid, R. D. *J. Chromatogr.* **1988,** 427, (1), 9–17.
54. Valleix, A.; Carrat, S.; Caussignac, C.; Léonce, E.; Tchapla, A. *J. Chromatogr. A* **2006,** 1116, (1–2), 109–126.
55. Kimata, K.; Hosoya, K.; Araki, T.; Tanaka, N. *Anal. Chem.* **1997,** 69, (13), 2610–2612.
56. Ahn, S.; Im, K.; Chang, T.; Chambon, P.; Fernyhough, C. M. *Anal. Chem.* **2011,** 83, (11), 4237–4242.
57. Huang, J.; Wang, J.; Chen, N.; Yao, H.; He, W.; Jiang, Z. *J. Porphyr. Phthalocya.* **2011,** 15, (02), 140–148.
58. Trapp, O. *J. Chromatogr. A* **2010,** 1217, (7), 1010–1016.
59. Issaq, H. J.; Mangino, M. M.; Singer, G. M.; Wilbur, D. J.; Risser, N. H. *Anal. Chem.* **1979,** 51, (13), 2157–2159.
60. Takemura, T.; Saito, K.; Nakazawa, S.; Mori, N. *Tetrahedron Lett.* **1992,** 33, (42), 6335–6338.
61. Chizhkov, V. P.; Litvin, E. F.; Usorov, M. I.; Yakushina, L. M.; Matyukov, A. A. *B. acad. sci. ussr. Ch.* **1971,** 20, (6), 1068–1071.
62. Fish, B. J. *J. CHromatogr. A* **1997,** 768, (1), 81–87.
63. Sato, H.; Sasaki, M. *Polymer Journal* **1991,** 23, (1), 23–27.

64. Kramer, M.; Muhleis, A.; Conrad, J.; Leitenberger, M.; Beifuss, U.; Carle, R.; Kammerer, D. R. *Z. Naturforsch. C.* **2011,** 66, (7-8), 319–327.
65. Sinha, P.; Hiller, W.; Pasch, H. *J. Sep. Sci.* **2010,** 33, (22), 3494–3500.
66. Hiller, W.; Sinha, P.; Hehn, M.; Pasch, H.; Hofe, T. *Macromolecules* **2011,** 44, (6), 1311–1318.
67. Crne, M.; Park, J. O.; Srinivasarao, M. *Macromolecules* **2009,** 42, 4353–4355.
68. Macko, T.; Pasch, H. *Macromolecules* **2009,** 42, (16), 6063–6067.
69. Chitta, R.; Macko, T.; Brüll, R.; Kalies, G. *J. chromatogr. A* **2010,** 1217, (49), 7717–7722.
70. Pasch, H.; Hiller, W.; Haner, R. *Polym. J.* **1998,** 39, (8 - 9), 1515 –1523.
71. Sato, H.; Sasaki, M.; Ogino, K. *Polym. J.* **1989,** 21, (12), 965–969.
72. Morejón, L.; Mendizábal, E.; Delgado, J. A.; Davidenko, N.; López-Dellamary, F.; Manríquez, R.; Ginebra, M. P.; Gil, F. J.; Planell, J. A. *Lat. Am. appl. res.* **2005,** 35, 175–182.
73. Carriere, P.; Grohens, Y.; Spevacek, J.; Schultz, J. *Langmuir* **2000,** 16, (11), 5051–5053.
74. Goñi, I.; Gurruchaga, M.; Valero, M.; Guzmán, G. M. *Polymer* **1992,** 33, (14), 3089–3094.
75. Nguyen, G.; Matlengiewicz, M.; Nicole, D. *Analusis* **1999,** 27, (10), 847–853.
76. Grohens, Y.; Schultz, J.; Prud'homme, R. E. *Int. J. Adhes. Adhes.* **1997,** 17, (2), 163–167.
77. Brar, A. S.; Singh, G.; Shankar, R. *J. Mol. Struct.* **2004,** 703, (1–3), 69–81.
78. Hehn, M.; Hiller, W.; Wagner, T.; Thiel, J.; Pasch, H. *Macromol. Chem. and Phys.* **2012,** 213, (4), 401–410.
79. Hatada, K.; Ute, K.; Okamoto, Y.; Imanari, M.; Fujii, N. *Polym. Bull.* **1988,** 20, (3), 317–321.
80. Hatada, K.; Ute, K.; Kitayama, T.; Nishimura, T.; Kashiyama, M.; Fijimoto, N. *Polym. Bull.* **1990,** 23, 549–554.
81. Kitayama, T.; Janco, M.; Ute, K.; Niimi, R.; Hatada, K.; Berek, D. *Anal. Chem.* **2000,** 72, (7), 1518–1522.
82. Hiller, W.; Pasch, H.; Sinha, P.; Wagner, T.; Thiel, J. r.; Wagner, M.; Müllen, K. *Macromolecules* **2010,** 43, (11), 4853–4863.
83. Hiller, W.; Hehn, M.; Sinha, P.; Raust, J.; Pasch, H. *Macromolecules* **2012,** 45, (19), 7740–7748.
84. Grohens, Y.; Brogly, M.; Labbe, C.; Schultz, J. *Eur. Polym. J.* **1997,** 33, (5), 691–697.

85. Quintana, J. R.; Stubbersfield, R. B.; Price, C.; Katime, I. A. *Eur. Polym. J.* **1989,** 25, (9), 973–976.
86. Katime, I.; Quintana, J. R.; Valenciano, R.; Strazielle, C. *Polym. J.* **1986,** 27, (5), 742–746.
87. Zhao, Y.; Chen, W.; Hair, D.; Xu, J.; Wu, C. i.; Han, C. C. *Eur. Polym. J.* **2005,** 41, (3), 447–452.
88. Ute, K.; Miyatake, N.; Hatada, K. *Polymer* **1995,** 36, (7), 1415–1419.
89. Asai, S.; Kawano, T.; Hirota, S.; Tominaga, Y. i.; Sumita, M.; Mizumoto, T. *Polym. J.* **2007,** 48, (17), 5116–5124.
90. Kusanagi, H.; Chatani, Y.; Tadokoro, H. *Polym. J.* **1994,** 35, (10), 2028–2039.
91. Fox, T. G.; Garrett, B. S.; Goode, W. E.; Gratch, S.; Kincaid, J. F.; Spell, A.; Stroupe, J. D. *J. Am. Chem. Soc.* **1958,** 80, (7), 1768–1769.
92. Izzo, L.; Griffiths, P. C.; Nilmini, R.; King, S. M.; Wallom, K.-L.; Ferguson, E. L.; Duncan, R. *Int. J. Pharm.* **2011,** 408, (1–2), 213–222.
93. Tung, K.-L.; Lu, K.-T. *J. Membrane Sci.* **2006,** 272, (1–2), 37–49.
94. Gu, Q.; Song, R.; Shen, D. *Polym. Bull.* **2000,** 44, (5-6), 533–538.
95. Katime, I.; Quintana, J. R.; Veguillas, J. *Polymer* **1983,** 24, (7), 903–905.
96. Kitayama, T.; Fujimoto, N.; Terawaki, Y.; Hatada, K. *Polym. Bull.* **1990,** 23, (3), 279–286.
97. Liquori, A. M.; Anzuino, G.; D'Alagni, M.; Vitagliano, V.; Costantino, L. *J. Polym. Sci.Pol. Phys.* **1968,** 6, (3), 509–516.
98. Miyamoto, T. i.; Inagaki, H. *Polym. J.* **1970,** 1, (1), 46–54.
99. Fazel, N.; Brulet, A.; Guenet, J. l. *Macromolecules* **1994,** 27, (14), 3836–3842.
100. Lemieux, E. J.; Prud'homme, R. E. *Polym. J.* **1998,** 39, (22), 5453–5460.
101. Inagaki, H.; Miyamoto, T.; Kamiyama, F. *J. Polym. Sci.Pol. Lett.* **1969,** 7, 329–333.
102. Berek, D.; Jančo, M.; Kitayama, T.; Hatada, K. *Polym. Bull.* **1994,** 32, (5-6), 629–635.
103. Berek, D.; Janco, M.; Hatada, K.; Kitayama, T.; Fujimoto, N. *Polym. J.* **1997,** 29, (12), 1029–1033.
104. Macko, T.; Hunkeler, D.; Berek, D. *Macromolecules* **2002,** 35, (5), 1797–1804.
105. Janco, M.; Hirano, T.; Kitayama, T.; Hatada, K.; Berek, D. *Macromolecules* **2000,** 33, (5), 1710–1715.
106. Cho, D.; Park, I.; Chang, T.; Ute, K.; Fukuda, I.; Kitayama, T. *Macromolecules* **2002,** 35, (15), 6067–6069.
107. Cho, D.; Park, S.; Chang, T.; Ute, K.; Fukuda, I.-i.; Kitayama, T. *Analytical chemistry* **2002,** 74, (8), 1928-1931.

108. Belliardo, F.; Chiantore, O.; Berek, D.; Novak, I.; Lucarelli, C. *J. Chromatogr.* **1990,** 506, 371–377.

109. Forgács, E. *J. Chromatogr. A* **2002,** 975, 229–243.

110. Paisley, S. D. *Chromatographia* **2010,** 72, (3), 317– 319.

111. Wan, Q. H.; Shaw, N. P.; Davies, M. C.; Barrett, D. A. *J. Chromatogr. A* **1995,** 697, 219 –227.

112. Pereira, L. *J. Liq .Chromatogr. R. T.* **2008,** 31, (11–12), 1687–1731.

113. Gilbert, M. T.; Knox, J. H.; Kaur, B. *Chromatographia* **1982,** 16, 138–143.

114. Macko, T.; Cutillo, F.; Busico, V.; Brüll, R. *Macromol. Symp.* **2010,** 298, 182–190.

115. Ginzburg, A.; Macko, T.; Dolle, V.; Brüll, R. *Eur. Polym. J.* **2011,** 47, (3), 319–329.

116. Sinha, P.; Harding, G. W.; Maiko, K.; Hiller, W.; Pasch, H. *J. Chromatogr. A* **2012,** 1265, 95–104.

117. Hiller, W.; Hehn, M.; Hofe, T.; Oleschko, K.; Montag, P. *J. Chromatogr. A* **2012,** 1240, (0), 77–82.

118. Hehn, M.; Maiko, K.; Pasch, H.; Hiller, W. *Macromolecules* **2013,** 46, (19), 7678–7686.

119. Maiko, K.; Hehn, M.; Hiller, W.; Pasch, H. *Anal. Chem.* **2013,** 85, 9793–9798.

120. Allen, R. D.; Long, T. E.; McGrath, J. E., Synthesis of Tactic Poly(Alkyl Methacrylate) Homo and Copolymers. In *Advances in Polymer Synthesis*, Culbertson, B.; McGrath, J., Eds. Springer US: 1986; Vol. 31, pp 347–362.

121. Hatada, K., *NMR of polymers*. Springer-Verlag: Germany, 2004; p 228.